1969-12

A study of gyrator circuits

Kulesz, James John, Jr.

Monterey, California. U.S. Naval Postgraduate School

A STUDY OF GYRATOR CIRCUITS

James John Kulesz

United States
Naval Postgraduate School

THESIS

A STUDY OF GYRATOR CIRCUITS

by

James John Kulesz, Jr.

December 1969

A Study of Gyrator Circuits

by

James John Kulesz, Jr.
Lieutenant, United States Navy
B.S., United States Naval Academy, 1961

Submitted in partial fulfillment of the
requirements for the degree of

MASTER OF SCIENCE IN ELECTRICAL ENGINEERING

from the

NAVAL POSTGRADUATE SCHOOL
December 1969

ABSTRACT

Since the introduction of the gyrator in 1948, numerous papers have been written concerning the implementation and application of these network devices. Gyrators have been realized utilizing vacuum tubes, transistors, and operational amplifiers to obtain their non-reciprocal property. It is the purpose of this thesis to consolidate the current findings.

A section has been written on each of the active devices mentioned above. The individual sections consist of summaries of published gyrator realizations. The method used to obtain the gyrator properties, along with appropriate equations, is that of the original circuit designer. Some relations and equations have been modified to standardize notation, or to express them in a more convenient form. Where available, experimental test circuits have been included to support the synthesis method.

TABLE OF CONTENTS

ILLUSTRATIONS

I. INTRODUCTION

A. BACKGROUND

In 1948 B.D.H. Tellegen introduced the gyrator [1] as the fifth basic passive network element; the others being the capacitor, inductor, resistor and the ideal transformer. The uniqueness of the gyrator is that it is the first of the basic elements that violates the reciprocity relation.

The open-circuit impedance, short-circuit admittance, and hybrid parameters of a two-port network [Fig. 1.1] may be written in the generalized form

$$\begin{bmatrix} 0_1 \\ 0_2 \end{bmatrix} = \begin{bmatrix} k_{11} & k_{12} \\ k_{21} & k_{22} \end{bmatrix} \begin{bmatrix} U_1 \\ U_2 \end{bmatrix}, \tag{1-1}$$

where 0 and U are dummy variables representing input and output quantities. The relation that $k_{12}=-k_{21}$ is referred to as the reciprocity theorem [2]. A circuit is said to be passive if, upon being excited, the total energy delivered to the network is nonnegative [3].

Figure 1.2 shows the idea gyrator as a two-port device. The open-circuit impedance matrix of an ideal gyrator which describes the gyrator action is

$$\begin{bmatrix} V_1 \\ V_2 \end{bmatrix} = \begin{bmatrix} 0 & \mp R_1 \\ \pm R_2 & 0 \end{bmatrix} \begin{bmatrix} I_1 \\ I_2 \end{bmatrix}, \tag{1-2}$$

where the off-diagonal resistances of the gyrator impedance matrix are called gyration resistances. Inspection of this matrix reveals another interesting feature of ideal gyrators, zero output and input impedances.

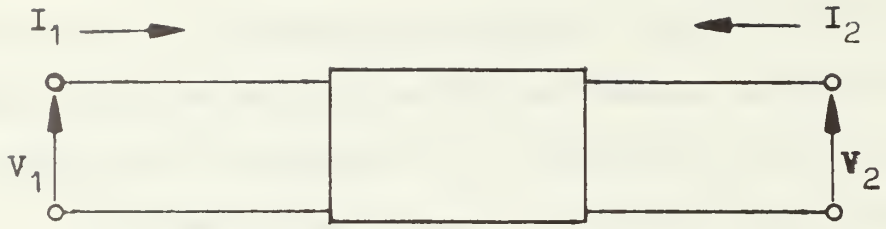

Fig. 1.1. Basic Two-Port Network

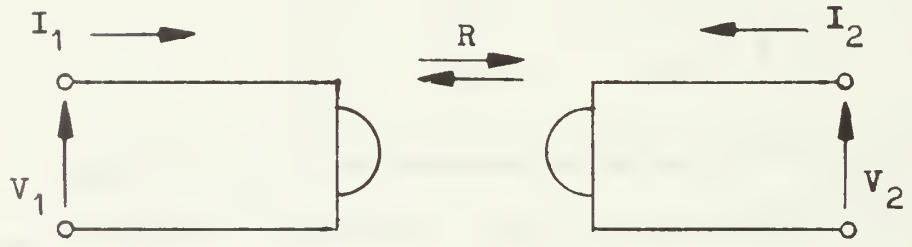

Fig. 1.2. Ideal Gyrator Two-Port Network

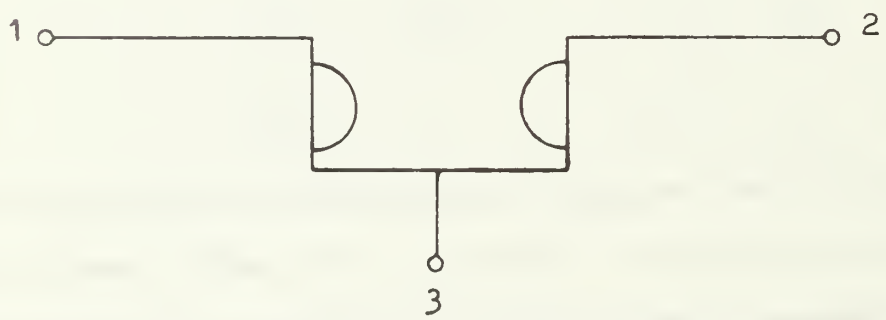

Fig. 1.3. Ideal Gyrator Three-Terminal Network

The short-circuit admittance may be easily derived from the impedance matrix as

$$\begin{bmatrix} I_1 \\ I_2 \end{bmatrix} = \begin{bmatrix} 0 & \pm G_2 \\ \pm G_1 & 0 \end{bmatrix} \begin{bmatrix} V_1 \\ V_2 \end{bmatrix}, \tag{1-3}$$

where the off diagonal conductances of the gyrator admittance matrix are known as gyration conductances. The chain parameters, also commonly referred to in the current literature on gyrators, are

$$\begin{bmatrix} V_2 \\ I_2 \end{bmatrix} = \begin{bmatrix} 0 & \pm R_2 \\ \pm G_1 & 0 \end{bmatrix} \begin{bmatrix} V_1 \\ I_1 \end{bmatrix}. \tag{1-4}$$

The term "ideal gyrator" applies to the condition that R_1 and R_2 are equal, and the network has zero output and input impedances. Devices for the condition that R_1 does not equal R_2 are referred to as "active gyrators." If R_2 does not equal R_1, the determinant is less than zero and the gyrator becomes an active device.

The gyrator is not restricted to a two-terminal network. Figure 1.3 shows the gyrator as a three-terminal network. The resultant indefinite-admittance matrix [4] is

$$\begin{bmatrix} I_1 \\ I_2 \\ I_3 \end{bmatrix} = \begin{bmatrix} 0 & G & -G \\ -G & 0 & G \\ G & -G & 0 \end{bmatrix} \begin{bmatrix} V_1 \\ V_2 \\ V_3 \end{bmatrix}. \tag{1-5}$$

With node one, two, or three grounded, the resultant matrix is the same as (1-3), with the possible exception of a reversal of plus and minus signs.

Reference [5] describes the concept of a multiterminal gyrator with n input terminals, m output terminals, and a common ground terminal. The derived admittance matrix is

$$\begin{bmatrix} I_{i1} \\ I_{i2} \\ \cdot \\ \cdot \\ I_{in} \\ \hline I_{o1} \\ I_{02} \\ \cdot \\ \cdot \\ I_{on} \end{bmatrix} = \left[\begin{array}{ccccc:ccccc} 0_1 & \cdot & \cdot & \cdot & 0_n & G_{11} & G_{12} & \cdot & \cdot & G_{1m} \\ \cdot & \cdot & \cdot & \cdot & \cdot & G_{21} & \cdot & \cdot & \cdot & G_{2m} \\ \cdot & \cdot & \cdot & \cdot & \cdot & \cdot & \cdot & \cdot & \cdot & \cdot \\ \cdot & \cdot & \cdot & \cdot & \cdot & \cdot & \cdot & \cdot & \cdot & \cdot \\ 0_n & \cdot & \cdot & \cdot & 0_m & G_{n1} & \cdot & \cdot & \cdot & G_{nm} \\ \hline -G_{11} & G_{21} & \cdot & \cdot & -G_{n1} & 0 & \cdot & \cdot & \cdot & 0_m \\ -G_{12} & \cdot & \cdot & \cdot & \cdot & \cdot & \cdot & \cdot & \cdot & \cdot \\ \cdot & \cdot & \cdot & \cdot & \cdot & \cdot & \cdot & \cdot & \cdot & \cdot \\ \cdot & \cdot & \cdot & \cdot & \cdot & \cdot & \cdot & \cdot & \cdot & \cdot \\ -G_{1m} & \cdot & \cdot & \cdot & -G_{nm} & 0_m & \cdot & \cdot & \cdot & 0_{mm} \end{array}\right] \begin{bmatrix} V_{i1} \\ V_{i2} \\ \cdot \\ \cdot \\ V_{in} \\ \hline V_{01} \\ V_{02} \\ \cdot \\ \cdot \\ V_{om} \end{bmatrix} , \quad (1\text{-}6)$$

where I_0 and V_0 represent output, and I_i and V_i input. If m=1 and n=1, the resultant admittance matrix is (1-3).

The most important present application of gyrators is in the field of RC network synthesis. Consider the ideal gyrator [Fig. 1.2] with a capacitor as the load at port two. The expression for input impedance of a two-port network is

$$Z_{in} = Z_{11} - Z_{12} Z_{21}/(Z_{22}+Z_L). \quad (1\text{-}7)$$

Using the ideal gyrator-impedance parameters (1-2), the calculated input impedance in the s-domain is

$$Z_{in} = R^2 Cs \quad (1\text{-}8)$$

The input impedance appears as an inductor of value R^2C. Therefore, RLC filters could be designed that would not required bulky and heavy inductors. Since a higher Q is more readily obtained with a capacitor than inductor, the advantages of producing low-frequency filter characteristics without large values of inductive reactive elements is

obtained [6] . Additional reasons for desiring to eliminate the wire-wound coils of inductance are [7] :

1. Reduction in size of volume necessary for the circuitry.

2. Variation of inductances with temperature, humidity and other environmental changes.

3. Reduction of labor costs for bonding.

4. Impossibility of inclusion into monolithic integrated circuits.

Figure 1.4 illustrates some of the suggested uses of gyrators to simulate inductances as suggested by Louis de Pian in his paper on active filters [8] .

B. Q FACTOR AND SENSITIVITY

With the increase of emphasis on the application of electronic gyrator circuits to simulate inductances in integrated filter circuits, it is imperative that the Q of the gyrator circuit used be investigated in order to ascertain the resonant frequency, equivalent inductance, and sensitivity of the filter. Figure 1.5 is a low-and medium-frequency equivalent circuit of a practical gyrator. By low-and medium-frequency equivalent circuit, it is meant that the inherent time delay between the input voltage and output current of each voltage-controlled current source (VCCS) does not significantly affect the result of any network calculations. The time delay is a result of interelectrode capacitances and motion of the charge carriers in the active components of the VCCS.

The ideal gyrator two-port admittance matrix (1-3) requires that the main diagonal terms be equal to zero. The practical realization will have some finite value for these terms. The two-port admittance

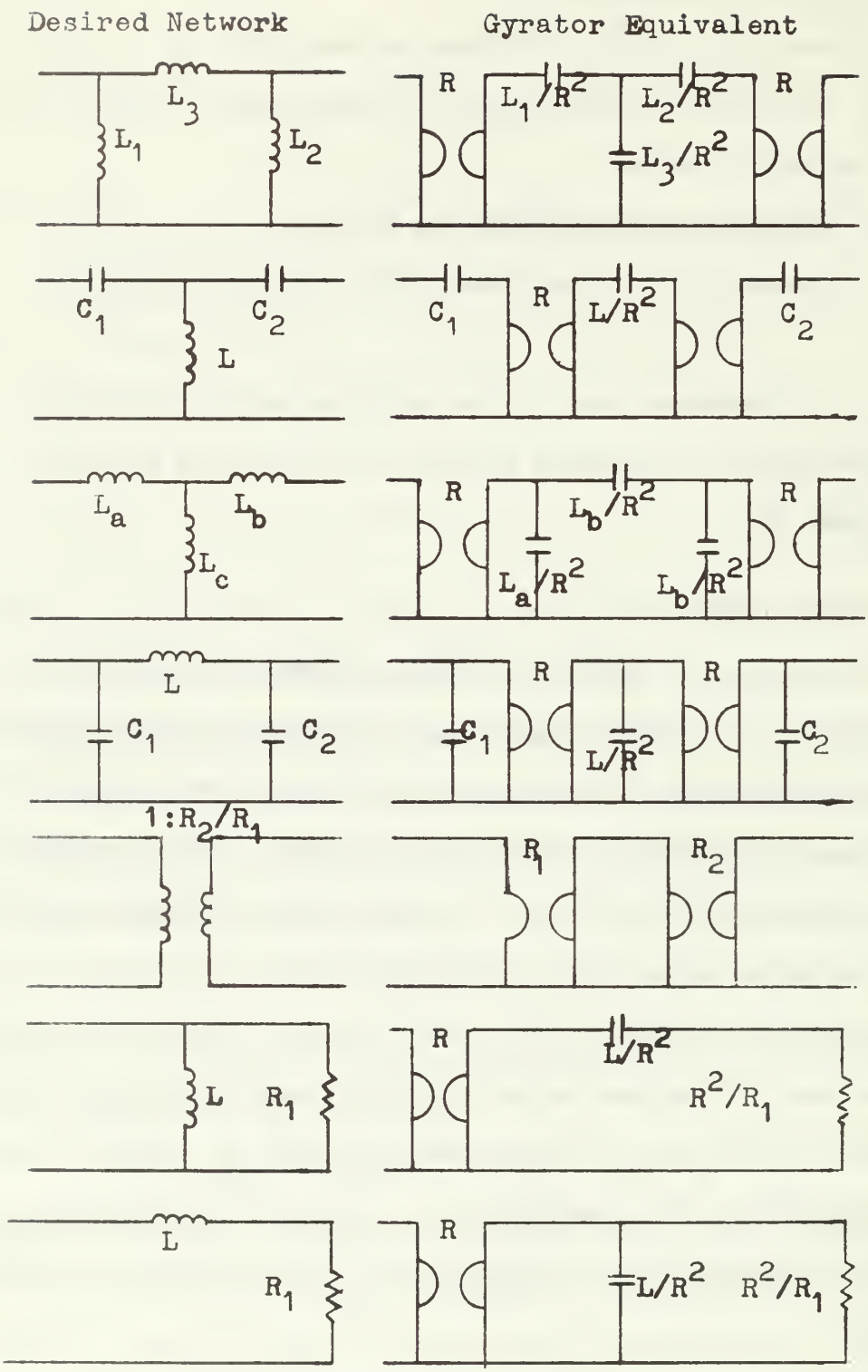

Fig. 1.4. Gyrator Equivalent Networks

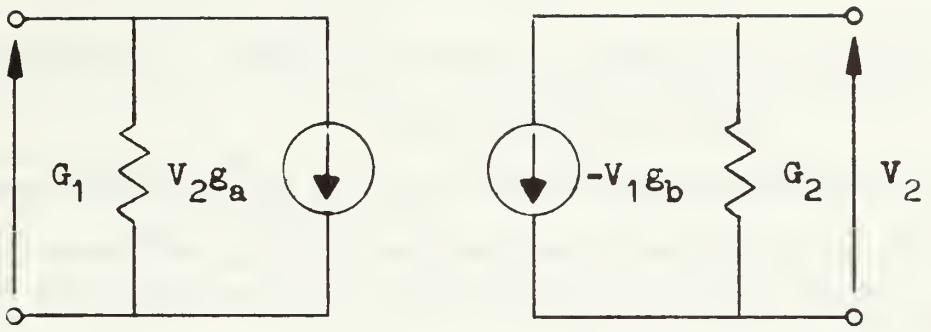

Fig. 1.5. Low-and Medium-Frequency Equivalent Gyrator

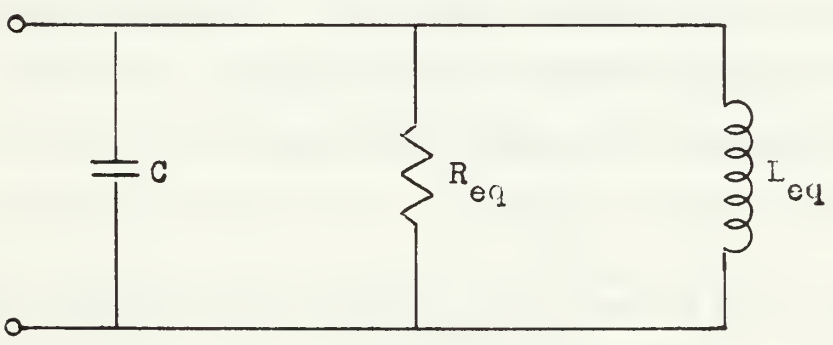

Fig. 1.6. $R_{eq}L_{eq}$ C Parallel Circuit

matrix for a practical gyrator can be written as

$$\begin{bmatrix} I_1 \\ I_2 \end{bmatrix} = \begin{bmatrix} G_1 & g_a \\ -g_b & G_2 \end{bmatrix} \begin{bmatrix} V_1 \\ V_2 \end{bmatrix} . \tag{1-9}$$

The input admittance for a two-port network is computed using

$$Y_{in} = Y_{11} - Y_{12}Y_{21}/(Y_{22}+Y_L) . \tag{1-10}$$

Using a capacitor as the load at port 2 of the equivalent gyrator results in a calculated input admittance, using the parameters of (1-8), of

$$Y_{in}(jw) = \frac{G_1G_2^2+G_2g_ag_b+G_1w^2C^2}{D} + \frac{g_ag_bwC}{jD} , \tag{1-11}$$

where $D = G_2^2+w^2C^2$.

Equation (1-11) has the form

$$Y_{in}(jw) = G_{eq}(W)+1/jwL_{eq}(w). \tag{1-12}$$

Equation (1-12) can be modeled by an equivalent circuit of a resistor and inductor in parallel. With the addition of a capacitor in parallel with the equivalent inductor and conductance, a parallel RLC resonant circuit is obtained [Fig. 1.6] . From this tuned circuit, the Q of the gyrator network can be determined.

The Q factor of any parallel RLC circuit is

$$Q = \frac{1}{wLG} . \tag{1-13}$$

Substituting the equivalent inductance and capacitance into (1-13), results in a Q factor equal to

$$Q(w) = wCg_ag_b/(G_1G_2^2+G_2g_ag_b+G_1w^2C^2). \tag{1-14}$$

The resonant frequency of the circuit is the frequency at which the slope of the Q(w) curve is equal to zero, which is also the point of maximum Q. Taking the derivative of Q(w) with respect to w, and

solving for the resonant frequency (w_0) results in

$$w_0 = G_2(1+X)^{\frac{1}{2}}/C, \tag{1-15}$$

where $X = g_a g_b / G_1 G_2$.

Generally $X >> 1$; therefore (1-15) is approximately equal to

$$w_0 = G_2(X)^{\frac{1}{2}}/C \ . \tag{1-16}$$

By substituting (1-15) into (1-14), the resultant maximum Q factor for the equivalent gyrator is

$$Q_{max} = X(1+X)^{-\frac{1}{2}}/2 \quad . \tag{1-17}$$

Again using the assumption $X >> 1$, the expression for Q_{max} may be approximated as

$$Q_{max} = X^{\frac{1}{2}}/2 \quad . \tag{1-18}$$

The sensitivity of the Q factor is defined by Bialko [9] as $d(\log Q)/d(\log X)$. Applying this definition to (1-14), results in a sensitivity (S) of

$$S_X^Q = K^2/(X+K^2) \ , \tag{1-19}$$

where $K = XC/G_2$.

The sensitivity at resonance can be determined by substituting (1-16) into (1-19). The sensitivity at resonance is equal to ½. This important result shows that at resonance a fractional change of Q is linearly dependent upon the fractional change of X, and independent of operating frequency and capacitance. A simulated inductor must possess this property if it is to be used in a network that requires stability of bandwidth, Q factor, and resonant frequency.

Figure 1.7 is a logarithmic plot of Q factor, equivalent inductance, and equivalent conductance verses w for an equivalent capacitor-loaded gyrator in which $G=G_1=G_2$ and $g=g_a=g_b$. Substitution of these values into the equations developed in this section was used to obtain

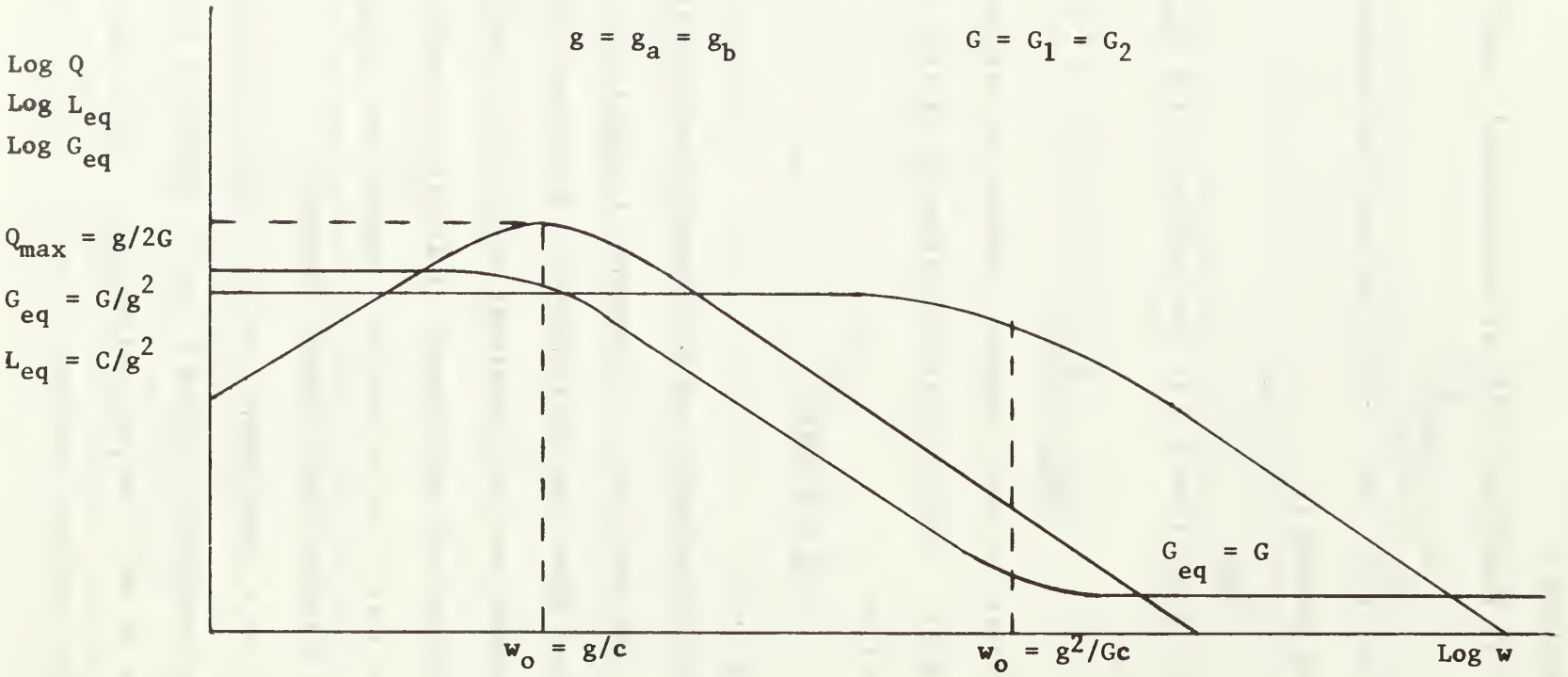

Fig. 1.7. Log Q, L_{eq}, G_{eq} verses Log w

the critical values labeled in the figure. The results agree with the work of T. N. Rao, P. Gary, and R. W. Newcomb [10] , which is based on an equivalent resistance, equivalent inductance, and capacitance in series.

Reference 11 discusses the adverse effect on the obtainable Q factor as a result of residual main diagonal terms of the gyrator admittance matrix. Analysis of equation (1-18) shows that as the values of the input and output conductances approach zero, the higher is the Q obtainable. As an example, consider that a Q_{max} of 500 is desired. With gyration conductances of the order of 10^{-3}mhos, input and output conductances G_1 and G_2 would require a value of 10^{-9}mhos.

Several articles have been written that examine the effect of time delay that accompanies actual gyrator realization [9, 12, 13, 14, 15, 16 and 17] . This time delay or phase shift is a very significant factor that must be taken into account at high frequences. The time delay can be attributed to the active devices used to construct the amplifiers used as voltage-controlled current sources. The delay is temperature-dependent and will increase as the operating temperature of the active devices is increased, particularly where transistorized circuits are employed. A typical time-delay magnitude would be in the order of nanoseconds.

The low-frequency equivalent gyrator circuit [Fig. 1.5] can be adapted to a high-frequency equivalent circuit by changing the gyration conductance terms to $g/(1+jwT)$ [12] . T represents the time delay of each VCCS. The two-port admittance matrix of the high-frequency equivalent gyrator can be written as

$$\begin{bmatrix} I_1 \\ I_2 \end{bmatrix} = \begin{bmatrix} G_1 & g_a/(1+jwT_1) \\ -/g_b/(1+jwT_2) & G_2 \end{bmatrix} \begin{bmatrix} V_1 \\ V_2 \end{bmatrix} . \tag{1-20}$$

The input admittance of a capacitor-loaded gyrator with equal time delay for each VCCS is calculated by substitution of (1-20) into (1-10). The input admittance, neglecting all w^2T^2 terms because of their negligible magnitude, is

$$Y_{in}(jw) = \frac{\left[G_1G_2+g_ag_b-2G_1Cw^2T\right] + jw\left[G_1C+2G_1G_2T\right]}{\left[G_2-2w^2CT\right] + j\left[wC+2G_2wT\right]} \tag{1-21}$$

Equation (1-21) can be further reduced, neglecting insignificant terms, to

$$Y_{in}(jw) = G_{eq} + 1/jwL_{eq} , \tag{1-22}$$

where $G_{eq} = \left[G_1G_2+g_ag_b(G_2-2w^2CT) + G_1w^2C^2\right] /D ,$

$$L_{eq} = D/\left[wg_ag_b(wC+2G_2wT)\right] ,$$

and $$D = G_2^2+w^2C^2 .$$

The equivalent inductance can be approximated for most applications by

$$L_{eq} = D/_w{}^2g_ag_b\ C , \tag{1-23}$$

since generally $2G_2wT << wC$.

The Q factor for a gyrator network with time delay can be calculated in the same manner as the low-and medium-frequency network (1-13). The delay dependent Q factor (Q_D), using (1-23) equivalent inductance is

$$Q_D(w) = XK/\left[1+X(1-2KwT) + K^2\right] . \tag{1-24}$$

The delay-dependent resonant frequency (w_D), derived from (1-24) is

$$w_D = \left[G_2/C\right]\left[(1+X)/(1-2XH)\right]^{\frac{1}{2}} , \tag{1-25}$$

where $H = G_2T/C$.

This is approximately equal to

$$w_D \approx [G_2/C]\, X^{\frac{1}{2}} q \ , \tag{1-26}$$

where $q=1/(1-2XH)^{\frac{1}{2}}$.

Equation (1-26) can be written in terms of the original resonant frequency (1-16) as

$$w_D = qw_0 \tag{1-27}$$

The maximum delay-dependent Q factor can be derived by substitution of (1-26) into (1-24). The result is

$$Q_{D\ max} = qX^{\frac{1}{2}}/2. \tag{1-28}$$

Expressed in terms of Q_{max}, (1-28) can be written

$$Q_{D\ max} = qQ_{max} \ . \tag{1-29}$$

The sensitivity of the filter considering the inherent time delay of each VCCS is derived from the definition of sensitivity and (1-24). The result is

$$S_X^{Q_D} = K^2 / [X-2XKwT + K^2] \ . \tag{1-30}$$

The sensitivity at the resonant frequency w_D is derived by substitution of (1-26) into (1-30). The resultant equation is

$$S_D = q^{2\frac{1}{2}} \ . \tag{1-31}$$

Equation (1-31) can be expressed in terms of $S_X^{Q_{max}}$ as

$$S_D = q^2 S_X^{Q_{max}} \ . \tag{1-32}$$

The equations for Q factor, equivalent inductance, equivalent conductance, sensitivity and resonant frequency for a capacitor-loaded gyrator are all dependent upon the time delay at high frequencies.

Equation (1-22) shows the effect of the negative part of the equivalent inductance. As the operating frequency increases, the magnitude of the equivalent conductance will decrease. Since the conductance is

the damping term of the characteristic equation for the RLC parallel circuit, a value may be reached at which the circuit will cease to act as a resonant circuit and become oscillatory.

The equivalent inductance is the term least affected by the phase delay of the circuit. It can be seen from equation (1-22), that the assumption of (1-23) will generally be valid. The inductance will respond similar to the low-frequency equivalent inductor.

The expressions for w_D (1-27), Q_D (1-29), and S_D max (1-32) illustrate that effect of the q parameter. With time delay, the resonant frequency will increase, and very high Q factors can be obtained. An increase of Q will also have the effect of decreasing the bandwidth of the circuit [15] . The high sensitivity of the network will make the simulated inductor impractical for many applications unless the effect of time delay can be kept to a minimum. The phase delay can be minimized by proper design of the voltage-controlled current sources [16 and 17] , or by the inclusion of additional resistances and capacitances across the input and output ports of the gyrator [18] . The value of the resistances and capacitances must be calculated very specifically to compensate for the phase shift.

Equations (1-12) thru (1-32) developed in this section, agree with the results derived by Bialko [9] . It should be noted that if the time delay is equal to zero, the high-frequency equations reduce to the low-frequency results.

C. THEORTICAL GYRATOR SYNTHESIS

1. VCCS Method

A method of synthesis for gyrator realizations can be obtained by decomposition of the gyrator admittance matrix (1-3) into two

matrices

$$\begin{bmatrix} I_1 \\ I_2 \end{bmatrix} = \begin{bmatrix} 0 & 0 \\ -g_1 & 0 \end{bmatrix} \begin{bmatrix} V_1 \\ V_2 \end{bmatrix} + \begin{bmatrix} 0 & +g_2 \\ 0 & 0 \end{bmatrix} \begin{bmatrix} V_1 \\ V_2 \end{bmatrix} . \tag{1-33}$$

The gyration conductance is the transconductance of the VCCS. Equation (1-33) shows that if two ideal VCCS with 180^{o} phase shift are connected together in parallel, an ideal gyrator is realized [Fig. 1.8] .

2. NIV-NIC Method

A negative-impedance inverter (NIV) [Figs. 1.9 and 1.10] has the chain matrix

$$\begin{bmatrix} V_2 \\ I_2 \end{bmatrix} = \begin{bmatrix} 0 & \pm R_2 \\ \mp G_1 & 0 \end{bmatrix} \begin{bmatrix} V_1 \\ I_1 \end{bmatrix} . \tag{1-34}$$

By changing the sign of one of the non-zero parameters, the gyrator chain matrix (1-4) is realized.

The chain matrix of a current negative-impedance converter (INIC) is

$$\begin{bmatrix} V_2 \\ I_2 \end{bmatrix} = \begin{bmatrix} 1 & 0 \\ 0 & -1 \end{bmatrix} \begin{bmatrix} V_1 \\ I_1 \end{bmatrix} . \tag{1-35}$$

The chain matrix of a voltage negative-impedance converter (VNIC) is

$$\begin{bmatrix} V_2 \\ I_2 \end{bmatrix} = \begin{bmatrix} -1 & 0 \\ 0 & 0 \end{bmatrix} \begin{bmatrix} V_1 \\ I_1 \end{bmatrix} . \tag{1-36}$$

Since the total chain matrix of networks connected in cascade is the product of the individual matrices, a gyrator can be realized by the cascade connection of a NIV with a INIC or VNIC [Fig. 11] [19] .

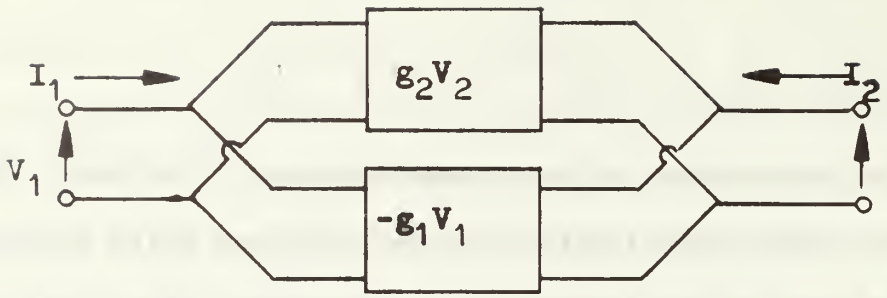

Fig. 1.8. VCCS Gyrator

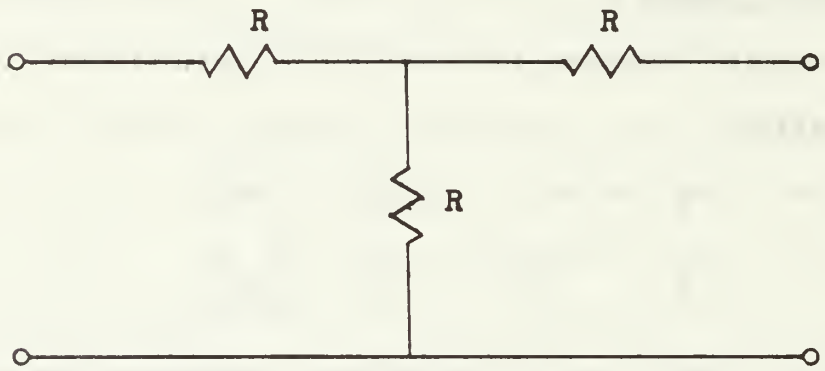

Fig. 1.9. Theoretical T Network NIV

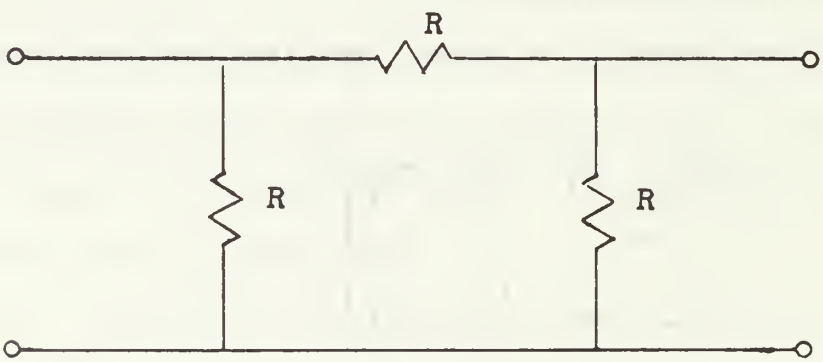

Fig. 1.10. Theoretical Network NIV

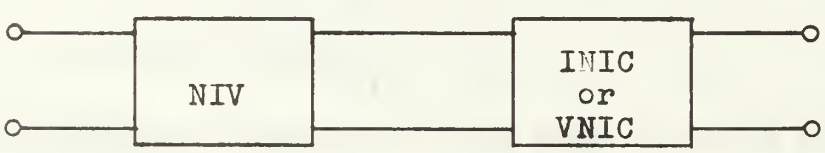

Fig. 1.11. NIV-NIC Gyrator

3. Synthesis Conclusions

The VCCS method, and the NIV-NIC method are the two basic ways to synthesize a gyrator. Although actual circuits have been built using tubes, transistors and operational amplifiers, analysis of the circuits will result in the majority of gyrators being classified as one of the two basic methods.

As mentioned in the section on Q factor (I.B.), a practical gyrator will have finite main-diagonal residual terms. Some of the actual circuit realizations use a negative resistance in series or in parallel, as applicable, to minimize these undesired terms. The use of NIV circuits, NIC circuits, and negative resistance in gyrator construction has been found to have an adverse effect on the Q factor and stability of a gyrator [11] . The NIV and NIC circuits suffer from high sensitivity, and the use of negative resistance to cancel another resistance is subject to component tolerances which may nullify the effort to achieve the desire magnitude of cancellation.

The VCCS method is the best of the two methods to synthesize a gyrator network, particularly where internal negative feedback in each VCCS is used to diminish the value of main diagonal residues [16 and 17] . This minimizes the problem of component tolerances, and offers the advantage of better stability, greater frequency range, and higher Q [20] .

II. VACUUM-TUBE GYRATORS

A. SHEKEL GYRATOR

The earliest vacuum-tube gyrator was proposed by Jacob Shekel [3 and 21] in 1953. The basic triode [Fig. 2.1] is used as the building block for the gyrator. The admittance matrix for the triode is

$$\begin{bmatrix} I_1 \\ I_2 \end{bmatrix} = \begin{bmatrix} 0 & 0 \\ g_m & g_p \end{bmatrix} \begin{bmatrix} V_1 \\ V_2 \end{bmatrix} , \tag{2-1}$$

where g_m is mutual conductance and g_p plate conductance. Equation (2-1) can be split into two matrices with the values

$$\begin{bmatrix} I_1 \\ I_2 \end{bmatrix} = \begin{bmatrix} 0 & \frac{1}{2}g_m \\ \frac{1}{2}g_m & g_p \end{bmatrix} \begin{bmatrix} V_1 \\ V_2 \end{bmatrix} + \begin{bmatrix} 0 & -\frac{1}{2}g_m \\ \frac{1}{2}g_m & \end{bmatrix} \begin{bmatrix} V_1 \\ V_2 \end{bmatrix} . \tag{2-2}$$

By adding a parallel admittance of $\frac{1}{2}g_m$ between terminals one and two, another of $-\frac{1}{2}g_m$ between one and three, and a third of $-(g_p+\frac{1}{2}g_m)$ between two and three [Fig. 2.2] the first matrix of (2-2) is eliminated and the resultant short-circuit admittance matrix is

$$\begin{bmatrix} I_1 \\ I_2 \end{bmatrix} = \begin{bmatrix} 0 & -\frac{1}{2}g_m \\ \frac{1}{2}g_m & 0 \end{bmatrix} \begin{bmatrix} V_1 \\ V_2 \end{bmatrix} . \tag{2-3}$$

The actual construction of a gyrator using such a triode was not practical because of the difficulty of realizing the $-\frac{1}{2}g_m$ and $(-g_p+\frac{1}{2}g_m)$ admittances. Negative resistors and negative circuit elements were known of at the time, but no literature is readily available indicating

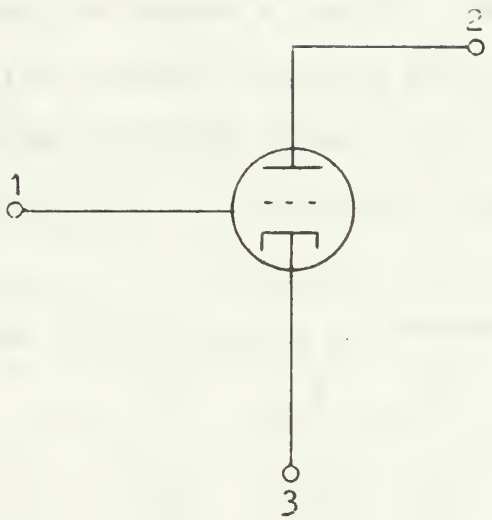

Fig. 2.1. Basic Triode

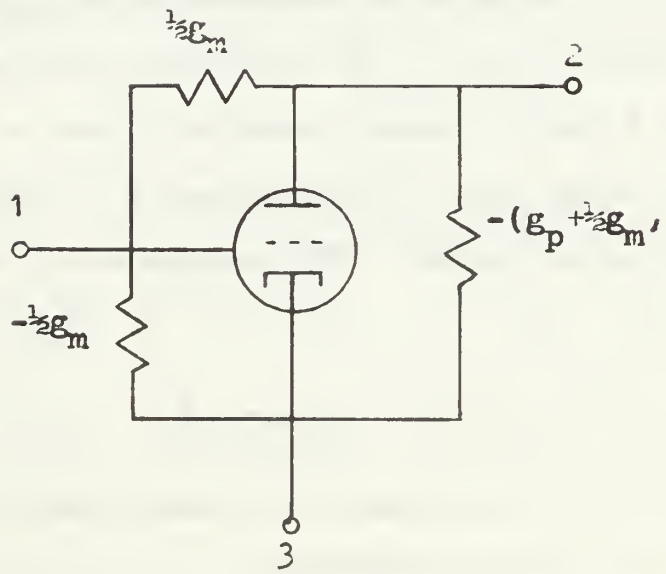

Fig. 2.2. Shekel Gyrator

that a Shekel gyrator was physically constructed or tested. At the time of proposal, the circuit was more of academic interest.

B. BOGERT GYRATOR

In 1955, B. P. Bogert proposed a vacuum-tube gyrator which obtained the gyrator properties from the use of feedback amplifiers [22] . The feedback amplifiers were used to obtain the impedance inversion that is a characteristic of the gyrator, and simulate negative resistances.

A basic two-port network has the open-circuit impedance parameters

$$\begin{bmatrix} V_1 \\ V_2 \end{bmatrix} = \begin{bmatrix} Z_{11} & Z_{12} \\ Z_{21} & Z_{22} \end{bmatrix} \begin{bmatrix} I_1 \\ I_2 \end{bmatrix} . \tag{2-4}$$

Assuming Z_{11} and Z_{12} are equal to zero, the product $Z_{12}Z_{21}$ is negative real, and when any load Z_L is connected across the output port, the resultant expression for input impedance using (1-7), is

$$Z_{in} = Z_{12}Z_{21}/Z_L \quad . \tag{2-5}$$

Equation (2-5) illustrates the impedance-inversion properties of a gyrator assuming Z_{12} and Z_{21} are the gyration resistances.

Figure 2.3 shows a Thevenin equivalent circuit of an amplifier with an unloaded voltage-gain A, input impedance R_1, output impedance R_2, and parallel-series feedback. The impedance matrix for this circuit is

$$\begin{bmatrix} V_1 \\ V_2 \end{bmatrix} = \begin{bmatrix} R_1 & -R_1 \\ -R_1(1-A) & R_1(1-A) + R_2 \end{bmatrix} \begin{bmatrix} I_1 \\ I_2 \end{bmatrix} . \tag{2-6}$$

Solving for the input impedance of the basic parallel-series feedback amplifier results in the expression

$$Z_{in} = R_1(R_2 + Z_L) \; / \; [R_1(1-A) + R_2 + Z_L] \quad . \tag{2-7}$$

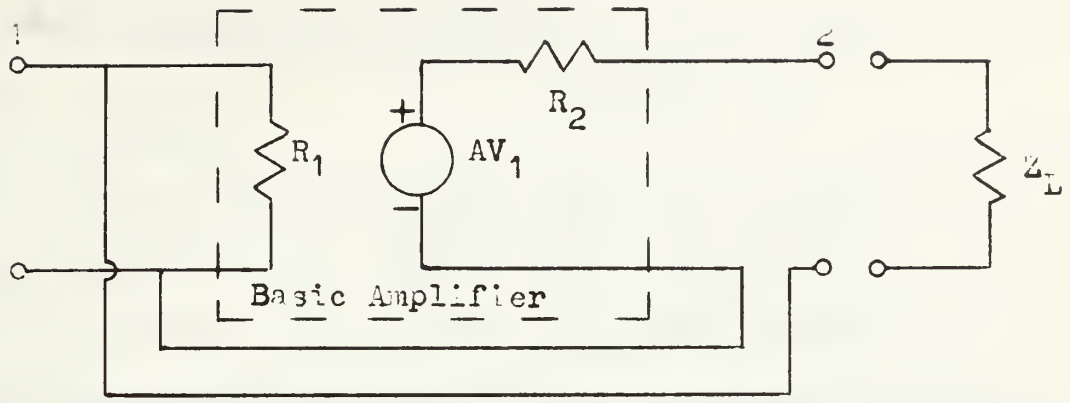

Fig. 2.3. Basic Parallel-Series Feedback Amplifier

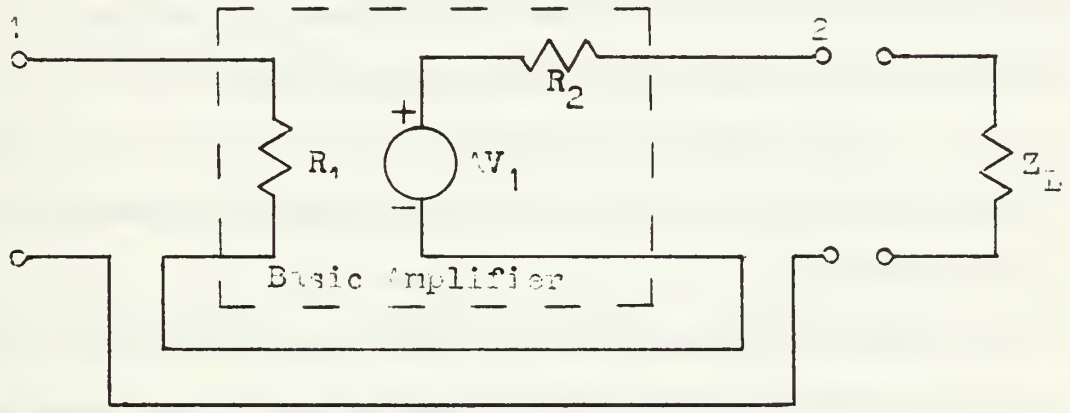

Fig. 2.4. Basic Series-Series Feedback Amplifier

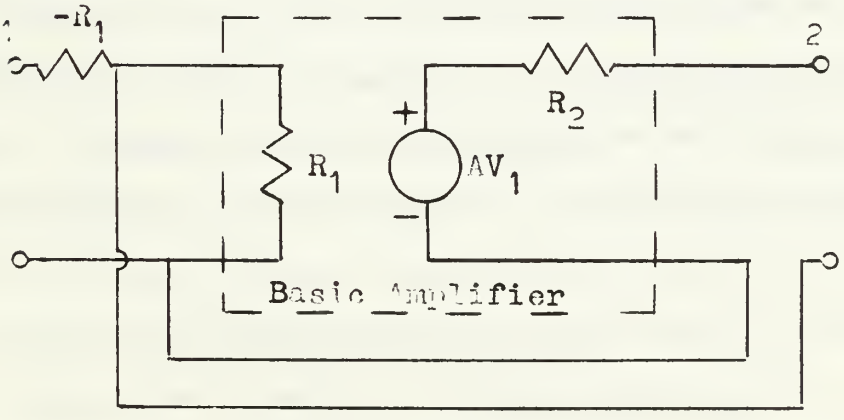

Fig. 2.5. Bogart Gyrator Equivalent Circuit

By proper selection of A, R_1 and R_2, $[R_1(1-A) + R_2]$ can be made approximately equal to zero. If in addition, $R_2 >> Z_L$, (2-7) reduces to

$$Z_{in} \approx R_1 R_2 / Z_L, \tag{2-8}$$

and (2-6) to

$$\begin{bmatrix} V_1 \\ V_2 \end{bmatrix} = \begin{bmatrix} R_1 & -R_1 \\ +R_1 & 0 \end{bmatrix} \begin{bmatrix} I_1 \\ I_2 \end{bmatrix} . \tag{2-9}$$

If a negative resistance of $-R_1$ is placedin the input lead of the parallel-series amplifier, the undesired main diagonal term R_1 of (2-9) will be cancelled. Figure 2.4 is a Thevenin equivalent circuit of an amplifier with series-series feedback with a load Z_L. The input impedance for this series-series feedback amplifier is

$$Z_{in} = (1-A)\ R_1 + R_2 + Z_L . \tag{2-11}$$

With proper selection of R_1, R_2, A and Z_L a negative resistance of $-R_1$ can be attained.

B. P. Bogert experimentally tested operation of a gyrator constructed of a parallel-series feedback amplifier with a series-series feedback amplifier used to create the desired negative resistance in series at the input [Fig. 2.5] . The negative impedance was obtained by using the series-series feedback amplifier with $R_1=R_2$, $Z_L=0$ and A=3. Substitution of these values in (2-11) gives a value of $-R_1$ for impedance. The parallel-series amplifier uses the same value of resistances with A=2. Substitution of these values in (2-6) results in (2-9).

The Bogert gyrator suffered from the disadvantages of variation of circuit parameter with increasing frequency, critical stability, and a low Q factor. These problems were caused by the effect of interelectrode

capacitances, the feedback existing in the network, and difficulty of perfectly matching resistances in the circuit, respectively.

C. SHARPE GYRATOR

The VCCS method was applied to realization of a gyrator by G. E. Sharpe [23 and 24] . His circuit is synthesized with a dual set of ideal active elements, called transactors because their method of operation is based on an irreversible electric-to-magnetic or magnetic-to-electric transfer action [25] .

The voltage-current transactor (v.c.t.) [Fig. 2.6] , which is basically a VCCS, is represented by a letter V laid on its side representing an applied input voltage. The output current branch is represented by the letter U, and a bar which represents that the voltage-to-current transmission is nonreciprocal. The current-voltage transactor (c.v.t.) [Fig. 2.7] has the voltage and current branches interchanged [26] . Although a gyrator could be constructed from either the v.c.t. or c.v.t., Sharpe used the v.c.t. to realize a gyrator.

An equivalent circuit for the v.c.t. gyrator [Fig. 2.8] illustrates that it consists of two VCCS of opposite polarity. Figure 2.9 illustrates the v.c.t. model of the derived gyrator.

A physical realization of the v.c.t. was made with a common cathode connection of two pentodes [Fig. 2.10] . Figure 2.11 is the actual proposed circuit, and Fig. 2.12 is an ac equivalent of that circuit after the following assumptions have been made [24] :

(1) If $R \gg R_L/2$, R may be neglected

(2) If $R_K \quad \frac{1}{g_{m1} + g_{m2}}$, R_K may be neglected.

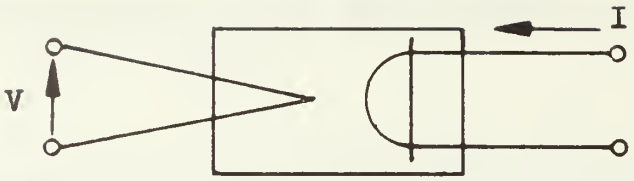

Fig. 2.6. Voltage-Current Transactor

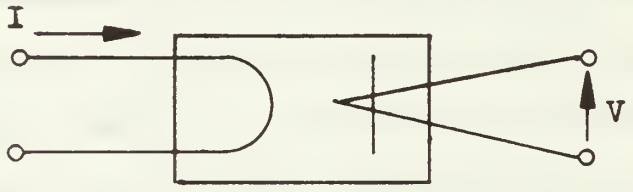

Fig. 2.7. Current-Voltage Transactor

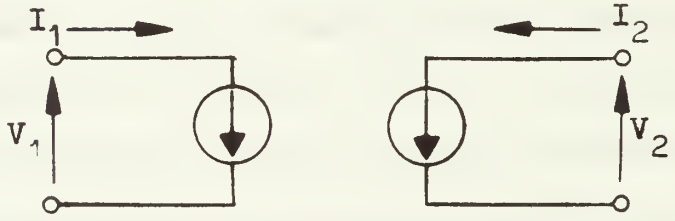

Fig. 2.8. V.C.T. Gyrator Equivalent Circuit

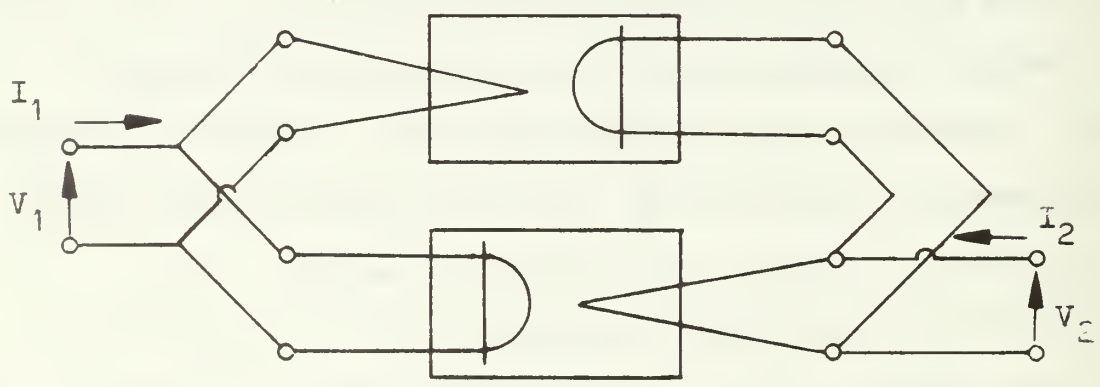

Fig. 2.9. V.C.T. Transactor Equivalent Circuit

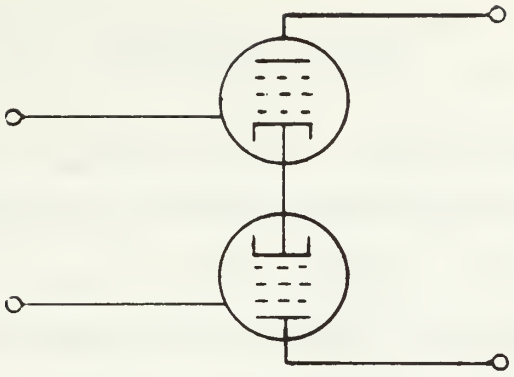

Fig. 2.10. Pentode V.C.T.

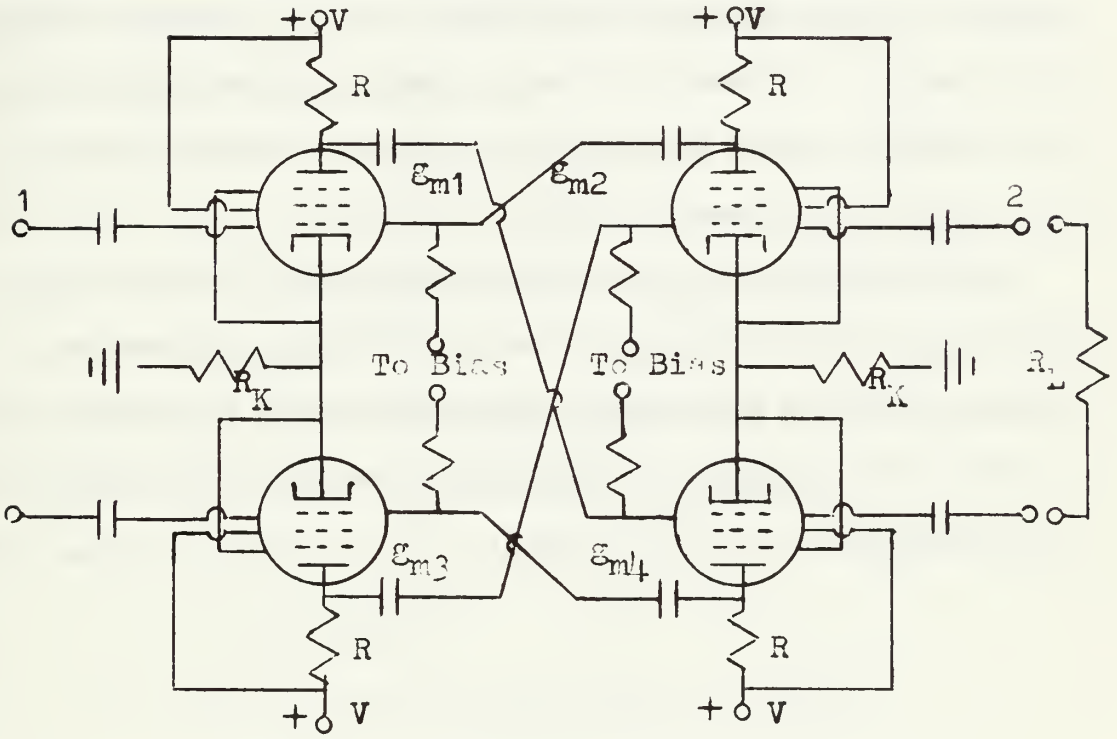

Fig. 2.11. V.C.T. Gyrator

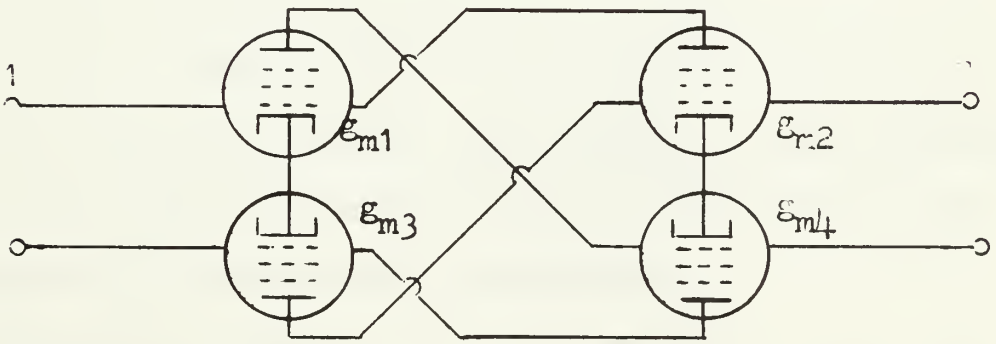

Fig. 2.12. AC Equivalent Gyrator

When a voltage V_1 is applied to the input, the device will act as a VCCS with output current $I_2 = -gV_1$ where

$$g = g_{m1}g_{m3}/(g_{m1}+g_{m3}) = g_{m2}g_{m4}/(g_{m2}+g_{m4}) \quad . \qquad (2\text{-}15)$$

When a voltage V_2 is applied to the output, an input current $I_1=gV_2$ will flow.

The gyrator derived by G. E. Sharpe was a demonstration that the v.c.t. and c.v.t. are more basic circuit elements than a transformer or a gyrator. Because of lack of documentation, it is assumed the Sharpe gyrator was not experimentally tested. The gyrator was realized to demonstrate that a gyrator could be broken down into two of these basic ideal active elements [23] .

Sharpe's articles, which were published in 1957, are the last articles that can be found on vacuum-tube gyrators. Vacuum-tube gyrators are more of historical significance than of a practical use. The rapid developement of the transistor after 1955, decreased interest in tube gyrators.

III. TRANSISTOR GYRATORS

A. SHENOI GYRATOR

A gyrator circuit was proposed in 1963 by B. A. Shenoi which employed only three transistors [27 and 28] . The method of synthesis is based on the VCCS method, with A and B [Fig. 3.1] representing the two amplifiers. The figure illustrates that the network is a shunt-shunt feedback network which characteristically has the property of low input and output impedances.

The gain of either amplifier can be adjusted to be equal in magnitude with that of the other amplifier, but opposite in phase. Amplifier A can be adjusted by variation of R_{ei}, and the gain of amplifier B by adjustment of R_4 and R_5. Figure 2.1 is the experimental circuit tested by Shenoi. Resistances indicated on the diagram were used to achieve a gyration resistance (R_0) of 118ohms.

The impedance parameters for the Shenoi gyrator are [26 and 27]

$$\begin{aligned} Z_{12} &\simeq R_{ei} + h_{ie1}/\beta_1 \\ Z_{21} &\simeq -R_4(1 + h_{ie3}/\beta_3 R_5) - (h_{ie3}/\beta_3)(1+h_{ie2}/\beta_2 R_5) \\ &\quad -h_{ie2}/\beta_2 \\ Z_{11} &\simeq R_o^2\,(G_{L1}+G_{b2}) \\ Z_{22} &\simeq R_o^2(G_{b1} + G_{L3}) \ , \end{aligned} \tag{3-1}$$

where, $R_o^2 = Z_{12}Z_{21}$, $G_{b1} = G_{V1}+G_{V2}$, $G_{b2} = G_{V3}+G_{V4}$, β is the transistor short-circuit forward current gain, and h_{ie} is the transistor input resistance in the common-emitter configuration.

Equation (3-1) is applicable for low-frequency operation of the gyrator. The circuit's gyrator properties deteriorate above 4 KHz as a result of the inherent time delay of the amplifiers.

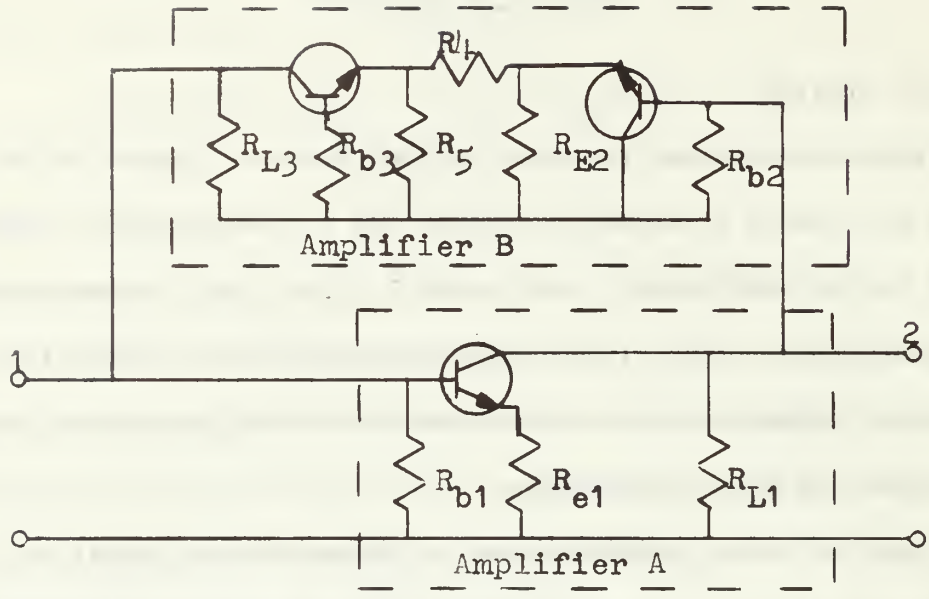

Fig. 3.1. Shenoi AC Equivalent Gyrator

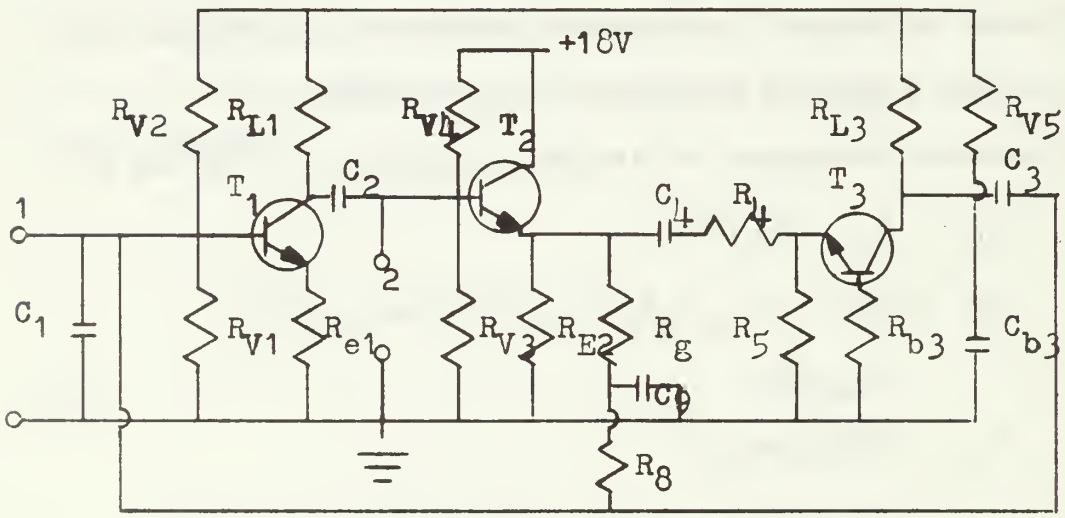

Fig. 3.2. Shenoi Gyrator (R_0 = 118)

R_{V2} = 4.7M	R_{V1} = 68K	C_4 = 25u
R_{L1} = 27K	R_{ei} = 110	R_4 = 92
R_{V4} = 150K	R_{V3} = 470	R_5 = 130
R_{L3} = 27K	R_{E2} = 1.5K	R_{b3} = 33K
R_{V5} = 470K	R_8 = R_9 = 100K	C_{b3} = 5u
C_1 = 400uu	C_9 = 5u	C_3 = 50u

B. ORCHARD-SHEAHAN GYRATORS

The gyrator developed by D. J. Orchard and D. F. Sheahan is synthesized by the VCCS method [16] . Figure 3.3 is the circuit schematic of the Orchard-Sheahan gyrator (Circuit 1).

Each VCCS has high input and output impedances to effectively reduce the main diagonal terms of the gyrator admittance matrix (1-3). The high input impedance of each VCCS is obtained with Darlinton pair transistors at the input ports. The high output impedance is obtained by common collector connection of a PNP and NPN transistor (T_6 and T_7, T_{13} and T_{14}).

One VCCS consists of transistors T_1 thru T_7. The gyration conductance, input impedance, and output impedance considering port one as the input port are

$$g_1 = 2R_4R_6/R_5R_7(R_4+R_6) , \tag{3-2}$$

$$Z_{in} = \beta^2 R_5(1 + R_4/R_6)/2 , \tag{3-3}$$

and $$Z_{out} = r_c R_7(1+R_4/R_6)/2R_4 , \tag{3-4}$$

where r_c is the collector-to-base resistance of the transistor.

The second VCCS is composed of transistor T_8 thru T_{14}. The gyration conductance, input impedance, and output impedance considering port two as the input port are

$$g_2 = 2R_{11}R_{14}/ R_{19}(R_{11}R_{14}+R_{12}R_{13}) , \tag{3-5}$$

$$Z_{in} = \beta^2(R_{12}+R_{19}+R_{11}R_{14}/R_{13})/2 , \tag{3-6}$$

and $$Z_{out} = r_c R_{19}R_{11}/2(R_{12}+R_{13}) . \tag{3-7}$$

It should be noted that the gyration conductances, (3-2) and (3-5), are only dependent upon the resistances in the circuit. They do not dependent on any of the transistor parameters such as the forward

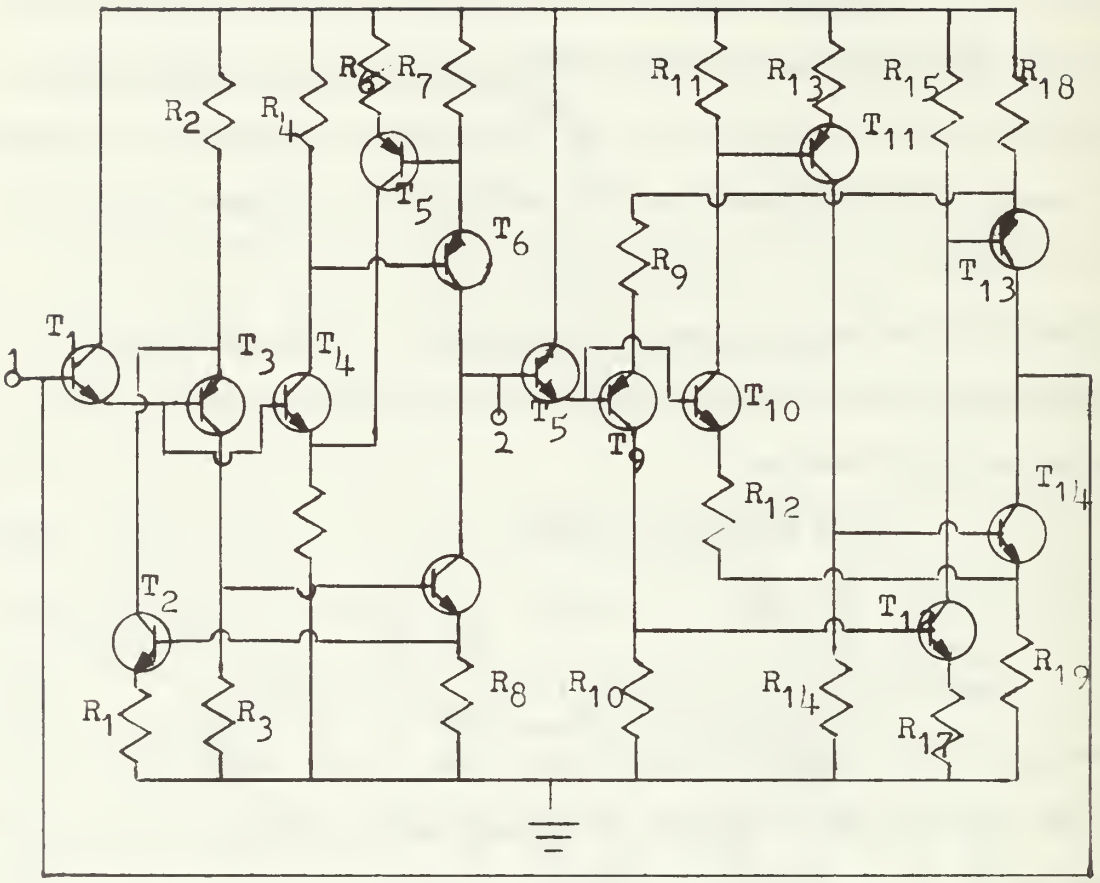

Fig. 33. Orchard-Sheahan Gyrator (Circuit 1)

R_1 = 1.0K
R_2 = 6.8K
R_3 = 10K
R_4 = 10K
R_5 = 6.8K
R_6 = 10K
R_7 = 2.0
R_8 = 2.0K
R_9 = 5.1K
R_{10} = 2.7K
R_{11} = 2.7K
R_{12} = 5.1K
R_{13} = 1.0K
R_{14} = 5.1K
R_{15} = 5.1K
R_{16} = None
R_{17} = 1.0K
R_{18} = 4.7K
R_{19} = 4.7K

current gain. Therefore, g_1 and g_2 should not change appreciably with variation of temperature or supply voltage which can cause change of the current gain. The input impedances (3-3) and (3-6), are the only parameters that change with such a variation. The relations derived for the Orchard-Sheahan gyrator are applicable to low-frequency synthesis. This circuit becomes sensitive to the inherent phase shift of each VCCS as discussed in Section I.B. The experimental circuit tested by Orchard and Sheahan [Fig. 3.3] , became oscillatory at frequencies as low as 1 KHz with low values of load capacitance. A majority of the phase shift is attributed to the Darlington pairs of transistors in which the time delay is extremely temperature-sensitive.

Using the same concept of gyrator realization, Orchard and Sheahan constructed a second gyrator (Circuit 2) [17] by replacing the Darlington pair of transistors at the input to each VCCS with a metal-oxide-semiconductor field-effect transistor (MOSFET). The MOSFET has the advantage of a higher imput impedance, and is not as temperature-sensitive as the Darlington pair [29] . As a result, this gyrator is able to operate with a capacitive load up to frequencies of 100 KHz.

Figure 3.4 is a network diagram of Circuit 2. As in circuit 1, the output impedance of each circuit uses a common collector connection of an NPN and a PNP junction transistor to give a high output impedance (T_3 and T_4, T_7 and T_8). The input VCCS at port 1 consists of transistors T_1 thru T_4 and associated resistors. The mutual transconductance (g_m) of a MOSFET is temperature-sensitive, and T_2 provides negative feedback around the MOSFET at port 1 to stabilize the g_m. In addition, resistor R_1 is used to stabilize the VCCS with local source feedback.

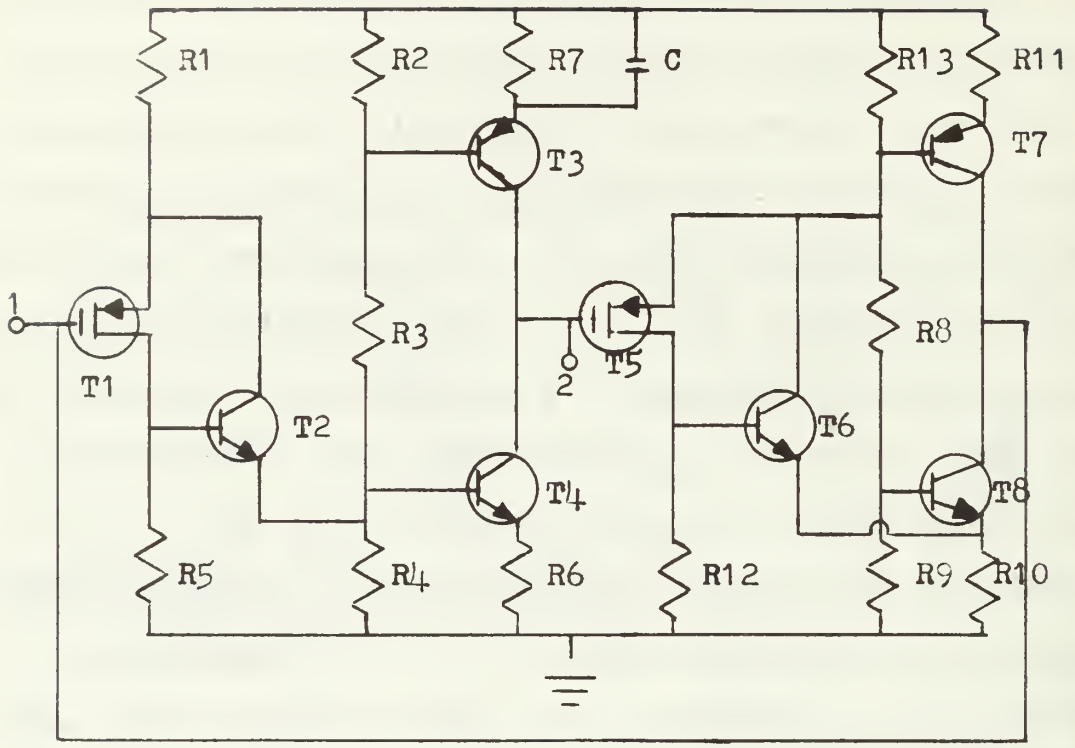

R_1 = 1.96K

R_2 = 3.16K

R_3 = 6.19K

R_4 = 1.62K

R_5 = 5.11K

R_6 = 5.11K

R_7 = 5.11K

R_8 = 6.19K

R_9 = 3.16K

R_{10} = 3.48K

R_{11} = 5.11K

R_{12} = 5.11K

R_{13} = 1.96K

C = 50p

Fig. 3.4. Orchard-Sheahan Gyrator (Circuit 2)

The gyration conductance for VCCS 1 is

$$g_2 = \frac{\dfrac{g_m R_5 R_7 (R_2+R_3) + R_2 R_5 R_6}{R_6 R_7 (R_2+R_3)}}{g_m R_1 \left[\dfrac{1+R_5(R_2+R_3+R_4)}{R_4(R_2+R_3)}\right] + 1} \tag{3-8}$$

The VCCS with input at port 2 is similar to the VCCS at port one. However, to achieve the 180^{o} phase shift of VCCS 2, the emitter of T_4 is connected to the emitter of T_8.

The gyration conductance equation is

$$g_2 = \frac{g_m \beta \left[1 + \dfrac{R_{13}}{R_{11}} + \dfrac{R_{13}R_8}{R_9 R_{11}} + \dfrac{R_{13}+R_8}{R_g} + \dfrac{R_{13}}{R_{10}} + \dfrac{R_{13}}{R_{12}}\right]}{-g_m R_{13} \beta \left[\dfrac{R_8}{R_9} + 1\right] + \left[\beta \dfrac{R_{13}-R_8}{R_{12}} - 1 - \dfrac{R_{13}+R_8}{R_9}\right]} \tag{3-9}$$

Circuit 2 as tested [Fig. 3.4] was an active gyrator because g_1 did not equal g_2. This does not affect inductance simulation. The important property that the product of the gyrator conductances provides the impedance-conversion property (1-8) is still applicable.

C. RAO-NEWCOMB GYRATOR

The gyrator developed by T. N. Rao and R. W. Newcomb is synthesized from the VCCS method [30 and 31] . The circuit as modeled in Fig. 3.5 consists of two differential voltage-to-current converters connected in parallel. With voltages V_1 and V_2 of the differential amplifier shorted to ground, the resultant admittance matrix is

$$\begin{bmatrix} I_1 \\ I_2 \end{bmatrix} = \begin{bmatrix} 0 & \dfrac{1}{R_a} \\ \dfrac{-1}{R_b} & 0 \end{bmatrix} \begin{bmatrix} V_1 \\ V_2 \end{bmatrix} . \tag{3-10}$$

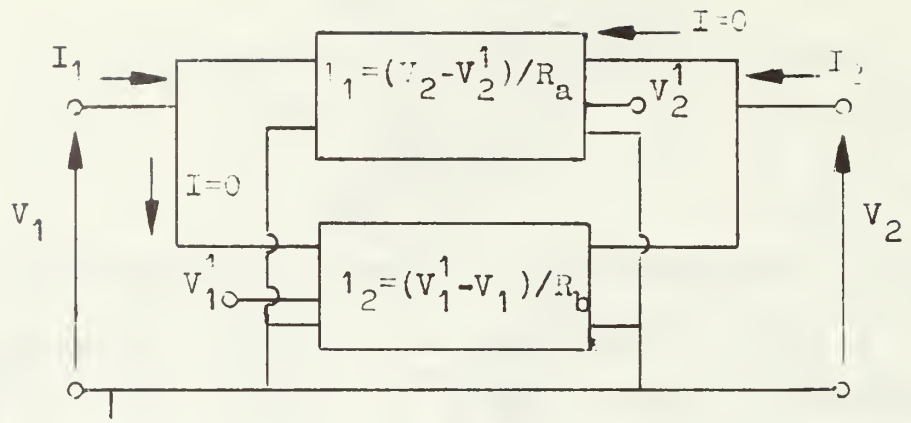

Fig. 3.5. Differential Voltage-to-Current Converter Gyrator

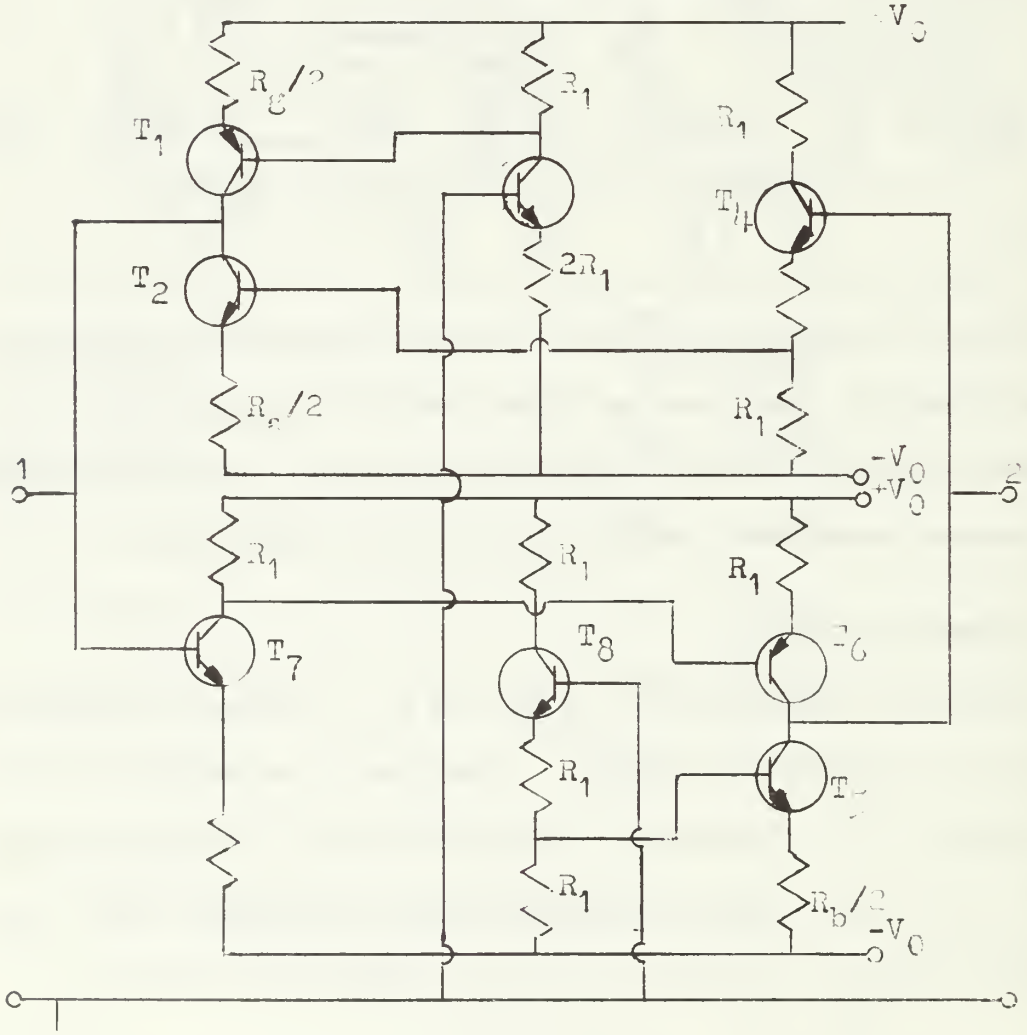

Fig. 3.6. Rao-Newcomb Gyrator

Figure 3.6 is the transistor realization of this circuit, with one voltage-to-current converter consisting of transistors T_1, T_2, T_3, and T_4, and the other of T_5, T_6, T_7 and T_8. The circuit operation depends upon the transistors having closely matched operating-point characteristics. When an input is not present, a zero dc level exists at the input and output. Figure 3.6 shows the biasing of transistor pairs T_1-T_2, and T_5-T_6 to be identical for zero inputs. When V_2 is nonzero, a current will flow in T_4. Neglecting the small voltage difference between the base and emitter of T_4, half of V_2 will appear across each R_1 resistor in the emitter circuit of T_4, since the two resistors comprise a voltage divider. The voltage divider places a voltage $V_2/2$ on the base of T_2. Neglecting the voltage difference between the base and emitter of the transistor T_2, the input current is closely approximated by the base voltage ($V_{2/2}$) divided by the resistance in the emitter circuit of T_2. The signal current, at the input and in transistor T_2 is V_2/R_a.

With V_1 applied at the input, a current is developed in T_7 which results in a negative voltage of $V_1/2$ applied to the base of T_6. The output current through T_6 can be closely approximated as the voltage at the base divided by the resistance, which gives a value of $I_2 = -V_1/R_b$.

The Rao-Newcomb gyrator was tested by R. Gary with V_o = 9V, R_1 = 680ohms, $R_a = R_b$ = 2400ohms, and input conductance of 1/(300K)mhos [31]. The circuit achieved a maximum Q factor of 60, but was limited by time-delay effect to peak resonant frequencies in the order of 10 KHz.

The Rao-Newcomb gyrator was modified by H. T. Chua and R. W. Newcomb for integrated circuit use [32]. The circuit [Fig. 3.7]

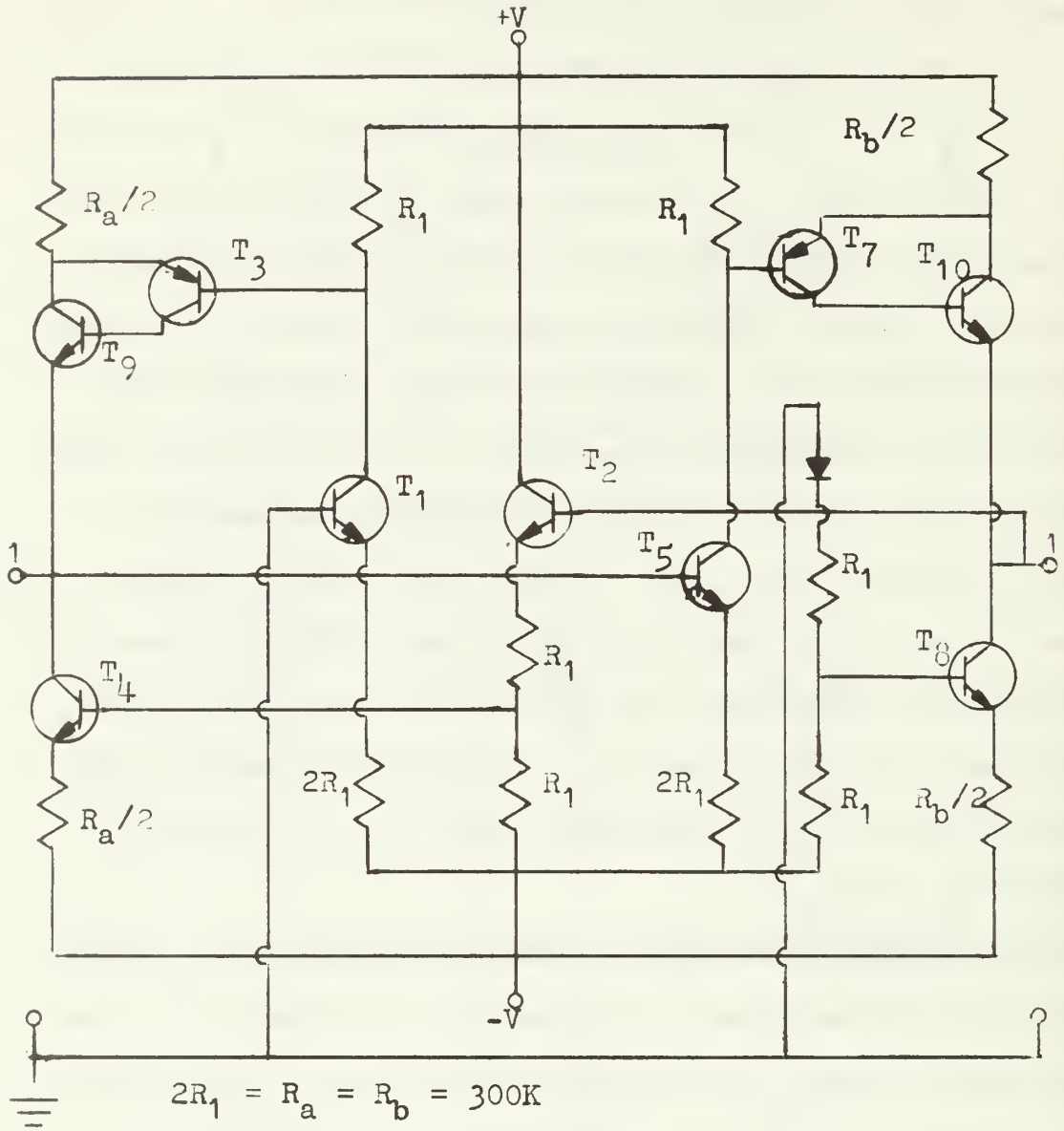

Fig. 3.7. Chua-Newcomb Gyrator

included compensation for variations of temperature and supply voltage. The circuit was stable at frequencies below 65 KHz, a significant improvement, but the Q factor decreased to a value of approximately 35.

D. YANAGISAWA GYRATORS

The original gyrator (Circuit 1) proposed by T. Yanazisawa in conjunction with K. Kawashima is based on the VCCS method [33] . The method of synthesis starts with separation of the gyrator chain matrix into the product of an ideal gyrator chain matrix and a power amplifier chain matrix

$$\begin{bmatrix} V_1 \\ I_1 \end{bmatrix} = \begin{bmatrix} 0 & (g_1 g_2)^{-\frac{1}{2}} \\ (g_1 g_2)^{\frac{1}{2}} & 0 \end{bmatrix} \begin{bmatrix} (g_1/g_2)^{\frac{1}{2}} & 0 \\ 0 & (g_1/g_2) \end{bmatrix}. \tag{3-11}$$

Converting (3-11) into an admittance matrix results in

$$\begin{bmatrix} I_1 \\ I_2 \end{bmatrix} = \begin{bmatrix} 0 & -G/A \\ AG & 0 \end{bmatrix} \begin{bmatrix} V_1 \\ V_2 \end{bmatrix}, \tag{3-12}$$

where $A = (g_2/g_1)^{\frac{1}{2}}$ and $G = (g_1 g_2)^{\frac{1}{2}}$.

An equivalent circuit [Fig. 3.8] , consisting of two VCCS and input and output conductances, can be described by an impedance matrix as

$$\begin{bmatrix} V_1 \\ V_2 \end{bmatrix} = \begin{bmatrix} 1/G_1 & -1/g_{m_2} \\ -1/g_{m_1} & 1/G_1 \end{bmatrix} \begin{bmatrix} I_1 \\ I_2 \end{bmatrix}. \tag{3-13}$$

Equation (3-14) can be converted to the admittance parameters

$$\begin{aligned} Y_{11} &= Y_{22} = -G_1 g_{m1} g_{m2}/D_1 \\ Y_{12} &= G_1^2 g_{m1}/D_1 \\ Y_{21} &= G_1^2 g_{m2}/D_1 \end{aligned} \tag{3-14}$$

where $D_1 = G_1^2 - g_{m1} g_{m2}$.

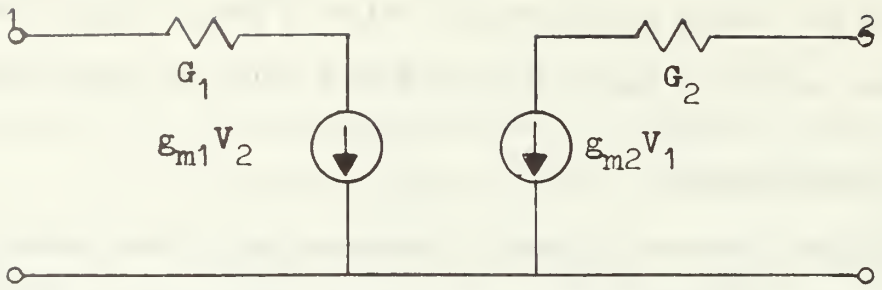

Fig. 3.8. Equivalent Amplifier

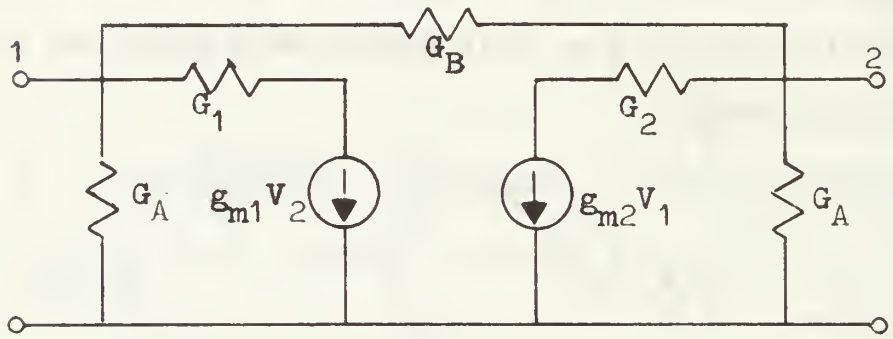

Fig. 3.9. Yanagisawa Equivalent Gyrator (Circuit 1)

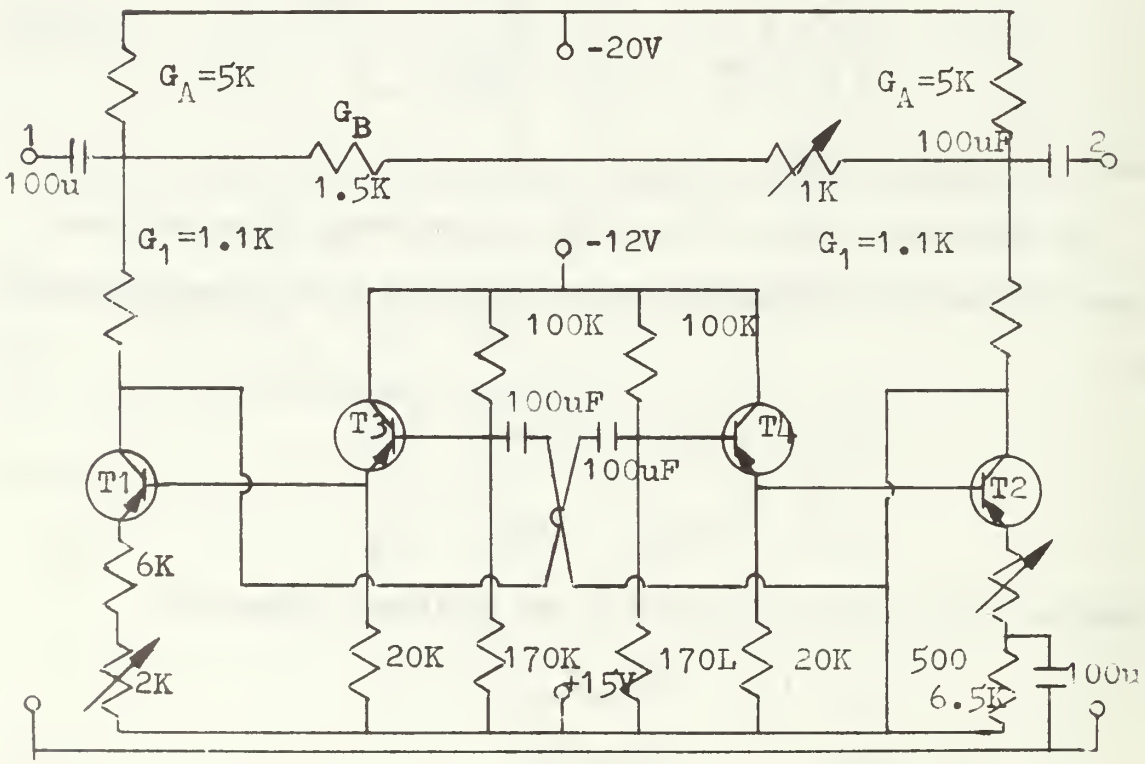

Fig. 3.10. Yanagisawa Gyrator (Circuit 1)

In order to achieve the desired gyrator admittance matrix (3-12) from (3-14), a proper positive conductance is added to the input and output ports to cancel the negative conductance of the equivalent amplifier circuit. In addition, since a sign change is needed between Y_{21} and Y_{12}, positive feedback is provided between ports 1 and 2. Figure 3.9 illustrates the equivalent gyrator circuit derived from the basic amplifier of Fig. 3.8. The admittance matrix for the gyrator equivalent circuit can be written as

$$\begin{bmatrix} I_1 \\ I_2 \end{bmatrix} = \begin{bmatrix} Y_{11}+G_A+G_B & Y_{12}-G_B \\ Y_{21}-G_B & Y_{22}+G_A+G_B \end{bmatrix} \begin{bmatrix} V_1 \\ V_2 \end{bmatrix} . \tag{3-15}$$

Equating (3-14) to (3-12), the relations that $Y_{11}+G_A+G_B = 0$, $Y_{12}-G_B<0$, and $Y_{21}-G_B>0$ are obtained. These constraints are satisfied if $G_1^2 > g_{m1}g_{m2}$, $g_{m2} > G_1$ and $g_{m2} > g_{m1}$. Additionally, (3-14) may be expressed as

$$\begin{aligned} Y_{11} = Y_{12} &= -(G_A+G_B) \\ Y_{12} &= G_B - G/A \\ Y_{21} &= G_B+AG . \end{aligned} \tag{3-16}$$

Assuming that G_B, G_A, A and G would be selected by the circuit designer, (3-16) provides the values of Y_{11}, Y_{22}, Y_{21} and Y_{12}. Equation (3-14) is used to solve for g_{m1}, g_{m2} and G_1 in terms of the equivalent amplifier parameters by

$$\begin{aligned} g_{m1} &= (Y_{12}Y_{21}-Y_{11}^2)/Y_{21} \\ g_{m2} &= (Y_{12}Y_{21}-Y_{11}^2)/Y21 \\ G_1 &= (Y_{12}Y_{21}-Y_{11}^2)/(-Y_{11}) . \end{aligned} \tag{3-17}$$

Since g_{m1} and g_{m2} are positive values, the relation that $Y_{12}Y_{21} > Y_{11}^2$ can be deduced from (3-17). Substitution of (3-16)into this constraint imposes another condition,

$$G_B G(A-\frac{1}{A}) > G_A(G_A+2G_B) + G^2 \quad . \tag{3-18}$$

Equation (3-18) implies A cannot equal 1. Because $A = (g_1/g_1)^{\frac{1}{2}}$, g_2 cannot equal g_1. Therefore, this gyrator must be realized as an active gyrator.

Figure 3.10 is the circuit experimentally tested by Yanagisawa and Kawashima with A = 4, G = 1 X 10^{-3}mhos G_A = 2 X 10^{-3}mhos, and G_B = 5 x 10^{-3}mhos.

This circuit has not been compensated for time delay of the VCCS, and satisfactory inductor simulation is limited to slightly above 1 KHz. Because the gyrators main diagonal admittance terms are achieved by cancellation of conductances, low Q factors can be expected for inductor simulation.

A second gyrator was proposed by T. Yanagisawa [34] in which the gyrator conductances Y_{21} and Y_{12} could be adjusted, and not affect the property that $Y_{11} = Y_{22} = 0$. As in circuit 1, the individual VCCS method with resistive feedback was the basis of the network synthesis.

Figure 3.11 is the gyrator equivalent circuit. It is noted that the current generator on the port 2 side of equivalent circuit is dependent upon the voltage at V_a, not V_1. The derived admittance matrix is

$$\begin{aligned} Y_{11} &= 1/R_5 + (1-g_{m1}R_3)/D_2 \\ Y_{12} &= g_{m2} - 1/D_2 \\ Y_{21} &= -(1 + g_{m1}R_2)/D_2 \\ Y_{22} &= 1/R_4 + (1-g_{m1}R_1)/D_2 \ , \end{aligned} \tag{3-19}$$

where $D_2 = R_2+R_3+R_1(1-g_{m1}R_3)$.

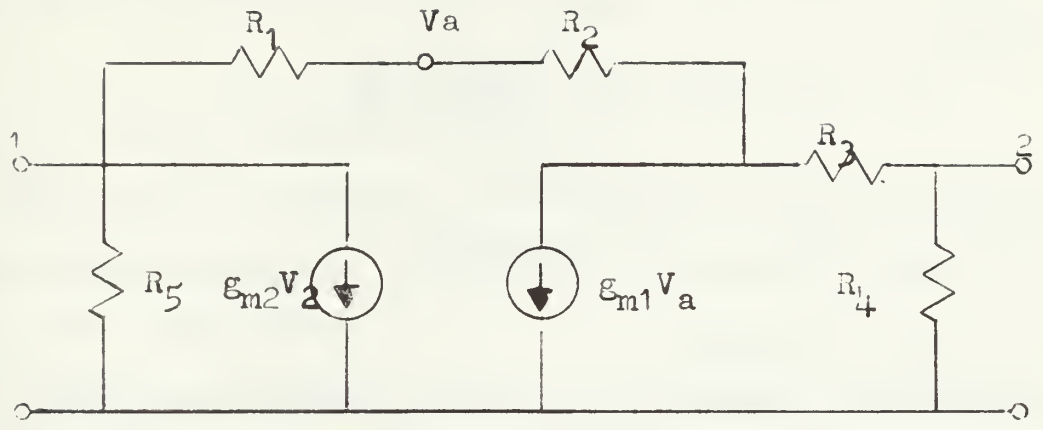

Fig. 3.11. Yanagisawa Equivalent Gyrator (Circuit 1)

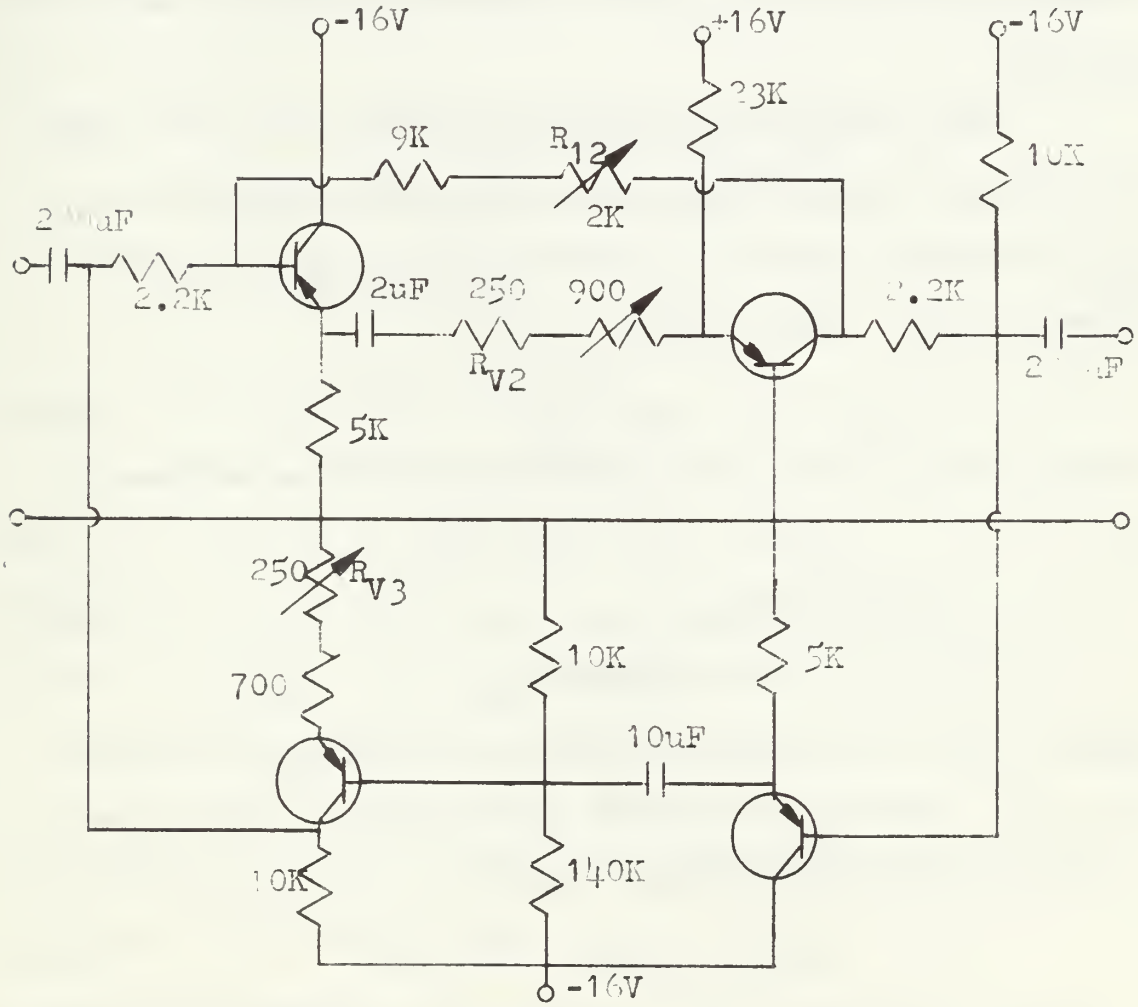

Fig. 3.12. Yanagisawa Gyrator (Circuit 2)

To satisfy the condition that $Y_{11} = Y_{22}$, R_4 must equal R_5 and R_3 must equal R_1. Applying these relations to (3-19) results in new admittance parameters

$$\begin{aligned} Y_{11} = Y_{22} &= 1/R_4 - (g_{m1}R_1-1)/D_3 \\ Y_{12} &= g_{m2} - 1/D_3 \\ Y_{21} &= -(1 + g_{m1}R_2)/D_3 , \end{aligned} \tag{3-20}$$

where $D_3 = R_2 + R_1(2-g_{m1}R_1)$.

From (3-20), it is evident that Y_{12} can be controlled by adjustment of g_{m2} alone.

Equating the Y_{11} and Y_{22} terms of (3-20) to zero results in the expression

$$R_4 = [R_2 + R_1(2-g_{m1}R_1)]/(g_{m1}R_1-1). \tag{3-21}$$

Before design values are chosen for R_1 and R_2, the expression for Y_{21} must be considered, since it is desired to vary Y_{21} without varying either Y_{11} or Y_{22}. The expression for Y_{21} is

$$Y_{21} = -(1 + g_{m1}R_2)/D_2 . \tag{3-22}$$

Solving (3-21) and (3-22) simultaneously results in two solutions for R_1:

$$R_1 = 1/g_{m1} , \tag{3-23}$$

and

$$R_1 = (1-R_4Y_{21}-R_4g_{m1})/g_{m1} . \tag{3-24}$$

Equation (3-23) is an impossible solution as can be seen by insertion into (3-21). Equation (3-24) is the proper solution. Substitution of (3-24) into (3-21) gives the value of R_2 as

$$R_2 = [(R_4^2 Y_{12}^2 + Y_{12}g_{m1}) - 1] /g_{m1}. \tag{3-25}$$

The design values g_{m1}, g_{m2}, R_1 and R_2 can be determined from (3-20), (3-24) and (3-25), given the resistance R_1 and gyration conductances Y_{12} and Y_{21}.

An experimental circuit [Fig. 3.12] was tested by Yanagisawa with $g_{m1} = .9 \times 10^{-3}$mhos, $g_{m2} = 1.1 \times 10^{-3}$mhos, $R_1 = 2.22$Kohms and $R_2 = R_4 =$ 10Kohms. Of the variable resistors shown in the circuit, R_{v1} is used to obtain the correct value of Y_{21}, R_{v2} is adjusted to minimize Y_{11} and Y_{22}, and R_{v3} to obtain the desired Y_{12}.

This circuit is vulnerable to time-delay effects, and is limited to low-frequency operation. It does have the advantage of adjustability of gyration conductances.

A third gyrator circuit (Circuit 3) was designed using the basic VCCS method with resistive feedback [35] . The equivalent gyrator [Fig. 3.13] is similar to Circuit 2 with the exception of the resistance R_4 at port two.

The short-circuit admittance parameters for Circuit 3 are

$$\begin{aligned} Y_{11} &= G_4 + G_1 - [(G_2 + G_3 + G_4)G_1^2]/D_4 \\ Y_{12} &= g_{m2} - G_1G_2G_3/D_4 \\ Y_{21} &= -(g_{m1} + G_2)G_1G_3/D_4 \\ Y_{22} &= G_3 - (G_1 + G_2)G_3^2/D_4 , \end{aligned} \tag{3-26}$$

where $D_4 = (G_2 + G_3 + G_4)(G_1 + G_2) - (g_{m1} + G_2)G_2$.

By equating (3-26) with the ideal gyrator admittance matrix

$$\begin{bmatrix} I_1 \\ I_2 \end{bmatrix} = \begin{bmatrix} 0 & g_1 \\ -g_2 & 0 \end{bmatrix} \begin{bmatrix} V_1 \\ V_2 \end{bmatrix} , \tag{3-27}$$

the quantities g_{m1}, g_{m2}, G_1 and G_2, for known values of g_1, g_2, and G_2 and G_4, can be computed from

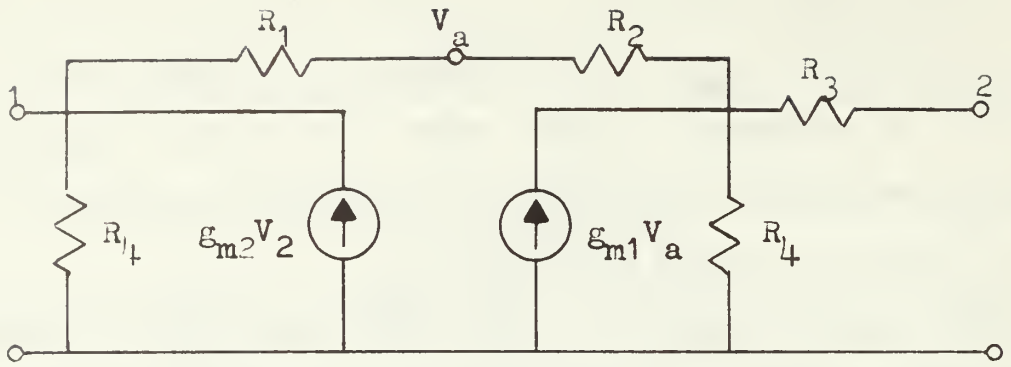

Fig. 3.13. Yanagisawa Equivalent Gyrator (Circuit 3)

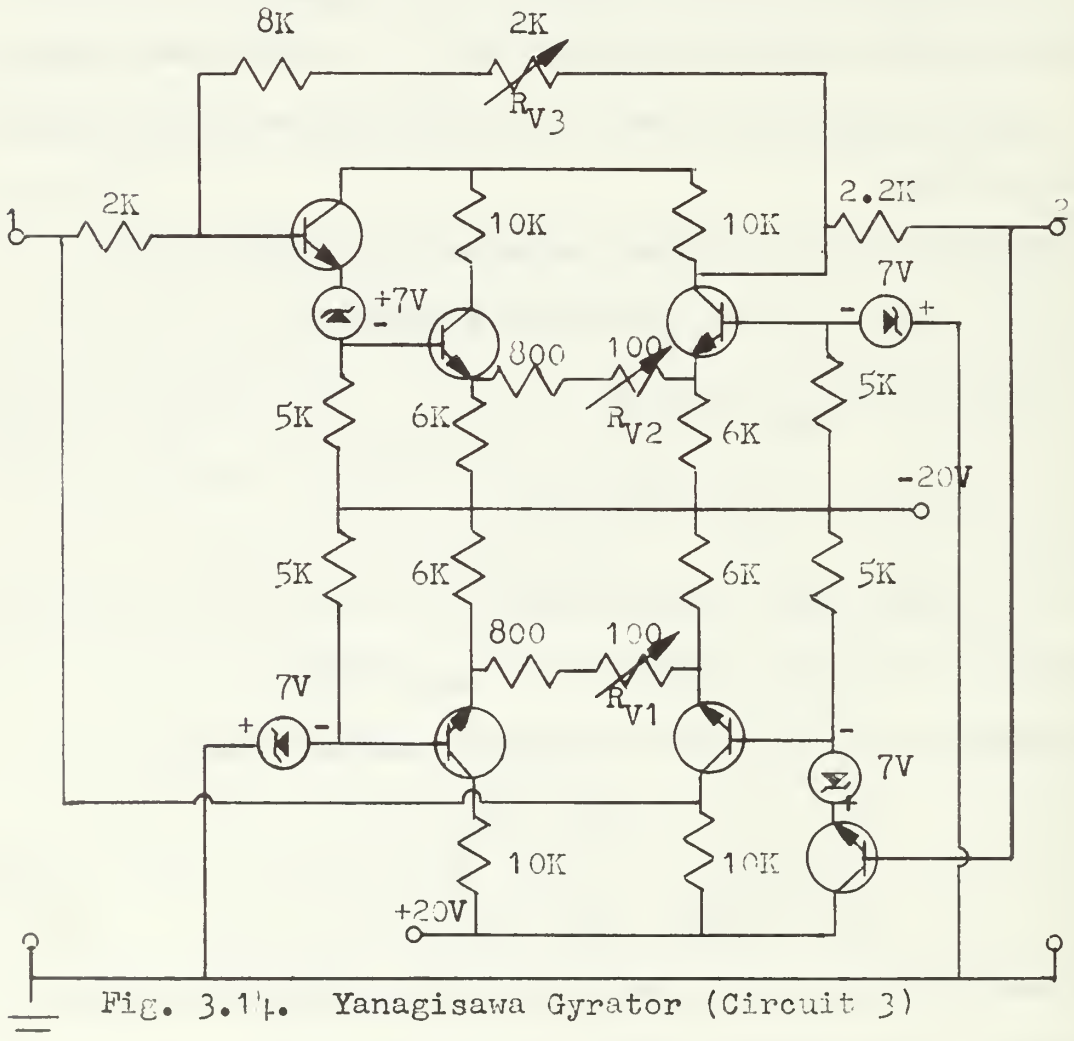

Fig. 3.14. Yanagisawa Gyrator (Circuit 3)

$$
\begin{aligned}
g_{m1} &= G_4 + g_2 \\
g_{m2} &= g_1 + G_1 G_2 G_3 / D_4 \qquad (3\text{-}28) \\
G_1 &= G_2 g_2 / (G_4 + G_2) \\
G_3 &= G_1 g_2 / G_4 + g_2 \quad .
\end{aligned}
$$

Figure 3.14 is the network that was tested with $g_1 = 1 \times 10^{-3}$mhos, $g_2 = 1 \times 10^{-3}$mhos, $R_2 = R_4 = 10$Kohms. From (3-28), $R_1 = 2$Kohms, $R_3 = 2.2$Kohms, $g_{m1} = 1.1 \times 10^{-3}$mhos and $g_{m2} = 1.083 \times 10^{-3}$mhos.

R_{V1} and R_{V2} of Figure 3.14 are used to adjust the values of g_{m1} and g_{m2} respectively. R_{V3} is used to obtain as low Y_{11} and Y_{22} values as possible.

As with Circuits 1 and 2, Circuit 3 is limited to low-frequency operation. It is superior to Circuit 2 because of the automatic balancing of the input and output dc operating voltages of both amplifiers.

IV. OPERATIONAL AMPLIFIER GYRATORS

A. INTRODUCTION

The operational amplifier has been used for network realization of gyrator circuits since 1964 [36 and 37] . The operational amplifier is commercially available and economic. It is usually fabricated as an integrated circuit, and has high open-loop gain, low dc drift, high output impedance, low output impedance and excellent bandwidth.

The ideal operational amplifier can be represented in general form using the concepts of the nullator and norator [38, 39, and 40] . The nullator [Fig. 4.1] is a two-terminal device which obeys the relationship, $V = I = 0$. The norator [Fig. 4.2] is a two-terminal device whose current and voltage can be any value, and are independent of each other. The norator relationships can be expressed as $V_1 = K_1$, $V_2 = K_2$. A nullor [Fig. 4.3] is a two-port device consisting of a nullator at the input port and a norator at the output port. The nullor is a generalization of the ideal operational amplifier. It can be used as an aid in obtaining dual networks from known circuits.

B. HUELSMAN-MORSE GYRATOR

L. P. Huelsman and H. S. Morse developed an operational-amplifier gyrator in 1964 [36 and 37] . Their method of synthesis was based upon the VCCS method.

The voltage-controlled current sources [Fig. 4.4] were constructed from single-input operational amplifier with the resultant admittance matrix

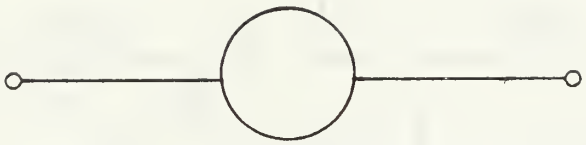

$V = I = 0$

Fig. 4.1. Nullator Model

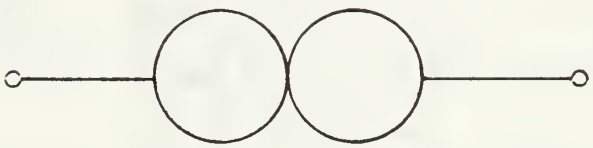

$V = K_1 \quad I = K_2$

Fig. 4.2. Norator Model

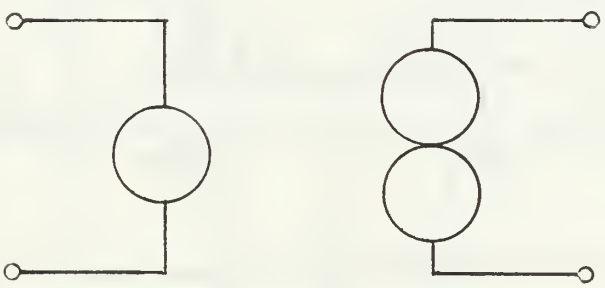

Fig. 4.3. Nullor Model

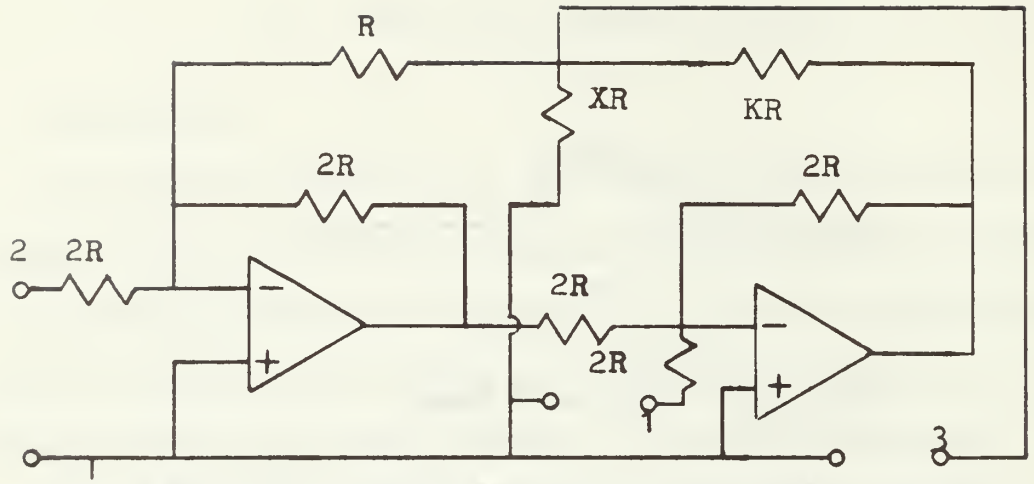

Fig. 4.4 Voltage-Controlled Current Source

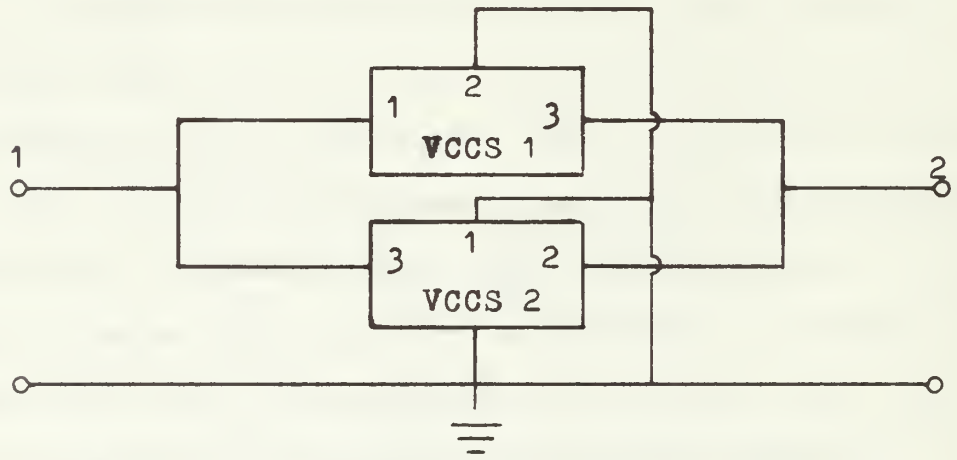

Fig. 4.5. Huelsman-Morse VCCS Gyrator Model

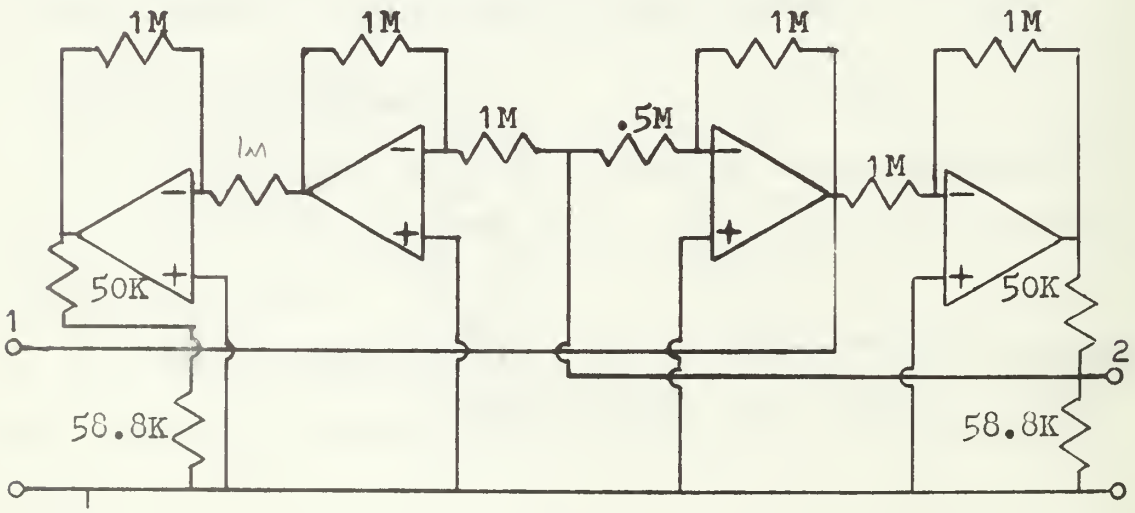

Fig. 4.6. Huelsman-Morse Gyrator

$$\begin{bmatrix} I_1 \\ I_2 \\ I_3 \end{bmatrix} = \begin{bmatrix} \frac{1}{2R} & 0 & 0 \\ 0 & \frac{1}{2R} & 0 \\ \frac{1}{KR} & \frac{-1}{KR} & G \end{bmatrix} \begin{bmatrix} V_1 \\ V_2 \\ V_3 \end{bmatrix}, \tag{4-1}$$

where $G = 1/R + 1/KR - 1/KR$.

Shorting port 2 results in the two-port admittance matrix

$$\begin{bmatrix} I_1 \\ I_3 \end{bmatrix} = \begin{bmatrix} \frac{1}{2R} & 0 \\ \frac{1}{KR} & G \end{bmatrix} \begin{bmatrix} V_1 \\ V_3 \end{bmatrix}. \tag{4-2}$$

Shorting port 1 results in the admittance matrix

$$\begin{bmatrix} I_2 \\ I_3 \end{bmatrix} = \begin{bmatrix} G & \frac{-1}{KR} \\ 0 & \frac{1}{2R} \end{bmatrix} \begin{bmatrix} V_2 \\ V_3 \end{bmatrix} \tag{4-3}$$

By connecting the two two-ports in parallel [Fig. 4.5] , the admittance matrix of the combination becomes

$$\begin{bmatrix} I_1 \\ I_2 \end{bmatrix} = \begin{bmatrix} (G + \frac{1}{2R}) & \frac{-1}{KR} \\ \frac{1}{KR} & (G + \frac{1}{2R}) \end{bmatrix} \begin{bmatrix} V_1 \\ V_2 \end{bmatrix}. \tag{4-4}$$

The ideal gyrator is now realized by equating the main diagonal terms to zero.

$$G + 1/2R = (3/2\ KX + K\text{-}X)/KXR = 0, \tag{4-5}$$

This constraint is satisfied if

$$K = X/(3/2X + 1) . \tag{4-6}$$

A typical Huelsman-Morse circuit is drawn in Fig. 4.6 with $K = 0.1$ and $X = 0.11765$. No experimental results were published with

the circuit. Since perfectly matched resistors are required to satisfy (4-6), this circuit should have a low Q factor because of the critical necessity of reducing the main diagonal terms of (4-4) as discussed in Section I.B..

C. HAWLEY GYRATOR

A. Hawley [41] used the VCCS method to synthesize a gyrator with an inverting and noninverting VCCS.

A noninverting VCCS [Fig. 4.7] realized with an operational amplifier has the admittance parameters

$$\begin{bmatrix} I_1 \\ I_2 \end{bmatrix} = \begin{bmatrix} 1/\beta R & -1/\beta R \\ -1/R & 0 \end{bmatrix} \begin{bmatrix} V_1 \\ V_2 \end{bmatrix}, \tag{4-7}$$

where β is the current gain of the transistor emitter follower. The inverting VCCS [Fig. 4.8] has the admittance parameters

$$\begin{bmatrix} I_1 \\ I_2 \end{bmatrix} = \begin{bmatrix} 0 & 1/R \\ -1/\beta R & 1/\beta R \end{bmatrix} \begin{bmatrix} V_1 \\ V_2 \end{bmatrix}. \tag{4-8}$$

The emitter followers are required to prevent loading when the circuits are connected in parallel.

The gyrator [Fig. 4.9] is realized by the parallel connection of the inverting and noninverting VCCS. Since the circuits are in parallel, (4-7) and (4-8) are added to give an overall matrix of

$$\begin{aligned} Y_{11} &= 1/\beta R \\ Y_{12} &= 1/R - 1/\beta R \\ Y_{13} &= -1/R - 1/\beta R \\ Y_{14} &= 1/\beta R \ . \end{aligned} \tag{4-9}$$

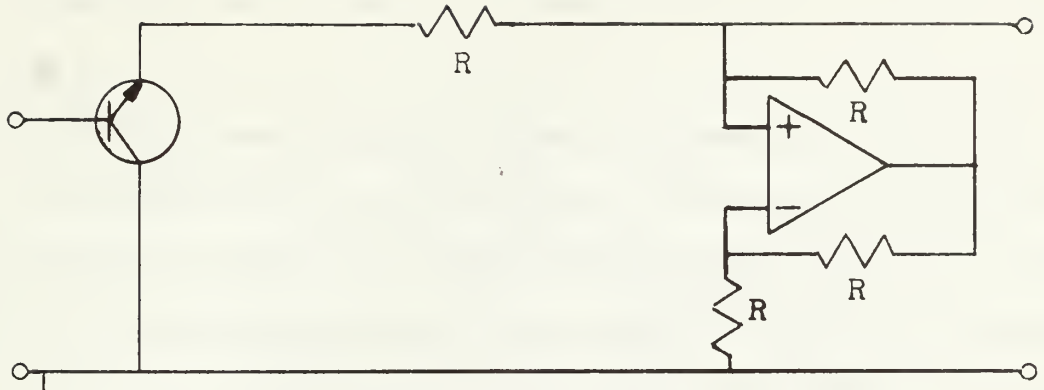

Fig. 4.7. Noninverting VCCS

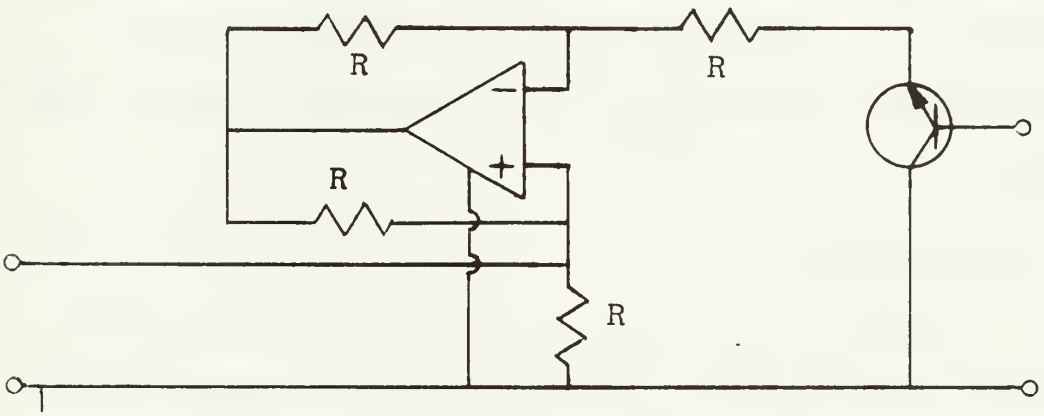

Fig. 4.8. Inverting VCCS

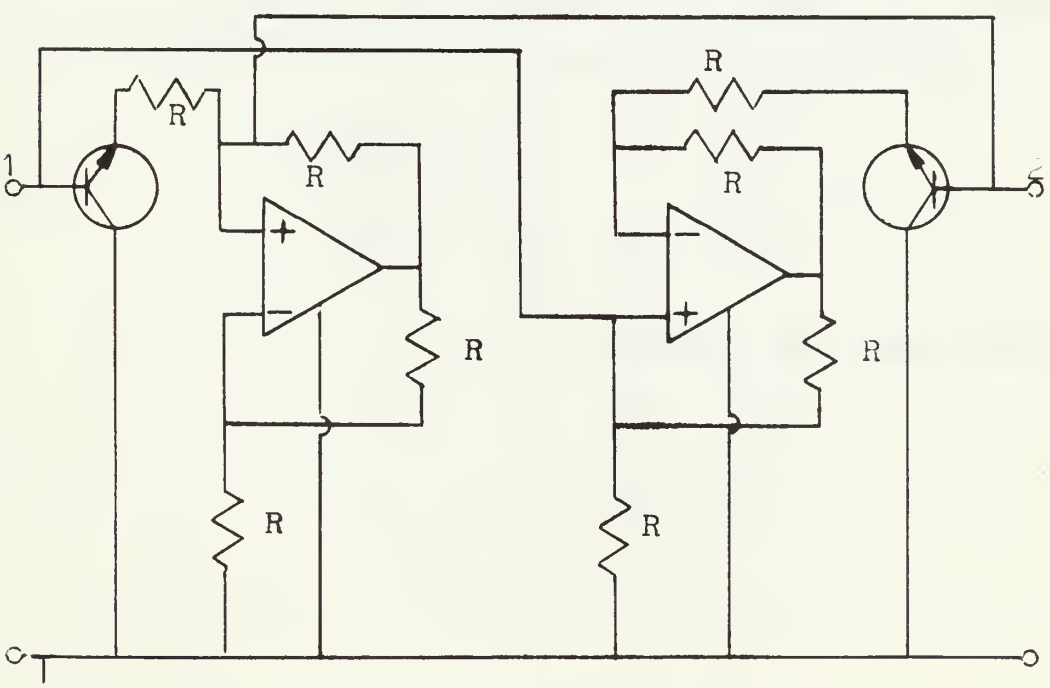

Fig. 4.9. Hawley Gyrator

As β increases, the circuit parameters approach those of an ideal gyrator (1-3).

Resistors of 31.6Kohms were used in the experimental circuit and a peak resonance frequency was obtained at 21KHz with an approximate Q factor of 38. The operational amplifiers of each VCCS were frequency compensated to insure that the amplifier would remain stable with the variation of feedback and load.

The circuit has the disadvantage of having all the terms of (4-9) dependent on β . This will result in a temperature-dependent Q factor, which is undesirable if the gyrator is to be used in a filter network.

B. BRUGLER GYRATOR

J. S. Brugler [42] constructed a gyrator circuit consisting of a negative-impedance inverter (NIV), cascaded with a current negative-impedance converter (INIC). Figure 4.10 is an elementary circuit diagram for the purpose of recognition of the NIV and INIC.

The chain matrix for the NIV is

$$\begin{bmatrix} V_2 \\ I_2 \end{bmatrix} = \begin{bmatrix} 0 & -R \\ \frac{1}{R} & 0 \end{bmatrix} \begin{bmatrix} V_1 \\ I_1 \end{bmatrix} \tag{4-10}$$

The chain matrix for the INIC is

$$\begin{bmatrix} V_2 \\ I_2 \end{bmatrix} = \begin{bmatrix} 1 & 0 \\ 0 & -1 \end{bmatrix} \begin{bmatrix} V_1 \\ I_1 \end{bmatrix} . \tag{4-11}$$

The resultant matrix, the matrix product of (4-10) and (4-11), is

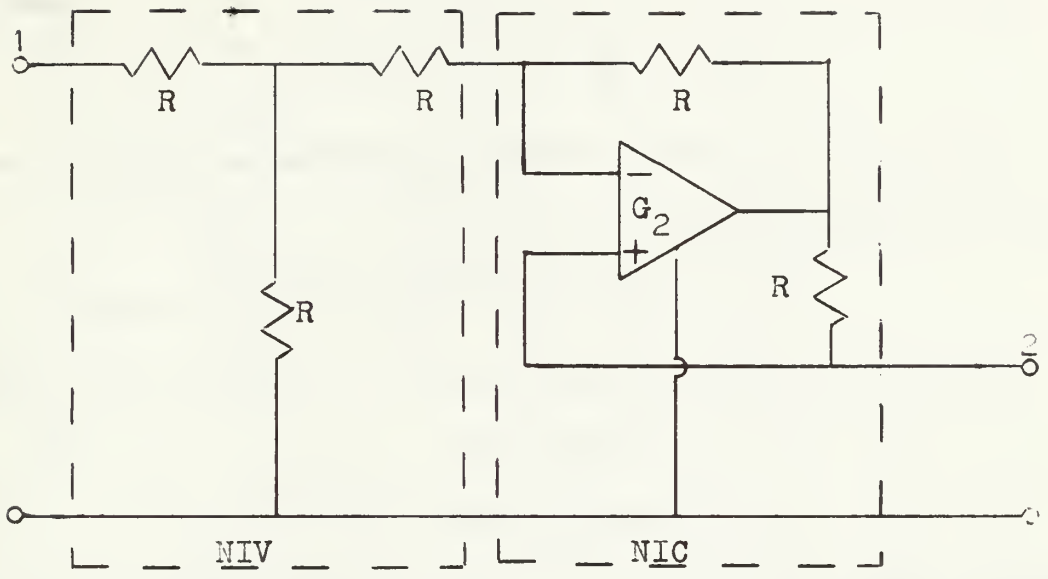

Fig. 4.10. Elementary Brugler Gyrator

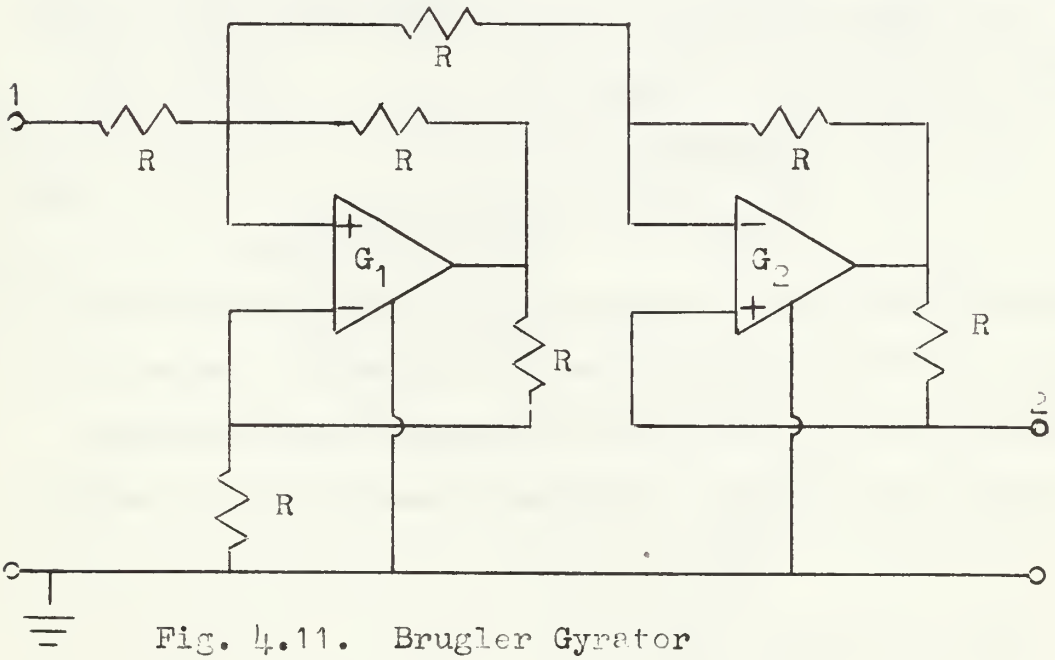

Fig. 4.11. Brugler Gyrator

$$\begin{bmatrix} V_2 \\ I_2 \end{bmatrix} = \begin{bmatrix} 0 & -R \\ \frac{-1}{R} & 0 \end{bmatrix} \begin{bmatrix} V_1 \\ I_1 \end{bmatrix} . \qquad (4\text{-}12)$$

Figure 4.11 is the circuit diagram for the Brugler gyrator. The derived impedance parameters are [43]

$$\begin{aligned} Z_{11} &= R(G_1-4G_2+10)/D \\ Z_{12} &= RG_2(G_1+2)/D \\ Z_{21} &= -RG_2(G_1+2)/D \\ Z_{22} &= R(4G_2-G_1+6)/D \ , \end{aligned} \qquad (4\text{-}13)$$

where $D = G_1G_2-G_1-2G_2+6$.

Using the assumption that the gains of the operational amplifier are infinite, equation (4-13) reduces to ideal gyrator impedance parameters (1-2).

The Llewellyn stability criterion [44] for a two-port network with passive termination is given by

$$\begin{aligned} &R_eZ_{11}, R_eZ_{22}Z \geq 0 \\ &2R_eZ_{11}R_eZ_{22} \geq |Z_{12}Z_{21}| + R_eZ_{12}Z_{21}. \end{aligned} \qquad (4\text{-}14)$$

The relations of (4-14), applied to (4-13), show that this gyrator can achieve low-frequency unstable modes of operation. Because a NIV is used in the circuit, low Q-factor values and critical stability tolerance can be expected. Experimental results were not published for this circuit.

E. PRESCOTT GYRATOR

A. J. Prescott [45] developed a gyrator [Fig. 4.12] for the purpose of simulating floating inductances. The actual circuit

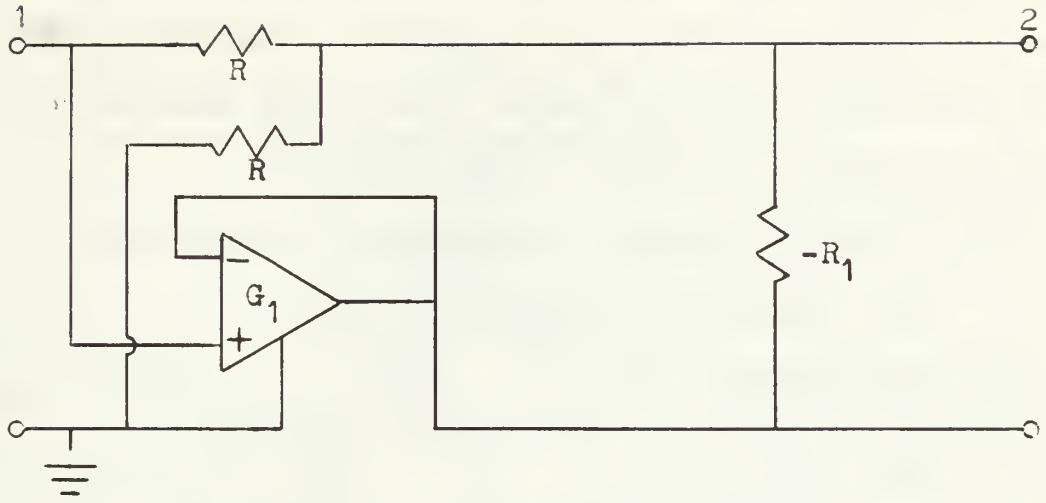

Fig. 4.12. Elementary Prescott Gyrator

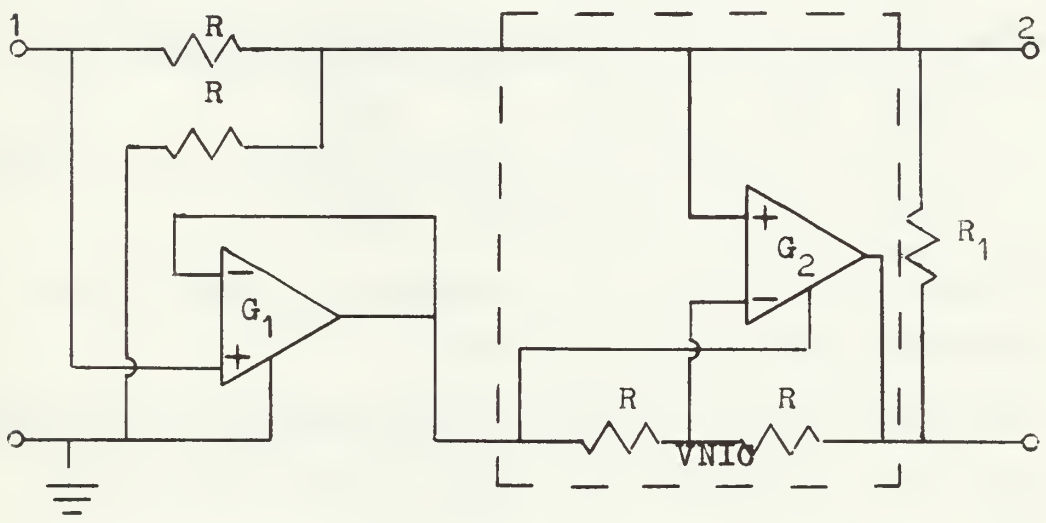

Fig. 4.13. Prescott Gyrator

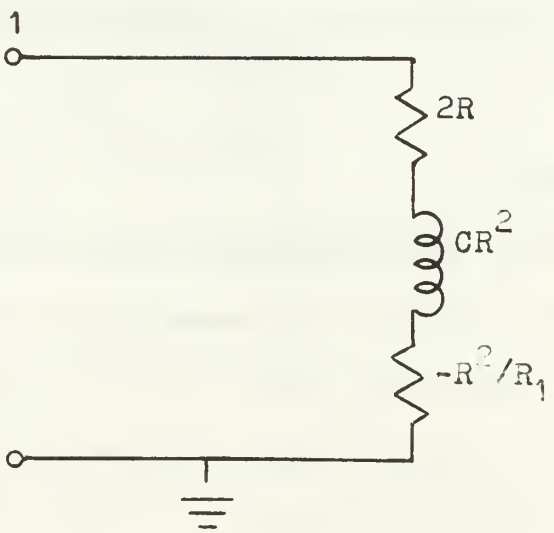

Fig. 4.14. Prescott Floating Inductor

[Fig. 4.13] illustrates the VNIC which is used to convert resistor R_1 into a negative resistance. If the gyrator is capacitively loaded, then an ungrounded inductor is realized [Fig. 4.14] which has both positive and negative resistances in series with it.

The short-circuit admittance parameters for this circuit are

$$\begin{aligned} Y_{11} &= [G_2(G_2-G_1)+G_1-2] \;/\; R(G_1+1)(G_2-2) \\ Y_{12} &= -1/R \\ Y_{21} &= 1/R \\ Y_{22} &= -G_2/\; R_1(G_2+2) + 1/R + 1/R \;. \end{aligned} \tag{4-15}$$

By assuming infinite amplifier gains, equation (4-15) reduces to

$$\begin{bmatrix} I_1 \\ I_2 \end{bmatrix} = \begin{bmatrix} 0 & -1/R \\ 1/R & (2R_1-R)/R_1R \end{bmatrix} \begin{bmatrix} V_1 \\ V_2 \end{bmatrix} . \tag{4-16}$$

An ideal gyrator can be realized by equating the Y_{22} term to zero. This condition is satisfied if $R_1 = R/2$.

This circuit uses the principle of exact cancellation of resistances to obtain a zero main diagonal term. Thus, a low Q factor can be expected. The Prescott gyrator is also subject to low-frequency unstable modes as determined from the Llewellyn stability criterion (4-14).

F. RIORDAN GYRATORS

R. H. S. Riordan [46] developed a gyrator which has a Q factor that appears to be limited by the losses in the capacitors used. The circuit was not synthesized by any of the basic methods, but instead employs feedback between two differential amplifiers. The circuit can be used with the load across amplifier 2 [Fig. 4.15] (Circuit 1), or across amplifier 1 [Fig. 4.16] (Circuit 2).

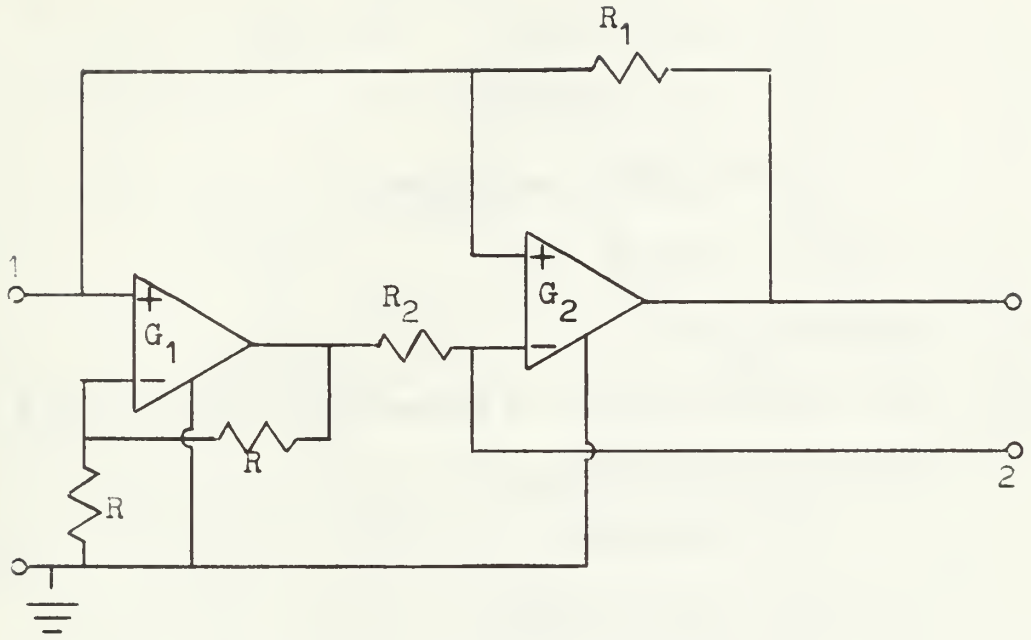

Fig. 4.15. Riordan Gyrator (Circuit 1)

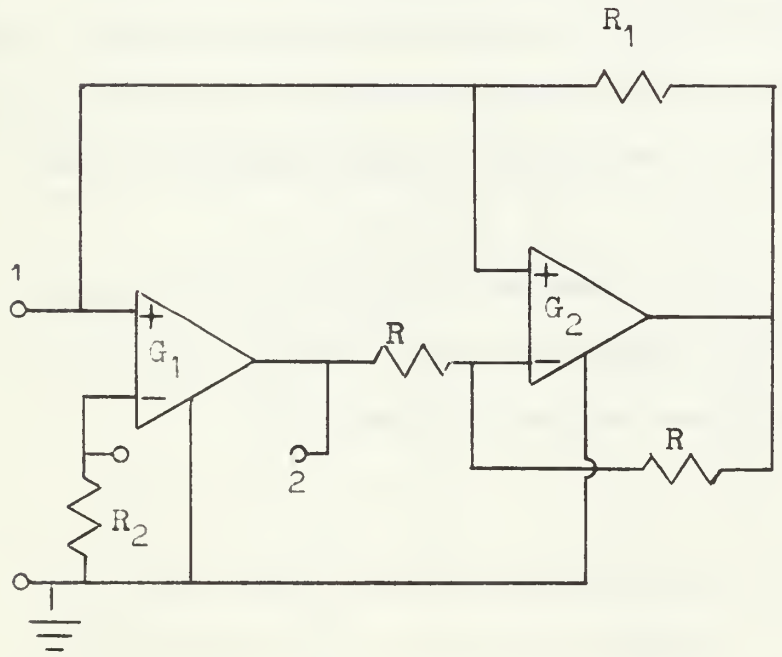

Fig. 4.16. Riordan Gyrator (Circuit 2)

The open-circuit impedance matrix for Riordan's Circuit 1 is [47]

$$\begin{aligned} Z_{11} &= R_1(G_1 + 2)/D_1 \\ Z_{22} &= -R_2G_2(G_1+2)/D_1 \\ Z_{21} &= R_1\left[G_1G_2+2(G_1-G_2)\right]/D_1 \\ Z_{22} &= R_2(G_1+2)\ /D_1\ , \end{aligned} \tag{4-17}$$

where $D_1 = G_1G_2+G_1-2G_1-2G_2+2$.

The open-circuit impedance matrix for Riordan's Circuit 2 is [47]

$$\begin{aligned} Z_{11} &= R_1(G_2+2)/D_2 \\ Z_{12} &= -R_2G_1G_2/D_2 \\ Z_{21} &= R_1G_1(G_2+2)/D_2 \\ Z_{22} &= R_2(2G_1-G_2+2)/D_2\ , \end{aligned} \tag{4-18}$$

where $D_2 = G_1G_2-G_2+2$.

Inspection of equations (4-17) and (4-18) reveals that both equations reduce to the ideal gyrator impedance matrix assuming infinite amplifier gains. The impedance parameters indicate that both circuits are subject to possible low-frequency unstable modes as per the criteria of (4-14).

The experimental results, conducted with various load capacitors and gyration resistances, indicated a peak Q factor of 2000 at 8 Hz. Q factors as high as 250 were achieved at 55 KHz.

G. DEBOO GYRATOR

G. J. Deboo's [48] three-terminal gyrator [Fig. 4.17] was constructed to realize ungrounded inductors. For analysis purposes, port two is grounded to realize a two-port gyrator. The resultant

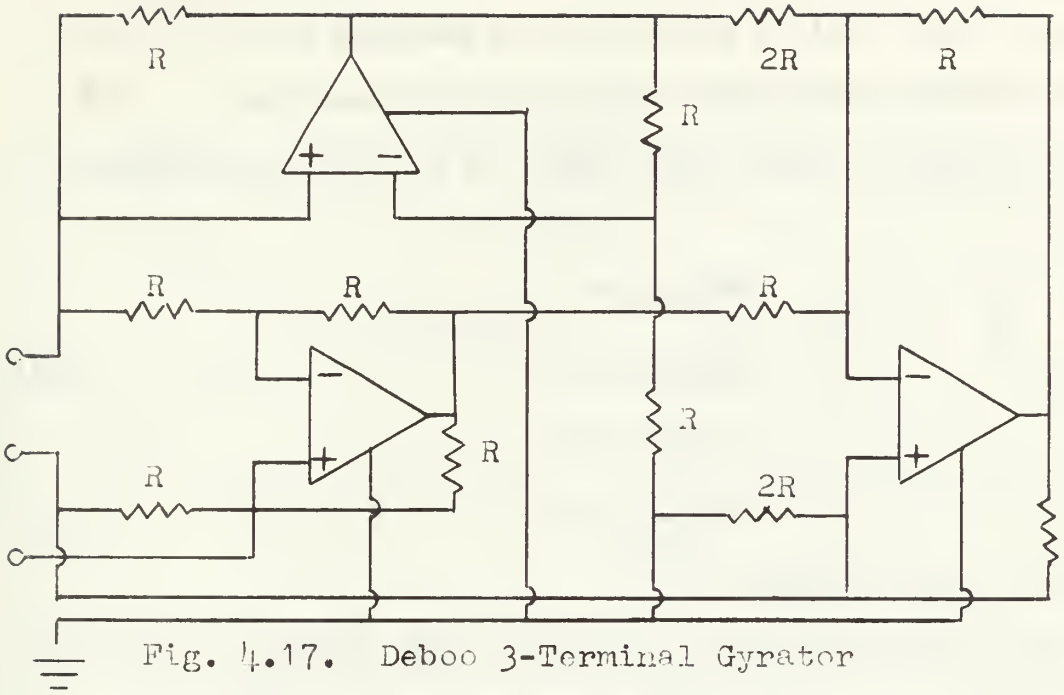

Fig. 4.17. Deboo 3-Terminal Gyrator

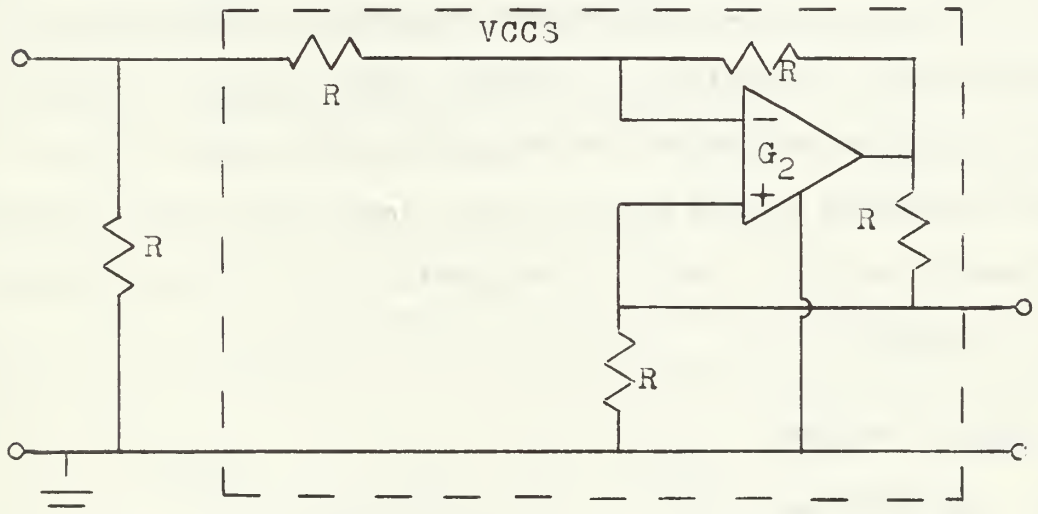

Fig. 4.18 Elementor Deboo Gyrator

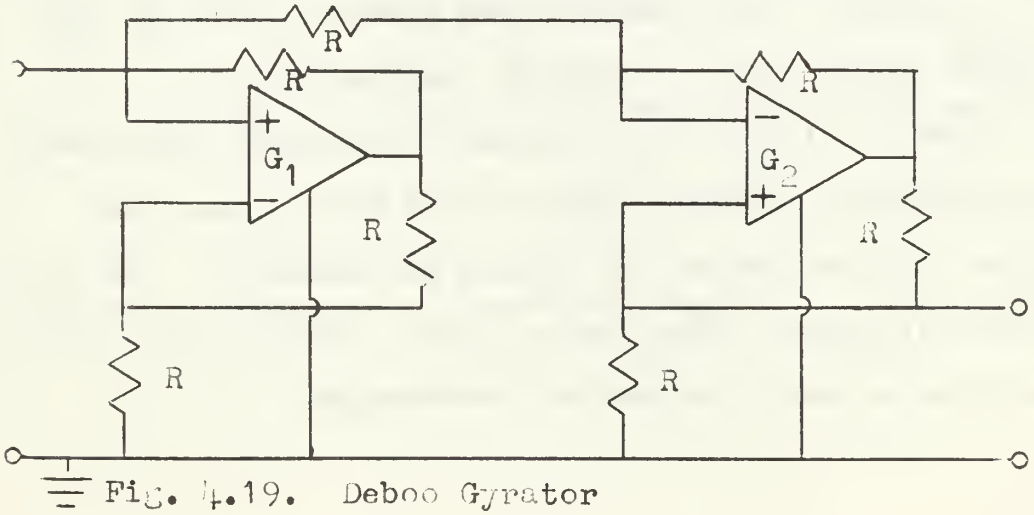

Fig. 4.19. Deboo Gyrator

circuit [Fig. 4.18] is realized with a Sheingold VCCS [42] with shunt negative conductance to reduce the input impedance.

The complete circuit [Fig. 4.19] has the impedance parameters [43]

$$\begin{aligned} Z_{11} &= 4R(G_1+2)/D \\ Z_{12} &= G_2R(G_1+2)/D \\ Z_{21} &= -G_2R(G_1+2)/D \\ Z_{22} &= R(4G_2-G_1+6)/D \quad , \end{aligned} \tag{4-19}$$

where $D = G_1G_2-2G_1+2G_2+12$.

Using the assumption that the gains of the operational amplifiers are infinite, the impedance parameters approach the ideal gyrator impedance matrix. Applying the Llewellyn criteria (4-14) to (4-19), shows the gyrator can achieve low-frequency unstable modes. Since a negative impedance is used in the circuit, low Q factor can be expected. Experimental data for a two-port configuration has not been published for this gyrator.

H. ANTONIOU GYRATORS

1. NIC-NIV Types

A. Antoniou [49] realized three gyrator circuits by using the cascade NIC-NIV method of synthesis (Section I.C.3).

Circuit 1 [Fig. 4.20] consists of the cascade connection of a Larky-type INIC [50] with a NIV realized from an operational amplifier. The INIC and NIV are outlined for recognition. The gyrator was similar in concept to the Brugler gyrator (Section IV.D), except the positions of the NIV and INIC are interchanged.

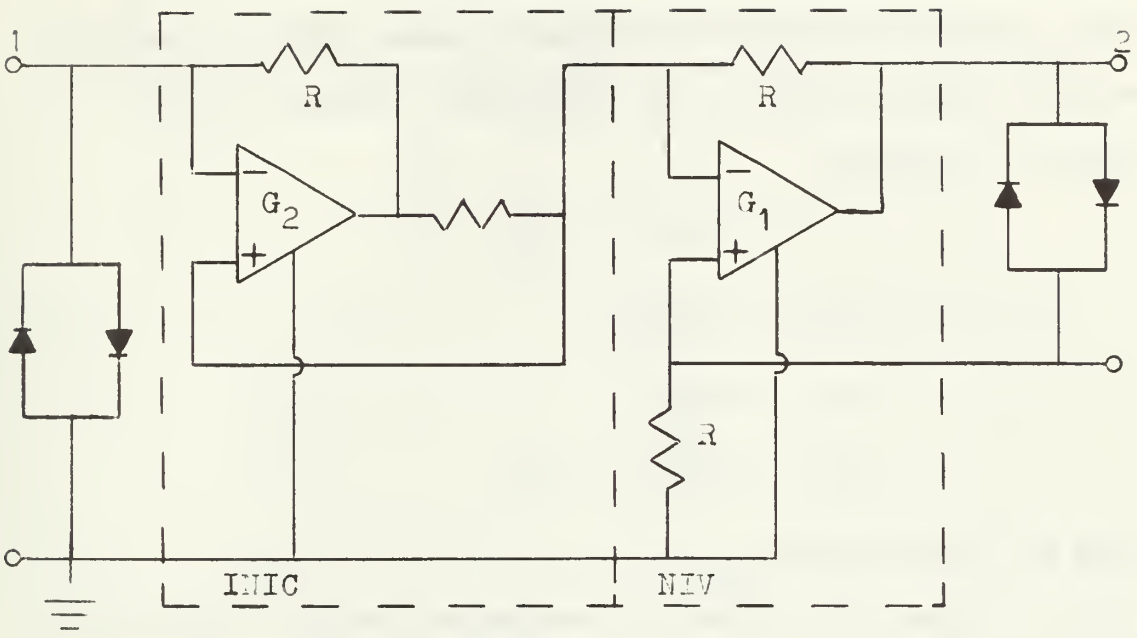

Fig. 4.20. Antoniou Gyrator (Circuit 1)

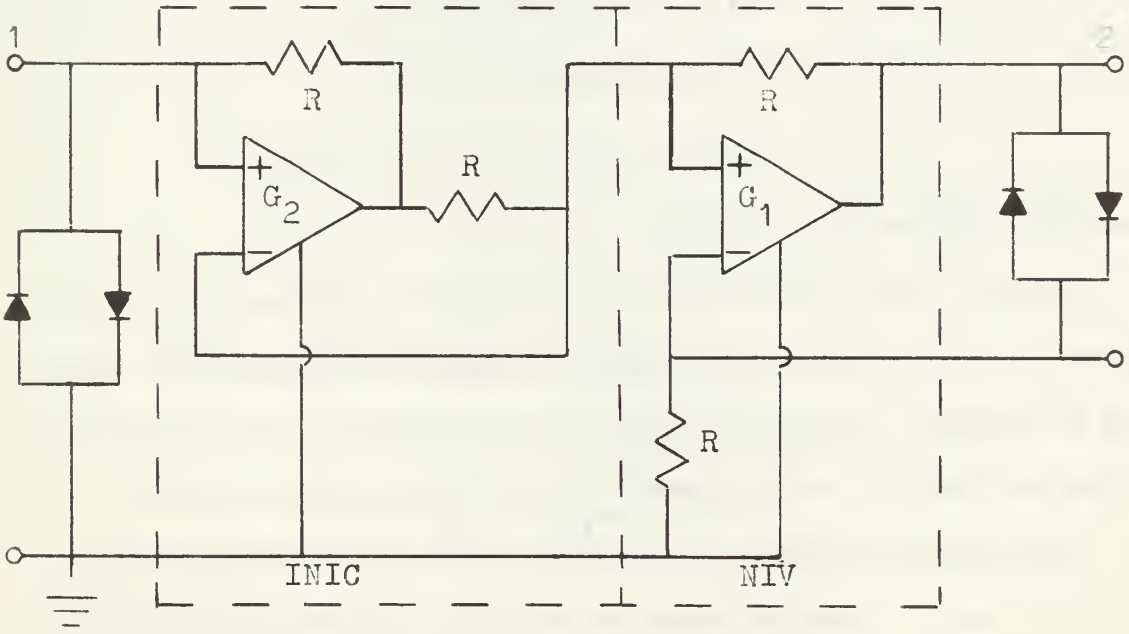

Fig. 4.21. Antoniou Gyrator (Circuit 2)

Since the operational amplifiers of the NIV and INIC can be connected either inverting or non-inverting, four circuit combinations exist. Antoniou's analysis shows that two combinations are unstable. Only the stable circuits will be considered. Circuit 1 has the admittance parameters

$$\begin{aligned} Z_{11} &= R(G_1-G_2+2)/D_1 \\ Z_{12} &= -RG_1G_2/D_1 \\ Z_{21} &= RG_1G_2/D_1 \\ Z_{22} &= R(G_2-G_1+2)/D_1 \quad , \end{aligned} \tag{4-20}$$

where $D_1 = G_1G_2+G_1+G_2+2$.

Circuit 2 [Fig. 4.21] , which is similar to Circuit 1 except for the interchange of input leads to the differential operational amplifiers, has the admittance parameters

$$\begin{aligned} Z_{11} &= R(G_2-G_1+2)(G_2G_1+G_1+G_2+2)/D_2 \\ Z_{12} &= -R(G_1G_2)(G_1G_2+G_1+G_2+2)/D_2 \\ Z_{21} &= R(G_1G_2)(G_1G_2+G_1+G_2+2)/D_2 \\ Z_{22} &= R(G_2-G_1+2)(G_1G_2+G_1+G_2+2)/D_2 \quad , \end{aligned} \tag{4-21}$$

where $D_2 = G_1^2G_2^2+R(2G_1G_2-G_1^2-G_2^2+4)$.

Antoniou [51] used the nullor concept to synthesize an additional gyrator circuit from Circuits 1 and 2. Figure 4.22 is a nullor equivalent of Circuits 1 and 2. By pairing the nullator of the INIC with the norator of the NIV, and the norator of the INIC with the nullator of the NIV, four possible circuits can be realized because each operational amplifier can be connected either inverting or noninverting. However, negative feedback is required around each operational amplifier

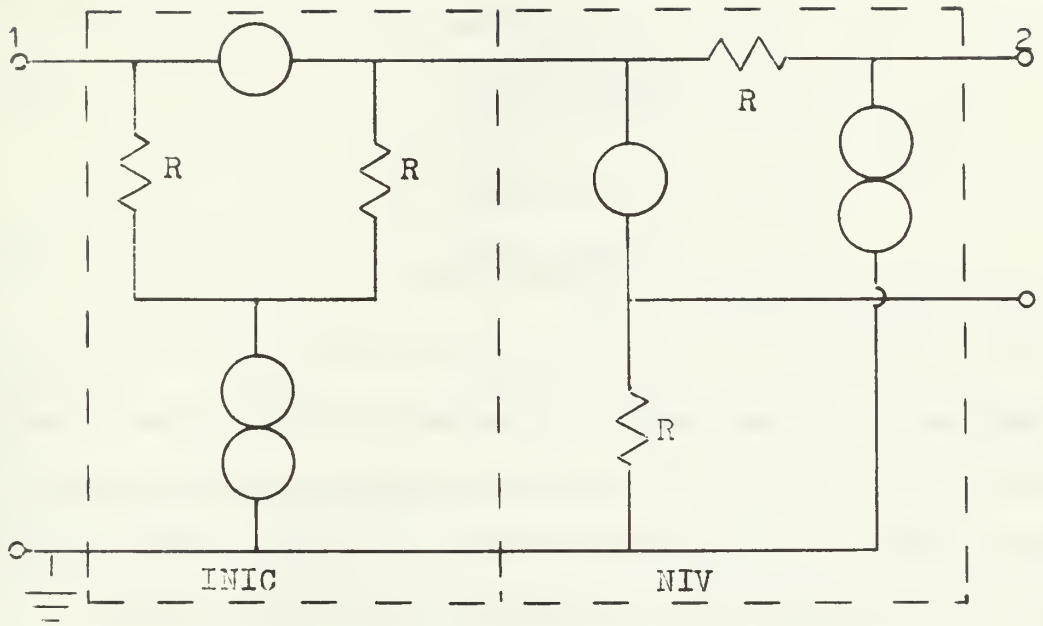

Fig. 4.22. Mullor Equivalent of Circuit 1 and 2

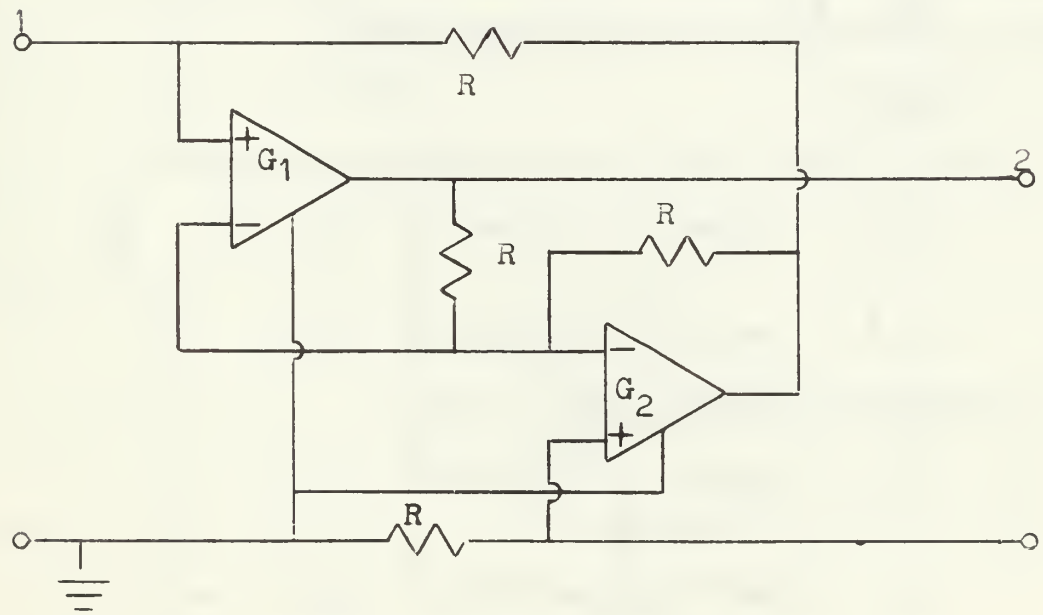

Fig. 4.23. Antoniou Gyrator (Circuit 3)

for circuit stability, and Circuit 3 [Fig. 4.23] is the only configuration possible. Circuit 3 has the admittance parameters

$$\begin{aligned} Z_{11} &= R(G_1+G_2+2)/D_3 \\ Z_{12} &= -G_2R(G_1+2)/D_3 \\ Z_{21} &= RG_1(G_2+1)/D_3 \\ Z_{22} &= R(G_1+G_2+2)/D_3 \quad , \end{aligned} \tag{4-22}$$

where $D_3 = G_1G_2+G_1+G_2+2$.

Equations (4-20, 4-21, and 4-22) approach the ideal gyrator impedance matrix if it is assumed the amplifier gains approach infinity. Circuits 1 and 2 can obtain unstable modes of operation during the period when the amplifiers are rising from zero voltage to full voltage gain. The instability is verified by the Llwellyn stability criterion (4-14). The addition of the limiting diodes to these circuits can prevent the amplifiers from saturating, but they reduce the voltage-handling capacity of the gyrator. The construction of Circuit 3 eliminates low-frequency unstable modes.

2. NIV type

The NIV [Fig. 4.24] has the impedance parameters

$$\begin{bmatrix} V_1 \\ \\ V_2 \end{bmatrix} = \begin{bmatrix} -R_2(G-1) & -GR/(G-1) \\ \\ -GR/(G-1) & -R_1/(G-1) \end{bmatrix} \begin{bmatrix} I_1 \\ \\ I_2 \end{bmatrix} . \tag{4-23}$$

If R_2 is a negative resistance, (4-23) becomes

$$\begin{bmatrix} V_1 \\ \\ V_2 \end{bmatrix} = \begin{bmatrix} R_2/(G-1) & -GR_1/G-1) \\ \\ GR_1/(G-1) & -R_1/(G-1) \end{bmatrix} \begin{bmatrix} I_1 \\ \\ I_2 \end{bmatrix} . \tag{4-24}$$

Assuming infinite amplifier gain and $R_1 = R_2$, equation (4-24) reduces to the ideal gyrator impedance matrix.

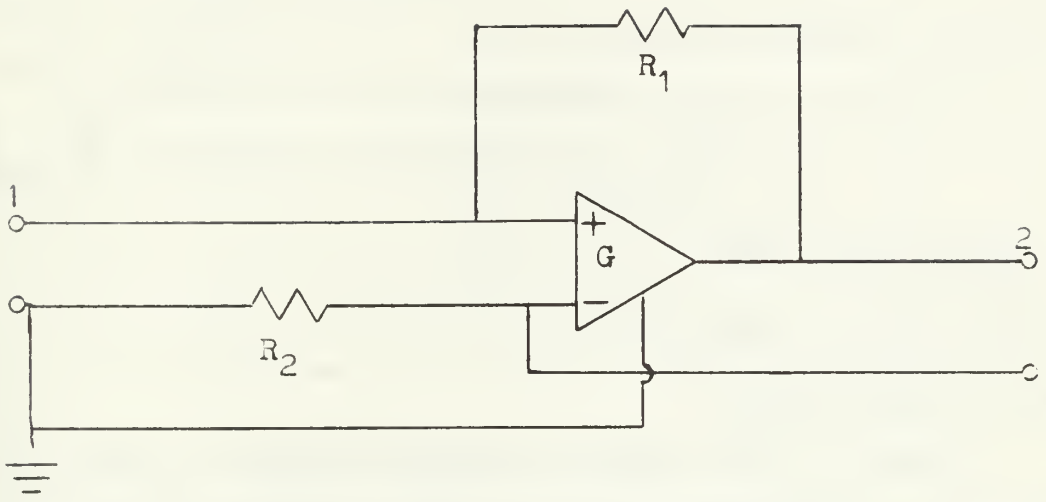

Fig. 4.24. Operational Amplifier NIV

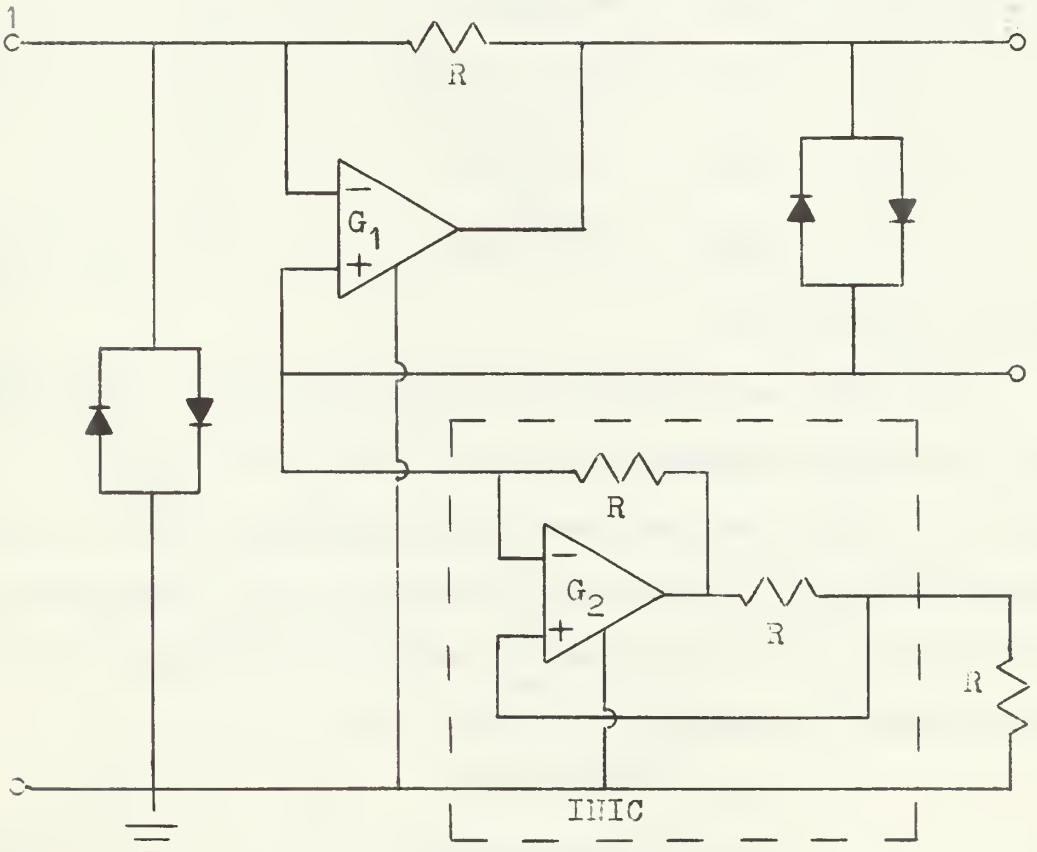

Fig. 4.25. Antoniou Gyrator (Circuit 4)

This method was applied by Antioniou [49] to synthesize two additional circuits. Circuit 4 [Fig. 4.25] achieves the required negative resistance with use of an INIC as shown in the network diagram. The Circuit 4 impedance parameters are

$$\begin{aligned} Z_{11} &= R/(G_1+1) \\ Z_{12} &= RG_1(G_2-2)/D_4 \\ Z_{21} &= -RG_1/(G_1+1) \\ Z_{22} &= -R(G_2-2)/D_4 \quad , \end{aligned} \tag{4-25}$$

where $D_4 = G_1G_2+2G_1+G_2+2$.

Circuit 5 [Fig. 4.26] is similar to Circuit 4, except for the interchange of input connections of both operational amplifiers. The impedance parameter for this gyrator are

$$\begin{aligned} Z_{11} &= -R/(G_1+1) \\ Z_{12} &= RG_1(G_2+2)/D_5 \\ Z_{21} &= -RG_1/(G_1-1) \\ Z_{22} &= -R(G+2)/D_5 \quad , \end{aligned} \tag{4-26}$$

where $D_5 = G_1G_2+2G_1+G_2+2$.

The nullor equivalent circuit [Fig. 4.27] drawn from Circuits 4 and 5 was used to synthesize Circuit 6 [Fig. 4.28] [51] . Negative feedback around each operational amplifier is required as in the case of Circuit 3. Hence, only one stable circuit configuration can be realized in which the limiting diodes are eliminated. The open-circuit impedance parameters for Circuit 6 are

$$\begin{aligned} Z_{11} &= 2R(G_1+1)/D_6 \\ Z_{12} &= -RG_2(G_1+2)/D_6 \end{aligned} \tag{4-27}$$

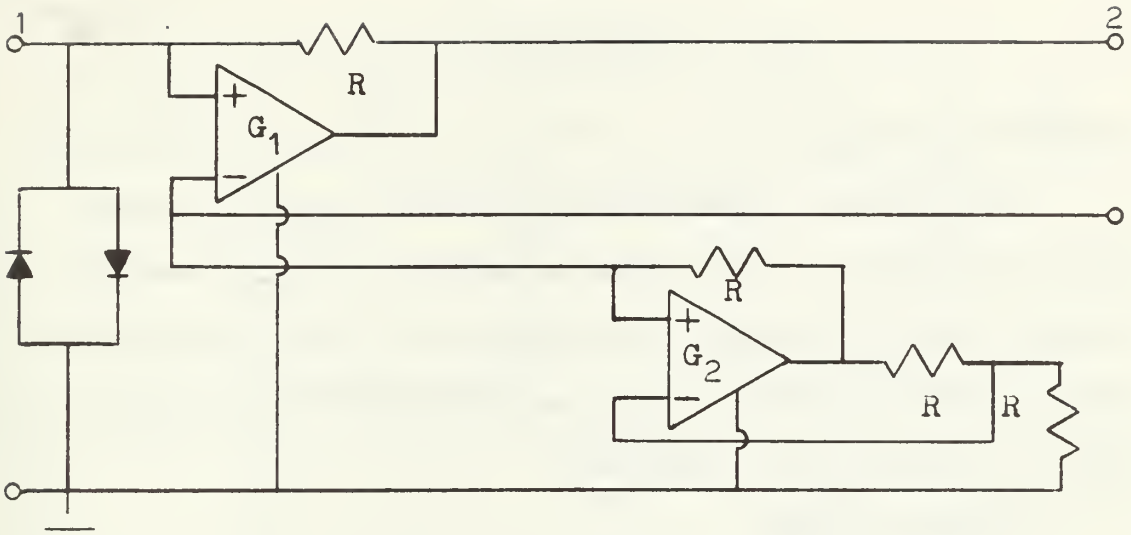

Fig. 4.26. Antoniou Gyrator (Circuit 5)

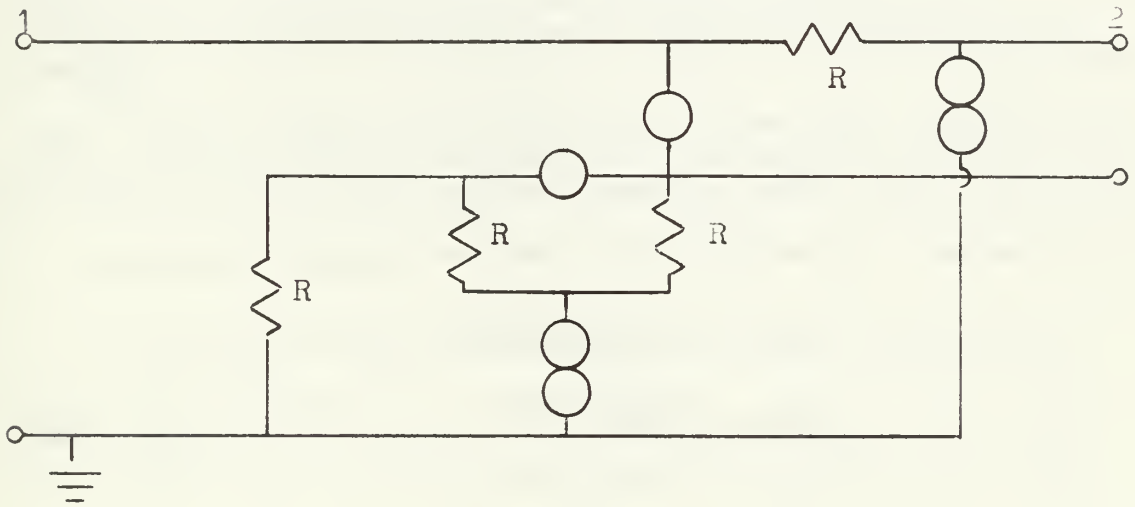

Fig. 4.27. Nullor Equivalent of Circuit 4 and 5

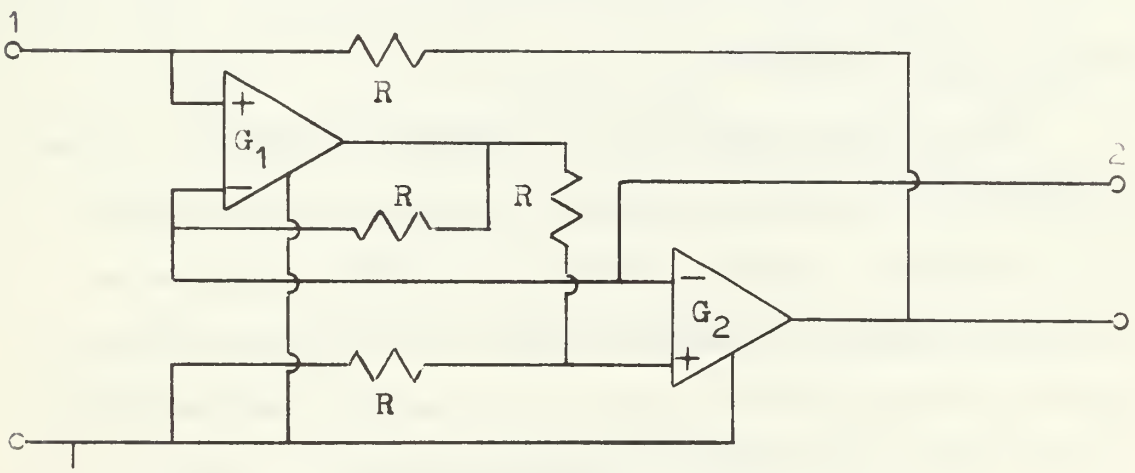

Fig. 4.28. Antoniou Gyrator (Circuit 6)

$$Z_{21} = RG_1(G_2+2)/D_6$$

$$Z_{22} = 2R(G_2+1)/D_6 \quad , \qquad \text{(4-27 Cont'd)}$$

where $D_6 = G_1G_2-2G_1+2$.

The impedance parameters of all the NIV circuits approach those of an ideal gyrator if infinite amplifier gains are assumed. Circuits 4 and 5 are subject to unstable modes for the same reason as Circuits 1 and 2. Circuit 6 is an improved gyrator that eliminates the stability problem at low frequencies.

3. Modified Circuits

A. Antoniou [43] applied the nullor technique to the Brugler circuit (Section IV.D) to obtain a new gyrator. The nullor equivalent circuit [Fig. 4.29] can be transformed into a modified Brugler network [Fig. 4.30] in the same manner as the other gyrators synthesized by this method. The modified circuit has the impedance parameters

$$Z_{11} = 2R(G_1+G_2+5)/D_7$$

$$Z_{12} = RG_2(G_1+4)/D_7 \qquad \text{(4-28)}$$

$$Z_{21} = -RG_1(G_2+4)/D_7$$

$$Z_{22} = 2R(G_1+G_2+3)/D_7$$

where $D_7 = G_1G_2+4(G_1+G_2)+12$.

When the series input resistor of Brugler's gyrator is removed and placed across the output terminals, the Deboo gyrator (Section IV.G) is realized. A nullor equivalent circuit [Fig. 4.31] can be made of this circuit. The modified Deboo circuit [Fig. 4.32] is similar to the Deboo circuit except for the resistor mentioned. The modified Deboo circuit has the impedance parameters

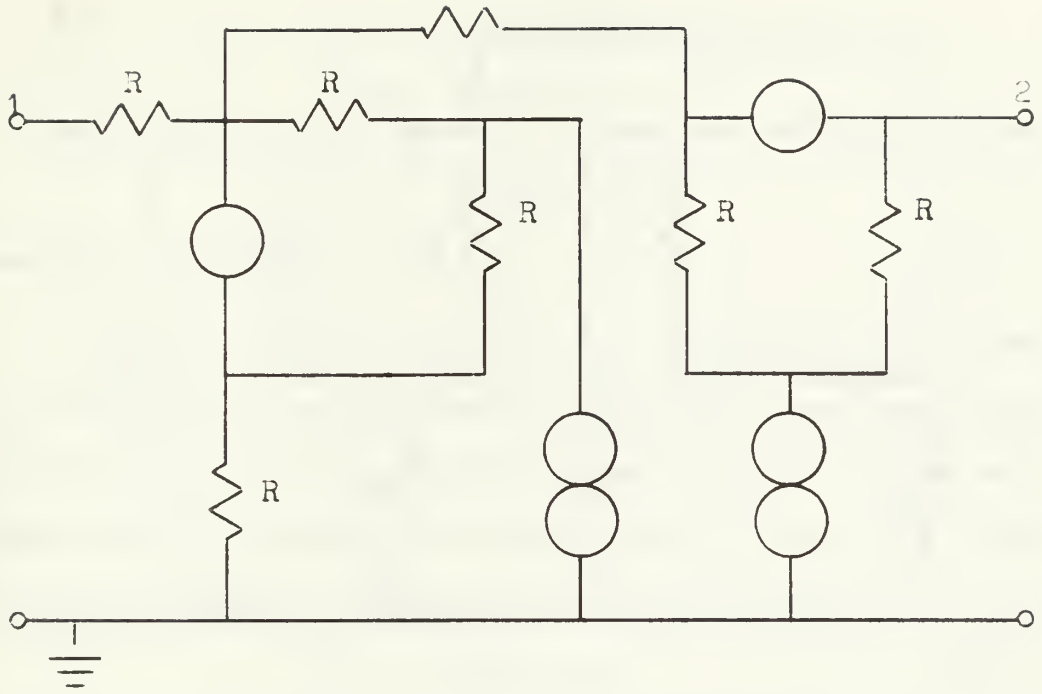

Fig. 4.29. Nullor Equivalent of Brugler's Circuit

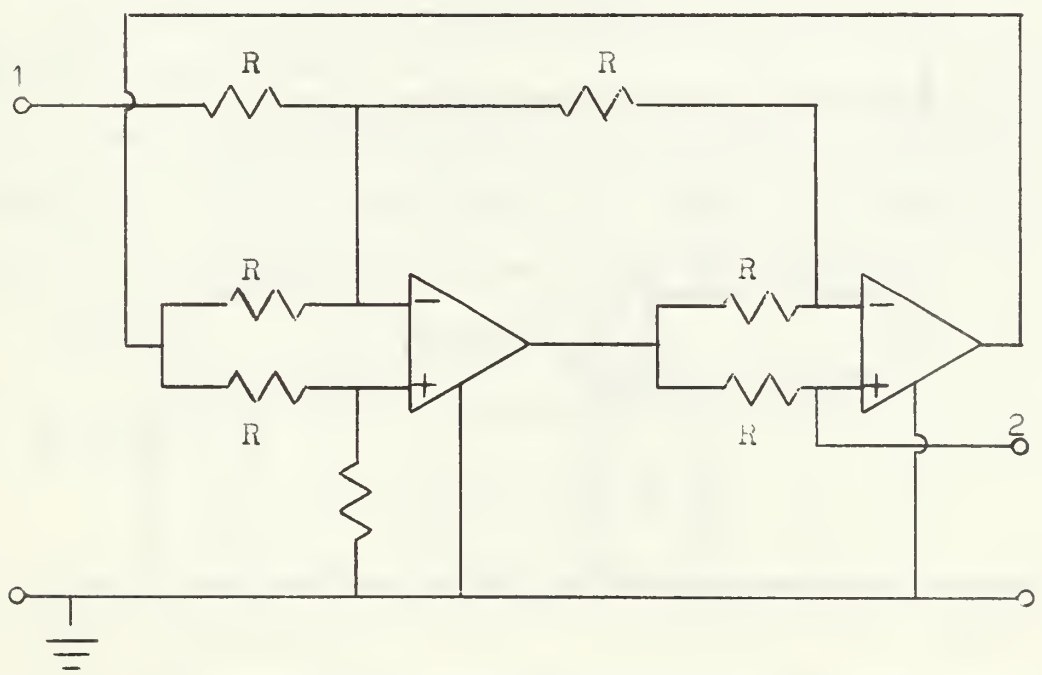

Fig. 4.30. Modified Brugler Gyrator

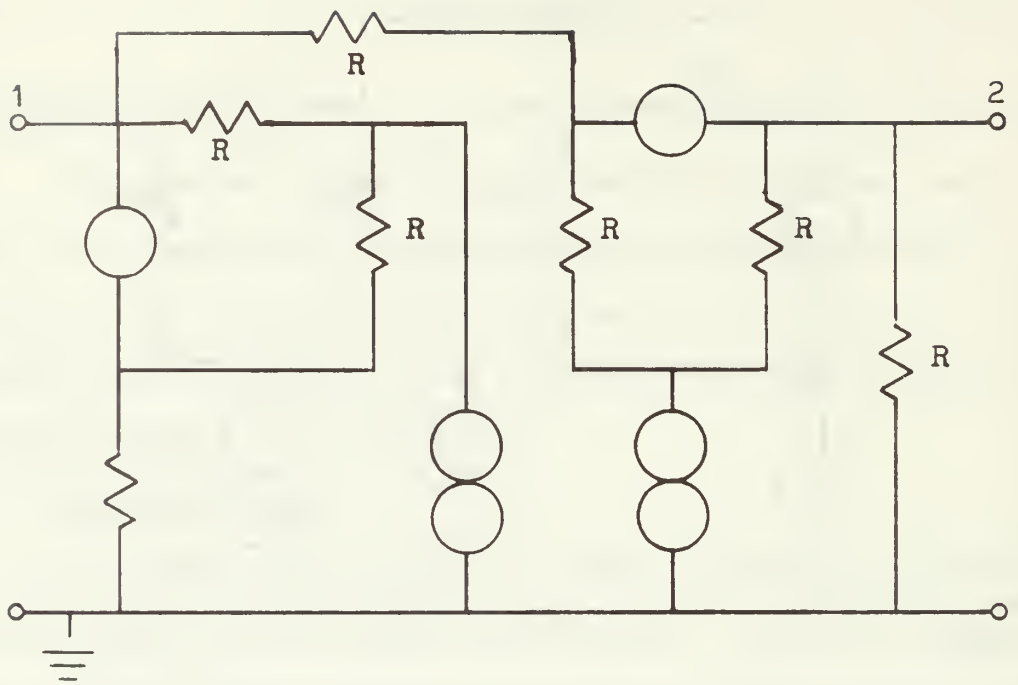

Fig. 4.31. Nullor Equivalent of Deboo's Gyrator

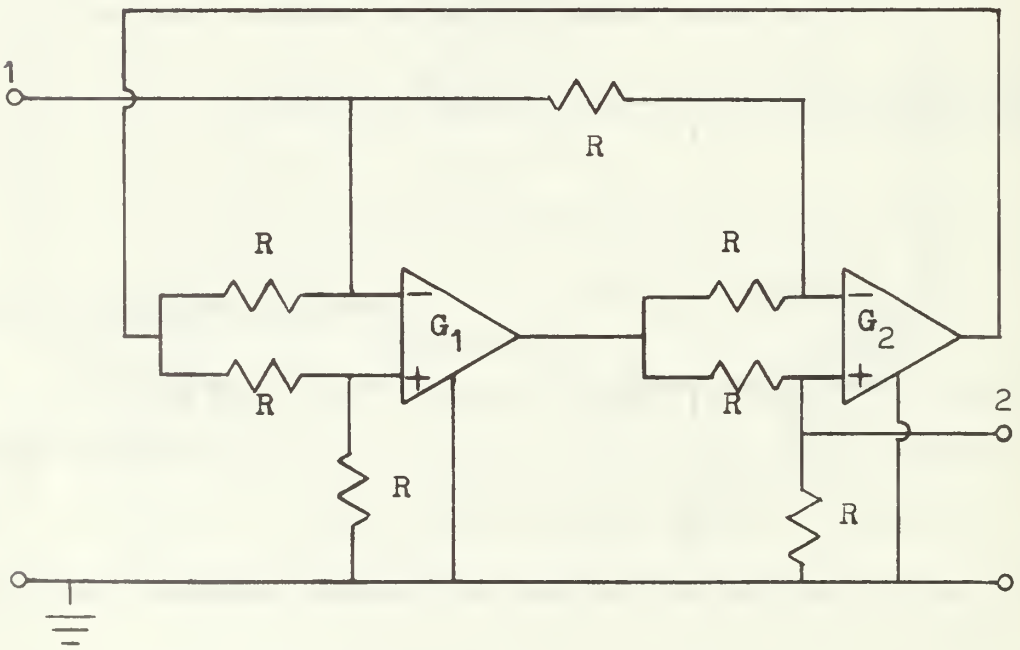

Fig. 4.32. Modified Deboo Gyrator

$$Z_{11} = 8R/D_8$$

$$Z_{12} = RG_2(G_1+4)/D_8 \qquad (4\text{-}34)$$

$$Z_{21} = -RG(G_2+4)/D_8$$

$$Z_{22} = 2R(G_1+G_2+3)/D_8 \ ,$$

where $D_8 = G_1G_2+4(G_1+G_2)+12$

Riordan's Circuit 1 and Circuit 2 were modified by Antoniou [51] making use of nullor equivalent circuits. The nullor equivalent circuit [Fig. 4.33] for Riordan's Circuit 1 (Section IV.F) can be synthesized into a modified Riordan Circuit 1 [Fig. 4.34] . The open-circuit impedance parameters for this gyrator are

$$Z_{11} = 2R(G_2+1)/D_9$$

$$Z_{12} = -RG_1G_2/D_9 \qquad (4\text{-}35)$$

$$Z_{21} = R(G_1G_2+2G_1+2G_2)/D_9$$

$$Z_{22} = 2R(G_1+1)/D_9 \ ,$$

where $D_9 = G_1G_2+2G_1+2G_2+2$.

The nullor equivalent circuit [Fig. 4.35] for Riordan's Circuit 2 is similarly synthesized into a modified Riordan Circuit 2 [Fig. 4.36] . The impedance parameters for this circuit are

$$Z_{11} = R(G_2+2)/D_{10}$$

$$Z_{12} = -RG_1(G_2+2)/D_{10}$$

$$Z_{21} = RG_2(G_1+2)/D_{10}$$

$$Z_{22} = R(2G_1+G_2+2)/D_{10} \ ,$$

where $D_{10} = G_1G_2+2G_1+G_2+2$.

As the gains of the operational amplifiers approach infinity, the open-circuit impedance parameters for the modified circuits approach that of an ideal gyrator.

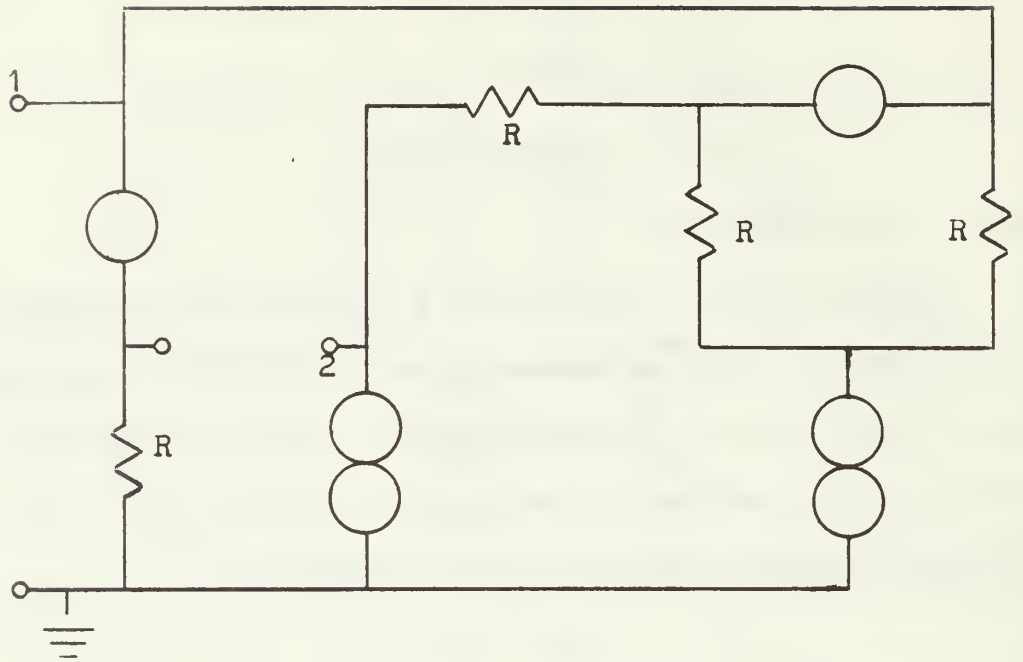

Fig. 4.33. Nullor Equivalent of Riordan's Circuit 1

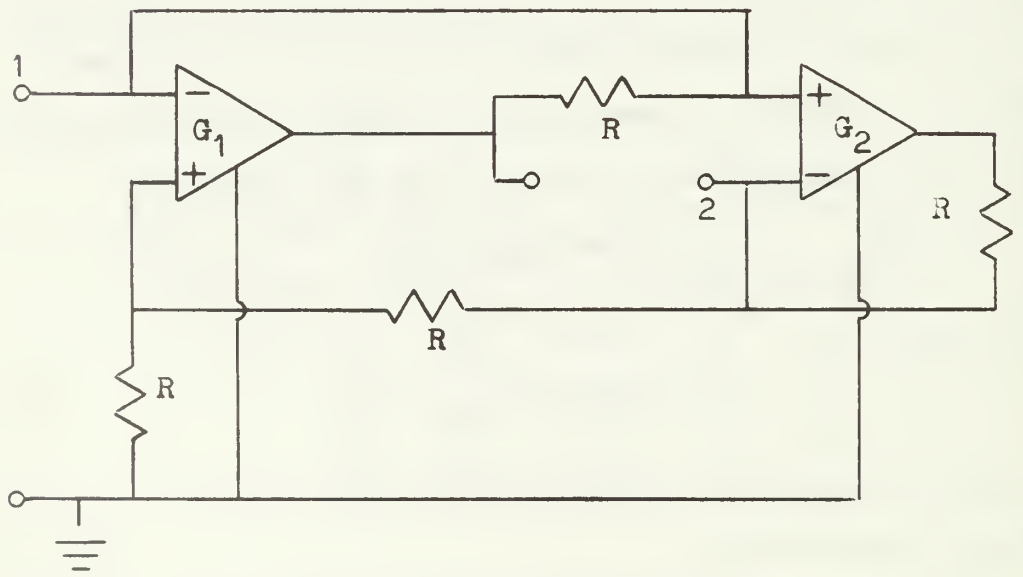

Fig. 4.34. Modified Riordan Gyrator (Circuit 1)

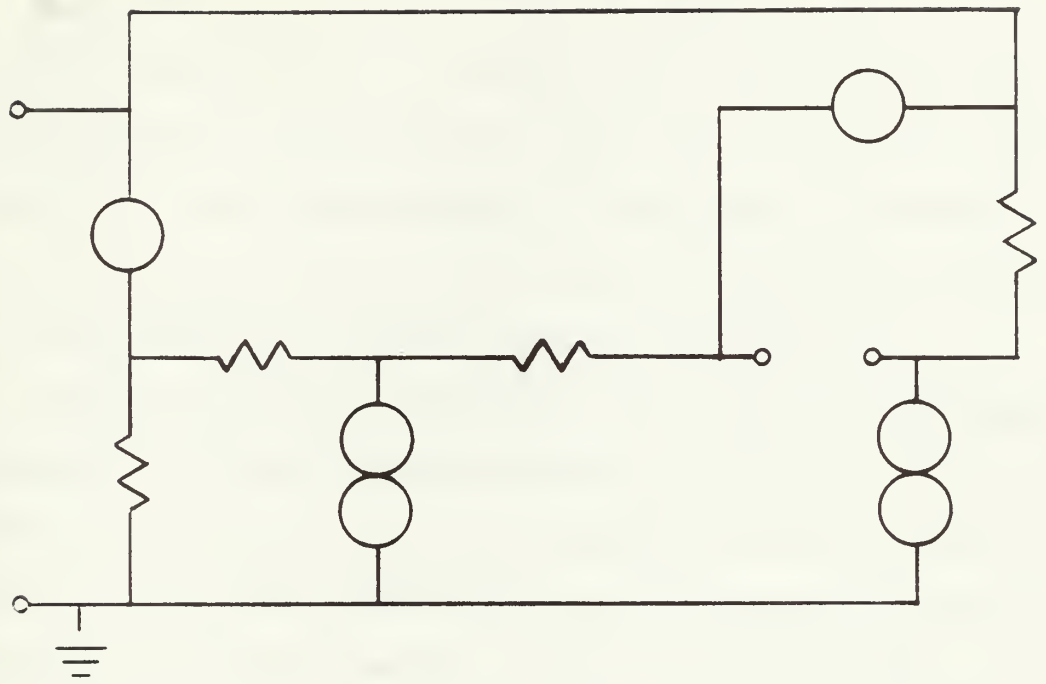

Fig. 4.35. Nullor Equivalent of Riordan's Circuit 2

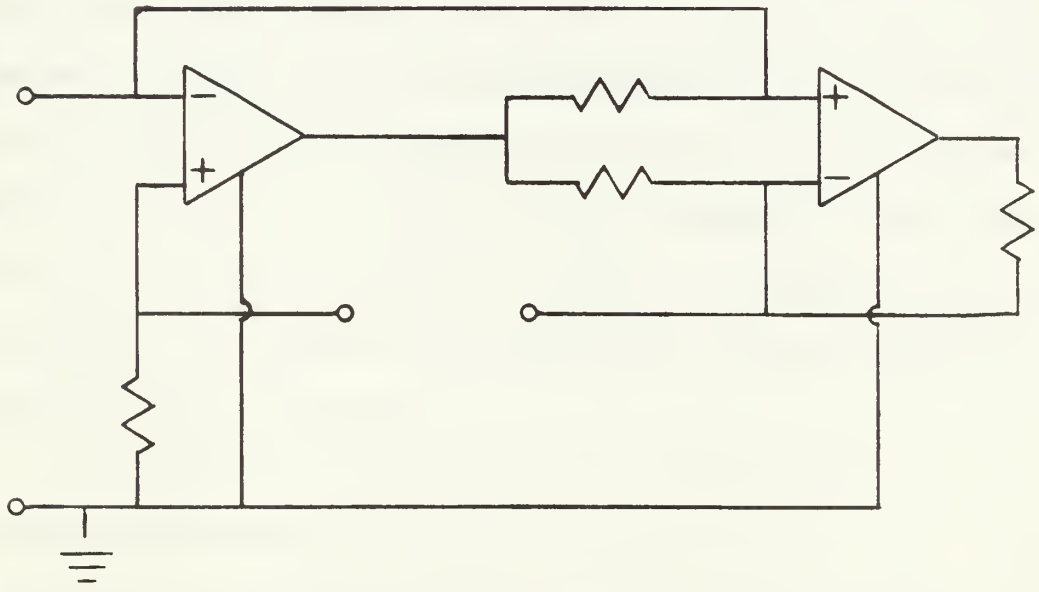

Fig. 4.36. Modified Riordan Gyrator Circuit 2

The modified circuits as synthesized by Antoniou eliminated unstable modes from the original circuits.

V. SUMMARY

The gyrator was at first an item of academic interest after its initial conception by H. B. Tellegren.. The earlier gyrators were synthesized and tested mainly for their impedance-conversion characteristics. But as the technology in transistors and integrated circuits developed, gyrators were seriously considered as one answer to the replacement of inductors in filter applications.

The most immediate problems that became evident when the known gyrators were tested in filter applications were due to their low Q factors and also their temperature-dependent sensitivity. The low Q factors can be mainly attributed to the residual terms of the gyrator's admittance or impedance matrix. The temperature dependence is related to the inherent time delay in the amplifiers used to physically construct the gyrator.

The unwanted residual terms can be significantly reduced by designing a gyrator from two independent VCCS of opposite polarity, such as the Orchard-Sheahan gyrators, or from two differential amplifiers with feedback as in the case of the Riordan gyrators. All the gyrators realized from the NIC-NIV circuit construction, or those that employ negative resistances to cancel undesired impedances or admittances, do not achieve sufficient cancellation because of component tolerances. In addition, the introduction of an NIV into a circuit can cause undesired stability problems.

The temperature-sensitivity problem can be partially corrected by additional compensating components designed into each VCCS. However, variations of operating conditions can reduce the effectiveness of this

solution because these added components can affect gyrator parameters. With the continuing development of the operational amplifier, the Riordan-type gyrator should prove to be the superior circuit. The feedback between the two amplifiers automatically compensates for changes in the operating environment, and the individual differential amplifiers are less temperature sensitive.

Table I gives a summary of typical values obtained when certain of the realizations were tested. The table is not complete. Many of the gyrator circuits discussed in this thesis were not accompanied by publicized experimental results.

TABLE I - SUMMARY OF PUBLISHED TEST RESULTS

GYRATOR	ACTIVE DEVICE	SYNTHESIS METHOD	GYRATION RESISTANCE CONDUCTANCE	OTHER PARAMETERS	TEST FREQUENCY RANGE (Hz)
BOGERT	VT	FEEDBACK AMPLIFIERS 1 NEGATIVE RESISTANCE	R=598ohms	Z_{11}=-2.8+j24.8 Z_{22}=-4.1+j3.8	400
SHENOI	T	VCCS	R=118ohms	Z_{11}=0.685ohms Z_{22}=2.2ohms	10-15K
ORCHARD-SHEAHAN CKT #1	T	VCCS	g=o.135X10^{3}mhos	Y_{11}=2.2X10^{-7}mhos Y_{22}=2.78X10^{-7}mhos	1-2000
ORCHARD-SHEAHAN CKT #2	T	VCCS	g_1=0.135X10^{-3}mhos g_2=.925X10^{-3}mhos	no data	1-100K
RAO-NEWCOMB	T	VCCS	R=2400ohms	Y_{11}=3.3X10^{-5}mhos Y_{22}=3.3X10^{-5}mhos	100-180K
YANAGISAWA CKT #1	T	VCCS	g_1=0.141X10^{-3}mhos g_2=2.54X10^{-3}mhos	no data	0-200K
YANAGISAWA CKT #2	T	VCCS	g_1=.9X10^{-3}mhos g_2=1.1X10^{-3}mhos	no data	0-200K

TABLE I - SUMMARY OF PUBLISHED TEST RESULTS (con't)

GYRATOR	ACTIVE DEVICE	SYNTHESIS METHOD	GYRATION RESISTANCE CONDUCTANCE	OTHER PARAMETERS	TEST FREQUENCY RANGE (Hz)
YANAGISAWA CKT #3	T	VCCS	$g_1=1.1X10^{-3}$mhos $g_2=1.083X10^{-3}$mhos	no data	1K
HAWLEY	OA	VCCS	R=31.6Kohms	no data	10-1000K
RIORDAN CKT #2	OA	VCCS with feedback	R=100Kohms R=3.3Kohms	no data	0-100K
DEBOO	OA	SHEINGOLD VCCS WITH NEGATIVE CONDUCTANCE	$g=1X10^{-4}$mhos	no data	10-100K
ANTONIOU CKT #2	OA	INIC-NIV	R=1Kohms	no data	10-10K
ANTONIOU CKT #6	OA	NIV WITH NEGATIVE RESISTANCE	no data	no data	10-10K

VT - VACUUM TUBE T - TRANSISTOR OA - OPERATIONAL AMPLIFIER

TABLE I - SUMMARY OF PUBLISHED TEST RESULTS

GYRATOR	CAPACITOR LOAD	SIMULATED INDUCTANCE	RESONANT FREQUENCY (Hz)	Q MAX	SUITABLE FOR INTEGRATED CIRCUITS
BOGERT	0.572uF	1.34H	no data	no data	NO
SHENOI	0.133uF	1.55mH (c)	15.1K (c)	67 (c)	YES
ORCHARD-SHEAHAN CKT #1	0.03uF	16.4mH (c)	480	385	YES
ORCHARD-SHEAHAN CKT #2	0.004uF 0.1uF	33mH .83H	30K .8	500 460	YES
RAO-NEWCOMB	2600pF	1.08H (c)	40K	57	YES
YANAGISAWA CKT #1	ONLY IMPEDANCE-INVERSION PROPERTY TESTED				YES
YANAGISAWA CKT #2	ONLY IMPEDANCE-INVERSION PROPERTY TESTED				YES
YANAGISAWA CKT #3	ONLY IMPEDANCE-INVERSION PROPERTY TESTED				YES
HAWLEY	1000pF	1.06H	21K	38	YES
RIORDAN CKT #2	.43uF .43uF	40mH 10mH	8 55K	2000 250	YES
DEBOO	1000pF	.1H	no data	no data	YES
ANTONIOU CKT #2	C=.01uF C=.1uF C=1uF	10mH(c) .1H(c) 1H(c)	.3K 3K 10K	no data	YES

TABLE I - SUMMARY OF PUBLISHED TEST RESULTS (con't)

GYRATOR	CAPACITOR LOAD	SIMULATED INDUCTANCE	RESONANT FREQUENCY (Hz)	Q MAX	SUITABLE FOR INTEGRATED CIRCUITS
ANTONIOUS CKT #6	no data	1H	200	2000	YES

C - CALCULATED

LIST OF REFERENCES

1. Tellegen, B. D. H., "The Gyrator, A new Network Element," Philips Res. Rep., V. 3, no. 2, pp. 81-101, April 1948.

2. Ghausi, M. S., Principles and Design of Linear Active Circuits, pp. 40-45, McGraw-Hill, 1965.

3. Parker, S. R., "Some Properties of Networks and Systems Passivity and Positive Real Functions," paper presented for Advance Network Theory Course EE-4121, Naval Postgraduate School, Monterey, California, June 1967.

4. Shekel, J., "The Gyrator as a 3-Terminal Element," Proc. I.R.E., V. 41, no. 8, pp. 1014-1016, August 1953.

5. Holt, A. G. J., and Linggard, R., "The Multiterminal Gyrator," Proc. IEEE, V. 56, no. 8, pp. 1354-1355, August 1968.

6. Huelsman, L. P., Theory and Design of Active RC Circuits, p. 165, McGraw-Hill, 1968.

7. Von der Pfordten, H. J., "Substitution of Inductances in Integrated Circuits", in "Papers on Integrated Circuit Synthesis," compiled by Newcomb, R. W., and Rao, T. N., Stanford University, Stanford, California, Technical Report 6560-4, p. 172, June 1966.

8. dePian, L., "Active Filters: Part 2 Using the Gyrator," Electronics, V. 41, no. 12, pp. 114-120, 10 June 1968.

9. Bialko, M., "On Q Factor and Q Sensitivity of an Inductor Simulated by a Practical Gyrator," Electronics Letters, V. 3, no. 4, pp. 168-169, April 1967.

10. Rao, T. N., Gary, P., Newcomb, R. W., "Equivalent Inductance and Q of a Capacitor-Loaded Gyrator," IEEE J. Solid-State Circuits, V. SC-2, no. 1, pp. 32-33, March 1967.

11. Orchard, H. J., "Inductorless Filters," Electronics Letters, V. 2, no. 6, pp. 224-225, June 1966.

12. Van Looij, H. TH., and Adams, K. M., "Phase-Compensation in Electronic Gyrator Circuits," Electronics Letters, V. 3, no. 4, pp. 430-431, October 1968.

13. Martinelli, G., "Time Delay in Ideal Gyrators," Proc. IEEE, V. 57, no. 2, pp. 249-250, February 1969.

14. McGregor, "Theoretical and Realizable Sensitivities of a Two-Pole Gyrator Active Filter," IEEE Trans. Circuit Theory, V. CT-15, no. 2, pp. 94-1000, June 1968.

15. Geffe, P. R., "Gyrator Bandwidth Limitations," IEEE Trans. Circuit Theory, V. CT-15, no. 4, p. 501, December 1968.

16. Sheahan, D. F. and Orchard, H. J., "High-Quality Transistorised Gyrator," Electronics Letters, V. 2, no. 7, pp. 274-275, July 1966.

17. Sheahan, D. F. and Orchard, H. J., "Integratable Gyrator Using M.O.S. and Bipolar Transistors," Electronics Letters, V. 2, no. 10, October 1966.

18. Van Looij, H. TH., "Wideband Electronic Gyrator Circuit," Electronics Letters, V. 4, No. 20, pp. 431-432, October 1968.

19. Su, K. L., Active Network Synthesis, p. 51, McGraw-Hill, 1965.

20. Hove, R. G. and Kleingartner, C. A., Silicon Monolithic Gyrator Using FET'S, paper presented at the Western Electronic Show and Convention, San Francisco, California, 19 August 1969.

21. dePian, L., Linear Active Network Theory, pp. 243-244, Prentice-Hall, 1962.

22. Bogert, B. P., "Some Gyrator and Impedance Inverter Circuits," Proc. IRE, V. 43, No. 7, pp. 793-796, July 1955.

23. Sharpe, G. E., "The Pentode Gyrator," IRE Trans. Circuit Theory, V. CT-4, No. 4, pp. 321-323, December 1957.

24. Sharpe, G. E., "Ideal Active Elements," J. IEE, V. 3, No. 7, pp. 430-431, July 1957.

25. Sharpe, G. E., "Transactors," Proc. IRE, V. 45, No. 5, pp. 692-693, May 1957.

26. Sharpe, G. E., "Ideal Active Elements," J. IEEE, V. 3, No. 1, pp. 33-34, January 1957.

27. Shenoi, B. A., "A 3-Transistor Gyrator with Variable Gyration Resistance," 1964 Proc. of 2nd Annual Allerton Conference on Circuit and System Theory, pp. 782-801, September 1964.

28. Shenoi, B. A., "Practical Realization of a Gyrator Circuit and RC-Gyrator Filters," IEEE Trans. Circuit Theory, VCT-12, No. 3, pp. 374-380, September 1965.

29. Millman, J. and Halkias, C. C., Electronic Devices and Circuits, p. 395, McGraw-Hill, 1967.

30. Rao, T. N. and Newcomb, R. W., "Direct-Coupled Gyrator Suitable for Integrated Circuits and Time Variation," Electronic Letters, V. 2, No. 7, pp. 250-251, July 1966.

31. Gary, P., "An Integrable Direct-Coupled Gyrator," in "Papers on Integrated Circuit Synthesis," compiled by Newcomb, R. W., and Rao, T. N., Stanford University, Stanford, California, Technical Report 6560-4, pp. 45-60, June 1966.

32. Chua, H. T. and Newcomb, R. W., "Integrated Direct-Coupled Gyrator," Electronics Letters, V. 3, No. 5, pp. 182-184, May 1967.

33. Yanagisawa, T., and Kawashima, Y., "Active Gyrator," Electronics Letters, V. 3, No. 3, pp. 105-107, March 1967.

34. Yanagisawa, T., "Realization of a Lossless Transistor Gyrator," Electronics Letters, V. 3, No. 4, pp. 167-188, April 1967.

35. Yanagisawa, T., "Direct-Coupled Transistor Lossless Gyrators," Electronics Letters V. 3, No. 7, July 1967.

36. Morse, A. S. and Huelsman, L. P., "A Gyrator Realization Using Operational Amplifiers," IEEE Trans. Circuit Theory, V. CT-11, No. 2, pp. 277-278, June 1964.

37. Huelsman, L. P., Theory and Design of Active RC Circuits, pp. 176-177, McGraw-Hill, 1968.

38. Davies, A. C., "The Significance of Nullators, Norators and Nullors in Active-Network Theory," Radio Electronic Engr., V. 34, No. 5, pp. 259-267, November 1967.

39. Bendik, J., "Equivalent Gyrator Networks with Nullors and Norators," IEEE Trans. Circuit Theory, V. CT-14, No. 1, p. 98, March 1967.

40. Braun, J., "Equivalent N.I.C. Networks with Nullators and Norators," IEEE Trans. Circuit Theory, V. CT-12, No. 3, pp. 441-442, September 1965.

41. Hawley, I. H., "A Gyrator Realization Using Operational Amplifiers," in "Papers on Integrated Circuit Synthesis," compiled by Newcomb, R. W., and Rao, T. N., Stanford University, Stanford, California , Technical Report 6560-4, pp. 61-92, June 1966.

42. Brugler, J. S., "RC Synthesis with Differential-Input Operational Amplifiers," in "Papers on Integrated Circuit Synthesis," compiled by Newcomb, R. W., and Rao, T. N., Stanford University, Stanford, California, Technical Report 6560-4, pp. 116-130, June 1966.

43. Antoniou, A., "3-Terminal Gyrator Circuits Using Operational Amplifiers," Electronics Letters, V. 4, No. 26, pp. 591-592, December 1968.

44. Llewellyn, F. B., "Some Fundamental Properties of Transmission Systems," Proc. Inst. Radio Engineers, V. 40, No. 3, pp. 271-283, March 1952.

45. Prescott, A. J., "Loss-Compensated Active Gyrator Using Differential-Input Operational Amplifiers," Electronics Letters, V. 2, No. 7, pp. 283-284, July 1966.

46. Riordan, R. H. S., "Simulated Inductors Using Differential Amplifiers," Electronic Letters, V. 3, No. 2, pp. 50-51, February 1967.

47. Antoniou, A., "Stability Properties of Some Gyrator Circuits," Electronics Letters, V. 4, No. 2, pp. 510-512, November 1968.

48. Deboo, G. J., "Application of a Gyrator-Type Circuit to Realize Ungrounded Inductors," IEEE Trans. Circuit Theory, V. CT-14, No. 1, pp. 101-102, March 1967.

49. Antoniou, A., "Gyrators Using Operational Amplifiers," Electronics Letters, V. 3, No. 8, pp. 350-353, August 1967.

50. Morse, A. S., "The Use of Operational Amplifiers in Active Network Theory," Proc. of the National Electronics Conferences, pp. 748, 1964.

51. Antoniou, A., "New Gyrator Circuits Obtained by Using Nullors," Electronic Letters, V. 4, No. 5, March 1968.

INITIAL DISTRIBUTION LIST

		No. Copies
1.	Defense Documentation Center Cameron Station Alexandria, Virginia 22314	20
2.	Library, Code 0212 Naval Postgraduate School Monterey, California 93940	2
3.	Naval Ordnance Systems Command Department of the Navy Washington, D. C. 20360	1
4.	Professor S. R. Parker, Code 52Px Department of Electrical Engineering Naval Postgraduate School Monterey, California 93940	2
5.	LT James John Kulesz 832 Florida Avenue Pittsburgh, Pennsylvania 15228	1

Security Classification

DOCUMENT CONTROL DATA - R & D

(Security classification of title, body of abstract and indexing annotation must be entered when the overall report is classified)

1 ORIGINATING ACTIVITY (Corporate author)	2a. REPORT SECURITY CLASSIFICATION
Naval Postgraduate School Monterey, California 93940	Unclassified
	2b. GROUP

3 REPORT TITLE

A Study of Gyrator Circuits

4 DESCRIPTIVE NOTES (Type of report and, inclusive dates)

Master's Thesis; December 1969

5. AUTHOR(S) (First name, middle initial, last name)

Lieutenant James John Kulesz, Jr.

6. REPORT DATE	7a. TOTAL NO. OF PAGES	7b. NO. OF REFS
December 1969	94	51

8a. CONTRACT OR GRANT NO.	9a. ORIGINATOR'S REPORT NUMBER(S)
b. PROJECT NO.	
c.	9b. OTHER REPORT NO(S) (Any other numbers that may be assigned this report)
d.	

10. DISTRIBUTION STATEMENT

This document has been approved for public release and sale; its distribution is unlimited.

11. SUPPLEMENTARY NOTES	12. SPONSORING MILITARY ACTIVITY
	Naval Postgraduate School Monterey, California 93940

13. ABSTRACT

Since the introduction of the gyrator in 1948, numerous papers have been written concerning the implementation and application of these network devices. Gyrators have been realized utilizing vacuum tubes, transistors, and operational amplifiers to obtain their nonreciprocal property. It is the purpose of this thesis to consolidate the current findings.

A section has been written on each of the active devices mentioned above. The individual sections consist of summaries of published gyrator realizations. The method used to obtain the gyrator properties, along with appropriate equations, is that of the original circuit designer. Some relations and equations have been modified to standardize notation, or to express them in a more convenient form. Where available, experimental test circuits have been included to support the synthesis method.

DD FORM 1 NOV 65 1473 (PAGE 1)

S/N 0101-807-6811

Security Classification

A-31408

14 KEY WORDS	LINK A		LINK B		LINK C	
	ROLE	WT	ROLE	WT	ROLE	WT
Gyrator						
Simulated Inductance						